

**COMPARISON OF FUNCTIONAL AND STRUCTURAL
PROPERTIES OF AN OUTER MEMBRANE PORIN
BETWEEN *Burkholderia pseudomallei*
AND *Burkholderia thailandensis***

Miss Jaruwat Siritapetawee

**A Thesis Submitted in Partial Fulfillment of the Requirements
for the Degree of Doctor of Philosophy in Biochemistry
Suranaree University of Technology**

Academic Year 2004

ISBN 974-533-325-5

การเปรียบเทียบสมบัติเชิงหน้าที่และเชิงโครงสร้างของโปรตีนพอรินใน
ผนังเซลล์ผิวนอกระหว่างเชื้อ *Burkholderia pseudomallei*
และ *Burkholderia thailandensis*

นางสาวจรรวรรณ สิริเทพทวี

วิทยานิพนธ์นี้เป็นส่วนหนึ่งของการศึกษาตามหลักสูตรปริญญาวิทยาศาสตรดุษฎีบัณฑิต

สาขาวิชาชีวเคมี

มหาวิทยาลัยเทคโนโลยีสุรนารี

ปีการศึกษา 2547

ISBN 974-533-325-5

**STUDY OF IMMUNOTOXICOLOGICAL EFFECTS OF
DOK DIN DAENG (*Aeginetia indica* Roxb.)**

Suranaree University of Technology has approved this thesis submitted in
partial fulfillment of the requirements for the Degree of Doctor of Philosophy

Thesis Examining Committee



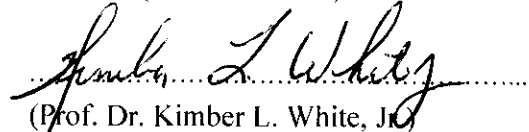
(Dr. Nuthawut Thanee)

Chairperson



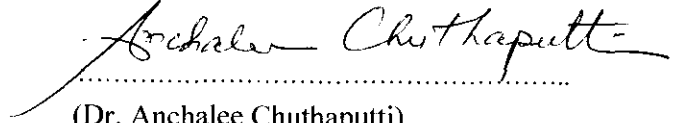
(Asst. Prof. Dr. Benjamart Chitsomboon)

Member (Thesis Advisor)



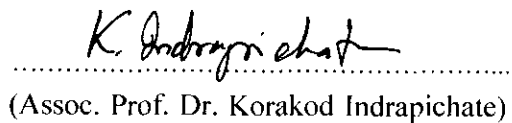
(Prof. Dr. Kimber L. White, Jr.)

Member



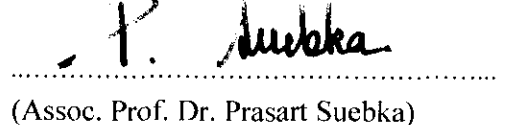
(Dr. Anchalee Chuthaputti)

Member

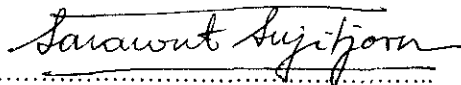


(Assoc. Prof. Dr. Korakod Indrapichate)

Member



(Assoc. Prof. Dr. Prasart Suebka)



(Assoc. Prof. Dr. Sarawut Sujitjorn)

Vice Rector for Academic Affairs

Dean of the Institute of Science

จรรุวรรณ สิริเทพทวี : การเปรียบเทียบสมบัติเชิงหน้าที่และเชิงโครงสร้างของโปรตีนพอรินในผนังเซลล์ผิวนอกระหว่างเชื้อ *Burkholderia Pseudomallei* และ *Burkholderia thailandensis*

(COMPARISON OF FUNTIONAL AND STRUCTURAL PROPERTIES OF AN OUTER MEMBRANE PORIN BETWEEN *Burkholderia pseudomallei* AND *Burkholderia thailandensis*)

อาจารย์ที่ปรึกษา : ดร. วิภา สุจินต์, 199 หน้า. ISBN 974-533-325-5

การศึกษาค้นคว้านี้ได้ทำการแยกโปรตีนพอรินสองชนิดคือ *BpsOmp38* และ *BthOmp38* ซึ่งเป็นโปรตีนผิวนอกของเชื้อ *B. pseudomallei* และ *B. thailandensis* ตามลำดับ พบว่าโปรตีนในสภาพธรรมชาติมีลักษณะเป็น 3 หน่วย (M_r 110,000) ซึ่งประกอบด้วยหน่วยย่อยที่เหมือนกัน (M_r 38,000) จากข้อมูลที่ได้จากการทำ peptide mass fingerprint ทำให้สามารถแยกชิ้น *Omp38* จากโครโมโซมของเชื้อทั้งสองได้ ลำดับนิวคลีโอไทด์ของยีน *BpsOmp38* และ *BthOmp38* พบว่าเหมือนกัน 98% และมีลำดับของกรดอะมิโนของโปรตีนเหมือนกัน 99.7% การวิจัยครั้งนี้ยังได้ทำการผลิตโปรตีน *Omp38* ในแบคทีเรีย *E. coli* ในรูป inclusion bodies และทำให้กลับมามีสภาพธรรมชาติโดยใช้ระบบบัฟเฟอร์ที่มี 10% (w/v) Zwittergent® 3-14 จากการศึกษาโครงสร้างทุติยภูมิโดยเทคนิค FTIR และ CD spectroscopy พบว่าโปรตีน *Omp38* มีองค์ประกอบหลักเป็น β -sheet จากการศึกษาหน้าที่ของพอรินด้วยวิธี liposome-swelling assays พบว่าโปรตีน *Omp38* มีคุณสมบัติเป็น non-specific channel ที่มีความสามารถให้สารละลายน้ำตาลที่มีน้ำหนักโมเลกุล <650 Da ผ่านเข้าออกได้ จากการทำนายโครงสร้างของพอริน พบว่ามีโครงสร้างเป็น β -barrel ประกอบด้วย 16-stranded β -barrel 8 periplasmic turns และ 8 external loops การศึกษาค้นคว้านี้ได้ทำการเตรียมผลึกโปรตีนด้วยเทคนิค sitting drop แต่ผลการทดลองภายใต้สภาวะที่ทดสอบสังเกตเห็นเฉพาะผลึกโปรตีนขนาดเล็ก ดังนั้นจึงต้องมีการทดสอบการเตรียมโปรตีนใน detergent ชนิดอื่นๆ และสภาวะการเกิดผลึกโปรตีนที่เหมาะสมต่อไป เพื่อให้ได้ผลึกที่มีคุณภาพสำหรับศึกษาโครงสร้างสามมิติของโปรตีน *Omp38* ต่อไปในอนาคต

สาขาวิชาชีวเคมี
ปีการศึกษา 2547

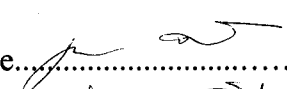
ลายมือชื่อนักศึกษา.....
ลายมือชื่ออาจารย์ที่ปรึกษา.....
ลายมือชื่ออาจารย์ที่ปรึกษาร่วม.....

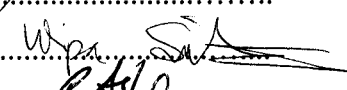
**JARUWAN SIRITAPETAWEE : COMPARISON OF FUNCTIONAL
AND STRUCTURAL PROPERTIES OF AN OUTER MEMBRANE
PORIN BETWEEN *Burkholderia pseudomallei* AND *Burkholderia
thailandensis***

THESIS ADVISOR : Wipa Suginta, Ph.D. 199 PP. ISBN 974-533-325-5

In this study, two outer membrane proteins, *BpsOmp38* and *BthOmp38* were isolated and purified from *B. pseudomallei* and *B. thailandensis*, respectively. The native conformation of Omp38 was found to be a trimer (M_r 110,000) consisting of three identical monomeric subunits (M_r 38,000). Based on peptide mass fingerprinting information, the gene encoding Omp38 was identified and isolated from genomic DNA of both bacteria. Nucleotide sequences of *BpsOmp38* and *BthOmp38* were 98% identical, and their predicted amino acid sequences were 99.7% identical. Omp38 proteins were over-expressed in *E. coli*, recovered from inclusion bodies, and refolded into functional trimeric Omp38 using a buffer system containing 10% (w/v) Zwittergent® 3-14. FTIR and CD spectroscopy revealed that the secondary structure of Omp38 contained predominantly β -sheet content. Liposome-swelling assays showed that Omp38 was a non-specific channel, which allowed sugars of <650 Da to permeate. Structural topology prediction suggested that Omp38 contained a 16-stranded β -barrel with 8 periplasmic turns and 8 extracellular loops. The expressed Omp38 was also subjected to protein crystallization trials using the sitting drop method. However, only small crystals of Omp38 were observed under tested conditions. To obtain Omp38 crystals with high quality for 3D-structure determination, different detergents for protein refolding and crystallization conditions will still need to be optimized in the future.

School of Biochemistry
Academic Year 2004,

Student's Signature.....

Advisor's Signature.....

Co-adviser's Signature.....

Acknowledgements

I would like to express my sincere thank to my thesis advisor, Dr. Wipa Suginta for providing guidance, support, considerable and kind help. I am deeply grateful to my co-advisor, Dr. Richard, H. Ashley, Department of Biomedical Sciences, University of Edinburgh, UK, who gave me the useful guidance, valuable advice and provided the bacterium, *Burkholderia thailandensis* type strain ATCC700388.

I would like to thank PD. Dr. Heino Prinz, Max Planck Institute for Molecular Physiology, Dortmund, Germany who helped with MALDI-TOF MS and ESI MS and peptide mass analysis, and Prof. Dieter Naumann, Robert-Koch Institute, Berlin, Germany with FTIR measurements. I also appreciate Miss Worada Samosornsuk, Faculty of Allied Health Science, Thammasat University, Thailand, for providing essential facilities for *Burkholderia pseudomallei* culture and drug susceptibility tests, and Dr. Chartchai Krittanai, Institute of Molecular Biology and Genetics, Mahidol University, Thailand, who kindly provided the CD spectropolarimeter for secondary structure determination.

I would like to thank Shell studentship grant and Suranaree University of Technology grant for financial support throughout the project.

Special thanks are extended to all friends, scientist and technician in the School of Biochemistry for their kind help and made me happy to work.

Finally, I would like to express my deepest gratitude to my parents and members of my family for their kind, understanding and encouragement. I also express my deepest gratitude to my dearest sister Asst. Prof. Mookhada Siritapetawee, for her kind help in preparing this thesis. Without her endless patience, this thesis will not be possible.

Jaruwan Siritapetawee

Contents

	Page
Abstract in Thai	I
Abstract in English	II
Acknowledgements	III
Contents	V
List of Tables	XII
List of Figures	XIII
List of Abbreviations	XVIII

Chapters

I Introduction	1
1.1 <i>Burkholderia pseudomallei</i>	1
1.2 <i>Burkholderia thailandensis</i>	9
1.3 Mechanisms of antimicrobial resistance	12
1.4 Biological membrane proteins	13
1.5 Outer membrane of Gram-negative bacteria and porins	15
1.6 Objectives	26
II Materials and Methods	28
2.1 Materials	28
2.1.1 Bacterial strains and plasmids	28
2.1.2 Chemicals	28

Contents (Continued)

	Page
2.1.3 PCR primers	29
2.2 Methodology	30
2.2.1 Preparation of peptidoglycan-associated proteins.....	30
2.2.2 Purification of native Omp38 protein.....	31
2.2.3 Determination of protein concentration.....	31
2.2.4 SDS-PAGE gel electroporesis.....	32
2.2.5 In-gel digestion and peptide mass analysis of Omp38 protein using MALDI-TOF Ms and ESI/MS	33
2.2.5.1 In-gel digestion.....	33
2.2.5.2 Peptide mass analysis and identification of Omp38 by MALDI-TOF MS and ESI/MS.....	34
2.2.6 Production of anti-Omp38 polyclonal antibodies and immunoblot analysis.....	35
2.2.7 Preparation of genomic DNA from <i>B. pseudomallei</i> and <i>B. thailandensis</i> (Miniprep protocol)	37
2.2.8 DNA analysis by agarose gel electrophoresis	38
2.2.9 Quantitation of DNA.....	39
2.2.10 Gene isolation, cloning and sequencing	39
2.2.10.1 Primers and PCR conditions.....	39
2.2.10.2 Ligation PCR product into the pGEM®T vector.....	40

Contents (Continued)

	Page
2.2.10.3 Transformation, selection and nucleotide sequence analysis.....	41
2.2.11 Purification of PCR products from an agarose gel.....	42
2.2.12 Analysis of DNA inserts by boiling miniprep.....	43
2.2.13 QIAGEN plasmid miniprep	44
2.2.14 DNA Sequencing and amino acid sequence analysis.....	45
2.2.15 Subcloning of <i>Omp38</i> inserts to an expression vector.....	45
2.2.15.1 Primer and PCR conditions.....	45
2.2.15.2 Insert and vector preparation for restriction enzyme digestion.....	46
2.2.15.3 Ligation of the <i>Omp38</i> fragments to an expression vector.....	47
2.2.15.4 Transformation of the recombinant plasmids into the expression <i>E. coli</i> host cells.....	47
2.2.15.5 Colony PCR.....	48
2.2.16 Expression of <i>BpsOmp38</i> and <i>BthOmp38</i> and preparation of inclusion bodies.....	48
2.2.17 Western blotting analysis.....	49
2.2.18 Purification and refolding of <i>Omp38</i> expressed in <i>E. coli</i> cells	50

Contents (Continued)

	Page
2.2.19 Protein identification and peptide mass analysis by MALDI-TOF MS and ESI/MS.....	51
2.2.20 Antibiotic susceptibility tests and functional study of Omp38	52
2.2.20.1 Antibiotic susceptibility tests.....	52
2.2.20.2 Proteoliposome-swelling assays.....	54
2.2.20.3 Effects of anti <i>Bps</i> Omp38 antibodies on permeability of Omp38.....	55
2.2.21 Secondary structure determination.....	55
2.2.21.1 Fourier Transform Infrared (FTIR) spectroscopy.....	55
2.2.21.2 Circular Dichroism (CD) spectroscopy	56
2.2.22 Molecular weight determination of Omp38.....	57
2.2.23 Membrane topology and 3D structural predictions	59
2.2.24 Preliminary crystallization studies of the expressed and refolding Omp38.....	60
III Results	62
3.1 Isolation and purification of outer membrane proteins from <i>B. pseudomallei</i> and <i>B. thailandensis</i>	62
3.2 Antibody production and Western blot analysis.....	68
3.3 Pore-forming activity of the native Omp38	71

Contents (Continued)

	Page
3.4 Secondary structure determination using Fourier Transform	
Infrared (FTIR) spectroscopy.....	77
3.5 Peptide mass analysis by MALDI-TOF MS and ESI/MS.....	78
3.6 Gene isolation, nucleotide and amino acid sequence analysis.....	81
3.6.1 Gene isolation and nucleotide sequencing.....	81
3.6.2 Amino acid sequence analysis.....	84
3.7 Subcloning of Omp38 DNA fragments into the pET23d(+)	
expression vector	88
3.8 Expression of Omp38 in <i>E. coli</i>	91
3.9 Mass analysis and refolding of the expressed Omp38	93
3.9.1 Mass analysis by MALDI-TOF mass spectrometry.....	93
3.9.2 Refolding of the expressed Omp38.....	95
3.10 Drug susceptibility test of <i>B. pseudomallei</i> and <i>B. thailandensis</i>	98
3.11 Pore-forming activity of the refolded Omp38.....	100
3.11.1 Penetration of neutral sugars through the refolded	
Omp38.....	99
3.11.2 Permeation of antibiotics through native and refolded	
Omp38 porins.....	106
3.11.3 Effects of anti- <i>Bps</i> Omp38 antibodies on pore-forming	
activity of the Omp38.....	109

Contents (Continued)

	Page
3.12 Secondary structure determination using Circular Dichroism (CD) spectroscopy.....	114
3.13 The M_r determination using Sephacryl S-200 HR filtration chromatography.....	118
3.14 Membrane topology and 3D structural prediction.....	120
3.15 Preliminary crystallization of the Omp38 porins.....	124
IV Discussion	129
4.1 Isolation and purification of the native Omp38 protein.....	129
4.2 Cloning and expression of <i>Omp38</i>	131
4.3 Refolding of the expressed Omp38	133
4.4 Biological activities of the native and refolded Omp38	136
4.5 Structural analysis.....	138
4.6 Topology and 3D structural model prediction.....	140
4.7 Preliminary crystallization.....	141
V Conclusion	144
References	148
Appendices	168
Appendix A 0.5 McFarland turbidity standard preparation.....	169

Contents (Continued)

	Page
Appendix B Stand curve of BSA by BCA Protein Assay.....	170
Appendix C Plasmid maps.....	171
Appendix D Competent cell preparation.....	175
Appendix E Solution preparation.....	177
Appendix F Crystal screening kit for membrane protein and scoring Sheet.....	186
Appendix G Typical observation in a crystallization experiment.....	188
Appendix H Journal publication.....	189
Curriculum Vitae	199

List of Tables

Table		Page
1.1	Outer membrane proteins of Gram-negative bacteria	18
2.1	A list of antibiotics used in agar disc diffusion method.....	53
2.2	Concentrations of standard proteins and blue dextran used for gel filtration chromatography.....	59
3.1	Purificationn of Omp38 from a 2-liter culture of <i>B. pseudomallei</i> and <i>B. thailandensis</i>	67
3.2	Susceptibility tests of bacteria to various antibiotics.....	99
3.3	Relative permeation rates of neutral sugars through native and refolded Omp38 proteins.....	105
3.4	A. Relative permeability rates of antibiotics through native and refolded <i>Bpsomp38</i> porins	107
3.4	B. Relative permeability rates of antibiotics through native and refolded <i>Bthomp38</i> porins	108

List of Figures

Figure	Page
1.1 Gram-negative staining of <i>Burkholderia pseudomallei</i>	1
1.2 <i>B. pseudomallei</i> culture grown on a selective medium.....	2
1.3 World map showing endemic areas of <i>B. pseudomallei</i>	5
1.4 Wrinkle colonies of <i>B. thailandensis</i> on MacConkey agar incubated at 37 °C for 48 h	9
1.5 Phylogenetic analysis of 16 bacterial species based on 16S rRNA gene sequences	11
1.6 Classes of membrane proteins.....	13
1.7 Diagram of the Gram-negative bacterial cell surface.....	16
1.8 Effect of loss outer membrane lipoprotein (Lpp) and OmpA on the cell envelope and shape of <i>E. coli</i>	19
1.9 View of the membrane exposed surface of maltoporin from <i>E. coli</i>	22
1.10 Three-dimensional representation of the structure of three different porins.....	23
1.11 A schematic representation of porin subunits.....	25
2.1 Crystallization setting by the sitting drop method.....	61
3.1 SDS-PAGE of peptidoglycan-associated proteins from <i>B. pseudomallei</i> ATCC23343.....	64

List of Figures (Continued)

Figure	Page
3.2 SDS-PAGE of peptidoglycan-associated proteins from <i>B. thailandensis</i> ATCC700388.....	65
3.3 SDS-PAGE of Omp38 purified from <i>B. pseudomallei</i> and <i>B. thailandensis</i> by Sephacryl S-200 HR filtration chromatography.....	66
3.4 Determination of the proper dilution of anti-BpsOmp38 polyclonal antibodies for Western blot analysis.....	69
3.5 Immunoblots of <i>BpsOmp38</i> , <i>BthOmp38</i> and <i>E. coli</i> BL21(DE3)pLysS porin	70
3.6 Liposome-swelling assays of <i>BpsOmp38</i>	72
3.7 Liposome-swelling assays of <i>BthOmp38</i>	73
3.8 Relative permeation rates of neutral sugars through liposomes reconstituted with the purified <i>BpsOmp38</i>	74
3.9 Relative permeation rates of neutral sugars through liposomes reconstituted with the purified <i>BthOmp38</i>	75
3.10 Relative permeability rates and size exclusion limit of <i>BpsOmp38</i> and <i>BthOmp38</i>	76
3.11 FTIR spectra of native <i>BpsOmp38</i> and <i>BthOmp38</i>	78
3.12 Determination of the M_r of native Omp38 using MALDI-TOF MS	80
3.13 Identification of the Omp38 gene in contig 836 of the incomplete <i>B. pseudomallei</i> genome	82

List of Figures (Continued)

Figure	Page
3.14 PCR amplification from genomic DNA of <i>B. pseudomallei</i> and <i>B. thailandensis</i>	83
3.15 The amino acid sequence alignment of Omp38.....	85
3.16 Identification of conserved domains and protein family of Omp38.....	86
3.17 <i>Bps</i> Omp38 and <i>Bth</i> Omp38 were aligned with other outer membrane porins.....	87
3.18 PCR amplification of <i>Omp38</i> DNA fragments lacking a signal peptide sequence.....	89
3.19 Subcloning of recombinant <i>Omp38</i> frgments into the pET23d(+) plasmid.....	90
3.20 Expression of Omp38 expressed in <i>E. coli</i> Origami(DE3).....	92
3.21 SDS-PAGE analysis of the expressed Omp38 after DEAE Fast Flow HiTrap™ column chromatography.....	93
3.22 The peptide fragments of the expressed Omp38 were identified by MALDI- TOF MS	94
3.23 SDS-PAGE analysis of refolded Omp38	82
3.24 SDS-PAGE of refolded and native Omp38	82
3.25 Liposome-swelling assays of refolded <i>Bps</i> Omp38	101
3.26 Liposome-swelling assays of refolded <i>Bth</i> Omp38.....	102
3.27 Relative permeation rates of sugar solutes through liposomes incorporated with refolded <i>Bps</i> Omp38	103

List of Figures (Continued)

Figure	Page
3.28	Relative permeation rates of sugar solutes through liposomes incorporated with refolded <i>Bth</i> Omp38 104
3.29	Effects of anti-Omp38 polyclonal antibodies on native <i>Bps</i> Omp38 channel activity 110
3.30	Effects of anti-Omp38 polyclonal antibodies on native <i>Bth</i> Omp38 channel activity.....111
3.31	Effects of anti-Omp38 polyclonal antibodies on refolded <i>Bps</i> Omp38 channel activity..... 112
3.32	Effects of anti-Omp38 polyclonal antibodies on refolded <i>Bth</i> Omp38 channel activity..... 112
3.33	CD spectra of native Omp38..... 115
3.34	CD spectra of native, refolded and unfolded <i>Bps</i> Omp38 116
3.35	CD spectra of native, refolded and unfolded <i>Bth</i> Omp38 117
3.36	Superimposition of the CD spectra of Omp38 obtained from a Jasco J-715 spectropolarimeter 118
3.37	Determination of M_r of Omp38.....119
3.38	Predicted transmembrane topology of <i>Bps</i> Omp38 and <i>Bth</i> Omp38 121
3.39	Predicted 3D structure of <i>Bps</i> Omp38 and <i>Bth</i> Omp38 using Swiss-Model..... 122
3.40	The predicted structured of trimeric Omp38 as displayed by Cn3D version 4.1 from RPS-BLAST 123

List of Figures (Continued)

Figure		Page
3.41	Preliminary crystallization of <i>BpsOmp38</i>	125
3.42	Preliminary crystallization of <i>BthOmp38</i>	126
3.43	The salt crystals obtained in preliminary crystallization experiments.....	127
3.44	SDS-PAGE of <i>BpsOmp38</i> and <i>BthOmp38</i> crystals.....	128

List of Abbreviations

A	Absorbance
bp	Base pairs
BSA	Bovine Serum Albumin
°C	Degree celsius
CD	Circular dichroism
cDNA	Complementary deoxynucleic acid
CSA	Nonhygroscopic ammonium (+)-10-comphorsulfonate
dmole	deci Mole
DNA	Deoxyribonucleic acid
DNTP mix	dATP, dCTP, dGTP and dTTP
DTT	Dithiotreitol
EDTA	Ethylene diamine tetraacetic acid
FTIR	Fourier Transform Infrared
g	Gravitational acceleration
(m, μ , n) g	(milli, micro, nano) Gram
h	Hour
IPTG	Isopropyl- β -D-thiogalactopyranoside
kDa	Kilo Dalton
LPS	Lipopolysaccharide
min	Minute

List of Abbreviations (Continued)

(m, μ) M	(milli, micro) Molar
(m, μ) L	(milli, micro) Liter
MRE	Mean residue ellipticity
mRNA	Messenger ribonucleic acid
M_r	Relative molecular mass
OD	Optical density
Omp	Outer membrane protein
PAGE	Polyacrylamide gel electrophoresis
PBS	Phosphate buffer saline
PCR	Polymerase chain reaction
pI	Isoelectric point
RNA	Ribonucleic acid
RNase	Ribonuclease
SDS	Sodium dodecyl sulfate
s	Second
TEMED	Tetramethylenediamine
Tris	Tris-(hydroxymethyl)-aminoethane
UV	Ultraviolet
v/v	Volume/volume
w/v	Weight/volume

Chapter I

Introduction

1.1 *Burkholderia pseudomallei*

General description

Burkholderia pseudomallei (formerly *Pseudomonas pseudomallei*) is a member of subdivision β -proteobacteria (Prescott *et al.*, 1999). *B. pseudomallei* is motile non-spore forming bacillus 0.4 – 0.6 μ m in width and 2 – 5 μ m in length. It is Gram-negative and has a characteristic bipolar staining and can be seen as either single colonies, in pairs, or sometimes in chains (Figure 1.1).

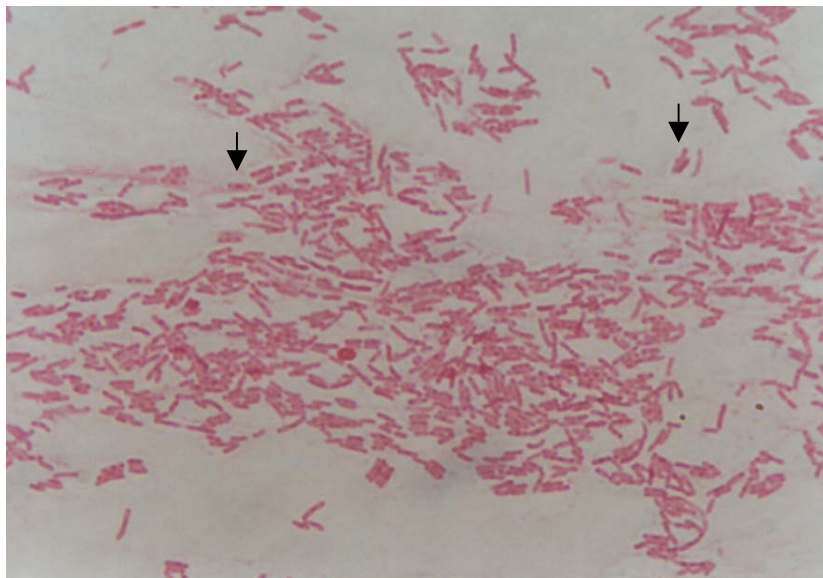


Figure 1.1 Gram-negative staining of *Burkholderia pseudomallei*.

Arrows show areas of the bacterial capsules, which cannot be stained with Gram's stain.

The organism grows aerobically in many simple media but will only grow under strictly anaerobic conditions in a complex medium containing nitrate. Based on the range of organic compounds, which the bacterium utilizes as carbon sources and for producing energy, this organism is classified in Genus *Burkholderia*. The colonies grown on solid media are highly variable. Shapes of bacterial colonies may range from rough to mucoid and colors may range from cream to bright orange (Figure 1.2). However, these phenotypic appearances do not seem to be associated with its virulence (Ellis and Titball, 1999).

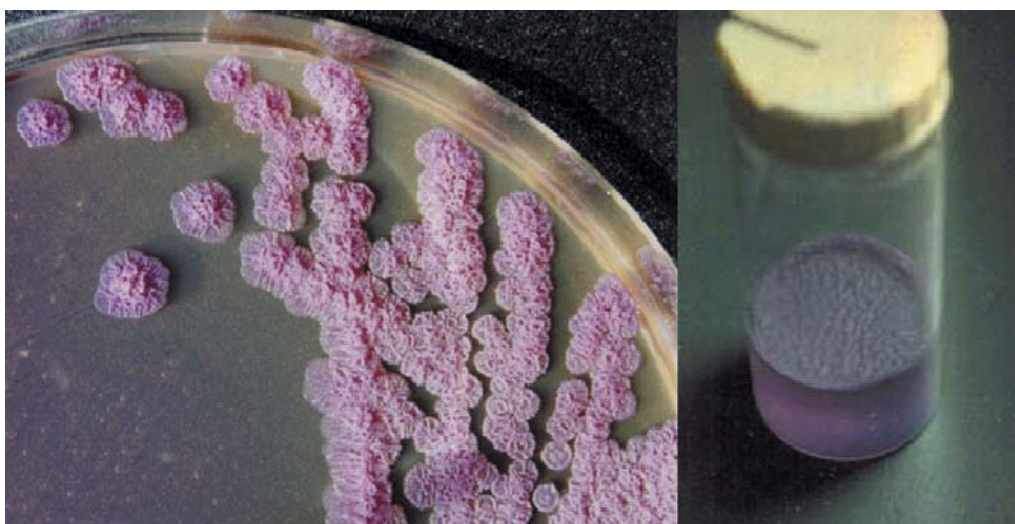


Figure 1.2 *B. pseudomallei* culture grown on a selective medium.

Left: *B. pseudomallei* grown on Ashdown's selective medium. Right: the organism forming a surface pellicle in Ashdown's selective broth. (White, 2003)

It has been suggested that the bacterium virulence may be dependent on the presence of the capsular antigen (Ellis and Titball, 1999). The bacterium seems to form a capsule-like structure comprising an abundant slime layer of polysaccharides called

glycocalyx. In vivo study has demonstrated that this capsule helps the bacterial cells to survive, divide and protect themselves from unsuitable environments (Ellis and Titball, 1999).

Recently, the *B. pseudomallei* genome has been analyzed, although incompletely, by pulsed field gel electrophoresis. Nucleotide sequences of *B. pseudomallei* genes have been determined by several investigators (Songsivilai and Dharakul, 2000) and deposited in a public genome database (<http://www.sanger.ac.uk/>). The resulting information shows that the *B. pseudomallei* genome consists of two large replicons. Both contain ribosome RNA sequences, which indicate the presence of two chromosomes. *B. pseudomallei* isolate K96243 has two chromosomes of approximately 3,563 +/- 73 and 2,974 +/- 40 kilobase-pairs in size, giving a predicted total genome size of about 6.5 million base-pairs (Songsivilai and Dharakul, 2000). Analysis of the publicly available nucleotide sequences has revealed that the average *B. pseudomallei* gene contains about 1,031 base-pairs, with an average G + C content of 65.7%. The genome is gene-rich in that 89% of the nucleotide sequence has been predicted as coding sequences. The entire *B. pseudomallei* genome contains about 5,600 genes (Songsivilai and Dharakul, 2000). The last update report has suggested that the total nucleotide sequence of *B. pseudomallei* is 7,247,547 bp in size (<http://www.ncbi.nlm.nih.gov/>).

Disease and pathogenesis

B. pseudomallei is a free-living organism that causes melioidosis, a potentially fatal disease in humans and animals including dolphins, sheeps, pigs and goats (Vendros *et al.*, 1988; Dance, 1991; Currie *et al.*, 1994). In human, the incubation

period generally takes about 2-3 days. However, it has been reported that the disease can be developed 6-26 years after exposure (Arakawa, 1990).

The clinical spectrum of melioidosis consists of four major forms including acute fulminant septicemia, sub-acute illness, chronic infection and subclinical disease. The disease may be localized or disseminated and affected many organs, depending on whether it is acute or chronic. Melioidosis can mimic other bacterial infections including typhoid, malaria, tuberculosis and septicemia from other common organisms (Ip *et al.*, 1995; Everett and Nelson, 1975). Each clinical case may represent the outcome of primary infection, reinfection, or reactivation of latent disease. Primary infection is most often found in children in northeast Thailand where two thirds of paddy fields yield the organism. Approx. 80% of northeastern Thai children have antibodies by the time they are 4 years old (Dance, 2000).

Definitive diagnosis requires culturing the organism from body fluids or blood. Severe urticaria has been reported with pulmonary melioidosis. Flushing and cyanosis may develop during septicemia. Inhalational melioidosis could lead to any of the skin manifestations, but only after metastatic abscesses to the skin are formed. In this case, the disease would likely to be associated with lymphangitis, cellulitis or regional lymphadenitis. Draining sinuses from lymph nodes or even bone may be present. Abscesses may ulcerate, and rarely ecthyma, gangrenosum-like lesions may form (Jawetz *et al.*, 1995). In most cases, adult melioidosis results from re-infection or re-activation of latent infections (Suputtamongkol *et al.*, 1994).

Transmission

In endemic areas (Figure 1.3), *B. pseudomallei* infection usually occurs as a consequence of soil and water contamination of skin abrasions.



Figure 1.3 World map showing endemic areas of *B. pseudomallei*.

B. pseudomallei is found in soil and aquatic environment in endemic areas represented in gray regions. The dark areas are severe infection (Ellis and Titball., 1999).

Arthropod-borne infection does not occur naturally but experimentally the disease can be transmitted by rat flea (*Xenopsylla cheopsis*) and mosquito (*Aedes aegypti*) (Prevatt and Hunt, 1957; Schlech *et al.*, 1981).

Human to human transmission has only been reported in one case. This case involved a patient's wife, who had raised haemagglutination titres to *B. pseudomallei* that indicated recent infection. People who have not been contacted with a source of *B. pseudomallei*, e.g. soil or endemic area, can be infected by sexual transmission (McCormick *et al.*, 1975). Ingestion, nasal instillation and inhalation are other possible routes of infection (Howe *et al.*, 1971).

Diagnosis and assessment

In northeast Thailand, *B. pseudomallei* is the most common cause of septicemic illness in adult diabetics during the rainy season (Dhiansiri *et al.*, 1988). Evidence of abscess formation is often noted either in the lungs on chest radiograph, or in the liver and spleen on ultrasound examination. Abdominal ultrasound is usually undertaken in all suspected cases, while radiolabelled white-cell scanning subsequently helps to indicate clinically hidden sites of infection (Ramsay *et al.*, 2001). Moreover, 95% of spleen abscesses are caused by *B. pseudomallei* (Walsh and Wuthiekanun, 1996). About 13% of septicemia patients can be detected to have subcutaneous abscesses with *B. pseudomallei*. Although evidence of the underlying predisposing condition, hyperglycemia or renal impairment is often recorded, *B. pseudomallei* is readily cultured from infected sites or blood .

Rapid diagnosis is important since antibiotic treatments of melioidosis, such as penicillin and gentamicin, are ineffective (Walsh *et al.*, 1996; Dance *et al.*, 1996). Typically, culture is normally grown on a routine blood agar and Ashdown's selective medium (Walsh *et al.*, 1996; Dance *et al.*, 1996). Swabs from open contaminated sites are also placed in a selective pre-incubation broth (Figure 1.2). Colonies are

usually seen in 24 h and an incubation time taken to obtain a positive blood culture normally takes 48 h. However, the incubation time can be shortened by performing a direct plate culture of the buffy-coat, or by lysis centrifugation (Tiangpitayakorn *et al.*, 1997; Simpson *et al.*, 1999).

Serological tests were widely used in the past. The disadvantage of serological tests is they are not specific for melioidosis diagnosis (Ashdown *et al.*, 1989). However, serological tests can help to diagnose melioidosis in areas where prevalence is low (Ashdown *et al.*, 1989), but they are of little use in endemic areas where most of the population is seropositive (White, 2003). Currently, latex agglutination tests based on polyclonal or specific monoclonal antibodies to *B. pseudomallei* lipopolysaccharide or exopolysaccharide can be used to identify melioidosis (Smith *et al.*, 1993; Steinmetz *et al.*, 1999). Direct immunofluorescence microscopy of infected sputum, urine, or pus is 98% specific and 70% sensitive compared with culture (Walsh *et al.*, 1994).

Treatment

Both lipopolysaccharide and flagellin proteins produced from *B. pseudomallei* have been suggested as possible protective immunogens (Brett *et al.*, 1994; Byran *et al.*, 1994). It has been reported that a cellular vaccine has been successfully used with captive marine mammals to protect against *B. pseudomallei* infection. The vaccine induces high levels of specific antibodies and significantly reduces mortality of such animals (Vendrous *et al.*, 1988). At present, there is no effective vaccine available against human melioidosis (Dannenberg and Scott, 1958;

Levine and Maurer, 1958), and the prospects for vaccine development seem poor, since repeated natural immunization does not prevent infection (White, 2003).

In Thailand, the conventional treatment of *B. pseudomallei* infection uses a combination of antibiotics including chloramphenicol, doxycycline and cotrimoxazole. Fluoroquinolone antibiotics were found to be inappropriate for the treatment of melioidosis. Currently, ceftazidime is widely used as a single drug treatment in septicemia patients because it is safe, well tolerated and also highly active against *B. pseudomallei in vitro* and its use in the treatment of melioidosis has been reported to reduce the mortality rate of severe cases to 50% (Ellis and Titball, 1999).

From 1986 to 1991, 602 patients with melioidosis were admitted in Sappasitprasong Hospital, Ubon Ratchatani, Thailand with a mortality rate in-hospital of 42%. Patients with severe symptoms showed multiple foci of infection or septicemia relapsed 4.7 times more frequently than patients with localized melioidosis. Relapses were 3.3 times more frequent following short-course (≤ 8 weeks) oral coamoxiclav than after the oral combination of chloramphenicol, doxycycline, and cotrimoxazole. However, the optimum choice and duration of antibiotic treatments to prevent relapses still remain to be determined (Chawagul *et al.*, 1993; Warawa and Woods, 2002).

1.2 *Burkholderia thailandensis*

Burkholderia thailandensis is a nonpathogenic soil organism originally isolated in Thailand (Brett *et al.*, 1997). The bacterial colonies grown on culture agar plate (Figure 1.4) and Gram's stain are similar to those of *B. pseudomallei*.



Figure 1.4 Wrinkle colonies of *B. thailandensis* on MacConkey agar incubated at 37 °C for 48 h.

Based on biochemical, immunological, and genetic data, *B. pseudomallei* and *B. thailandensis* are closely related species. The main characteristic for separation of the two species is the difference in their ability to utilize L-arabinose (Smith *et al.*, 1997). Almost clinical isolates of *B. pseudomallei* are unable to utilize L-arabinose as a single substrate (Ara^-), while *B. thailandensis* can utilize arabinose (Ara^+) (Dharakul *et al.*, 1999). In addition, the most distinct difference between these two species is

their relative virulence. The 50% lethal dose (LD₅₀) for *B. pseudomallei* in the Syrian hamster model of acute melioidosis is <10 organisms, whereas the LD₅₀ for *B. thailandensis* is about 10⁶ organisms (Reckseidler *et al.*, 2001). It has also been shown that the two species can be differentiated based on their tendency to cause disease in humans. In northeastern Thailand, 75% of soil isolates are *Ara*⁻ biotypes, while the other 25% are *Ara*⁺ biotypes, but there are no reports documenting mixed population of *B. pseudomallei* and *B. thailandensis* in epidemiological surveys. This may reflect the inability of current assays for appropriate identification of the mixed population (Sonthayanon *et al.*, 2002). Differences in a number of traits between the two organisms have led to classification of the two bacteria into two different species (Brett *et al.*, 1998).

Recently, a PCR-based method has been developed for differentiating these two species by using specific primers flanking a 15 bp deletion in the flagellin gene of the non-pathogenic *B. thailandensis*, which generate amplified products of 191 bp and 176 bp for *B. pseudomallei* and *B. thailandensis*, respectively. The PCR products have been proved to be a useful marker for epidemiological identification of the pathogenic *B. pseudomallei* species (Sonthayanon *et al.*, 2002).

A comparison of nucleotide sequences of *Burkholderia* and other related bacteria has shown that the 16S ribosomal RNA (rRNA) gene is highly conserved among the bacteria species (Figure 1.5). Only especially 15 nucleotide dissimilarities were observed within 1488 bp of the 16S rRNA from *B. pseudomallei* and *B. thailandensis* (Brett *et al.*, 1998). The 16S rRNA has now been used as a new identification of the bacteria. Based on this standard, phylogenetic trees of nucleotide

differences between *Burkholderia* species were constructed and some bacteria have been re-classified into new species (Olsen and Woese, 1993).

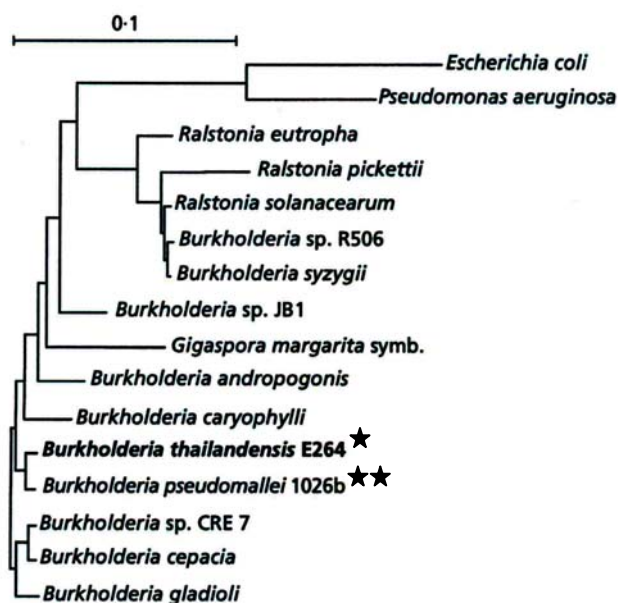


Figure 1.5 Phylogenetic analysis of 16 bacterial species based on 16S rRNA gene sequences (Brett *et al.*, 1998).

Despite the success in using 16S rRNA gene sequences for identifying most bacterial species, there are “blind spots” within some major genus, in which the 16S rRNA sequences seem to not be discriminative enough for the identification of certain species. In such circumstances, sequences of essential genes other than 16S rRNA, such as *groEL*, have been shown to be useful for the identification of the indiscriminate species (Goh *et al.*, 1996; Ringuet *et al.*, 1999). For instance, the nucleotide sequence of the *groEL* gene of *B. thailandensis* shows >99.8 % identity

with that of any of the other strains of *B. thailandensis*, but <97.6% identity with any of the strains of *B. pseudomallei* (Woo *et al.*, 2002).

1.3 Mechanisms of antimicrobial resistance

Microorganisms generally utilize various mechanisms to resist cytotoxic drugs. For example, they eliminate the drug target in the cell through the alteration or replacement of molecules that are normally bound by antibiotics (Spratt, 1994). Moreover, microorganisms may reduce the intracellular concentration of drugs by: (i) synthesizing enzymes that degrade antibiotic and inactivate the drugs, (ii) eliminating channels for transporting hydrophilic drugs, such as outer membrane porins in Gram-negative bacteria, and (iii) producing drug efflux systems that export lipophilic drugs before these compounds can find their cellular targets (Hendrik *et al.*, 1998).

Successful treatment of patients with melioidosis has proved to be difficult, due to the lack of effective and specific antibiotics. Moreover, *B. pseudomallei* is inherently resistant to a variety of antibiotics including β -lactams, aminoglycosides, marcolides, and polymyxins (Moore *et al.*, 1999). It has been suggested that the antibiotic resistance may be associated with low permeability of antibiotics through porin channels located at the outer membrane of the bacterium (Bianco *et al.*, 1997).

1.4 Biological membrane proteins

Membrane proteins are divided into five classes (Evans and Graham, 1991) as shown in Figure 1.6.

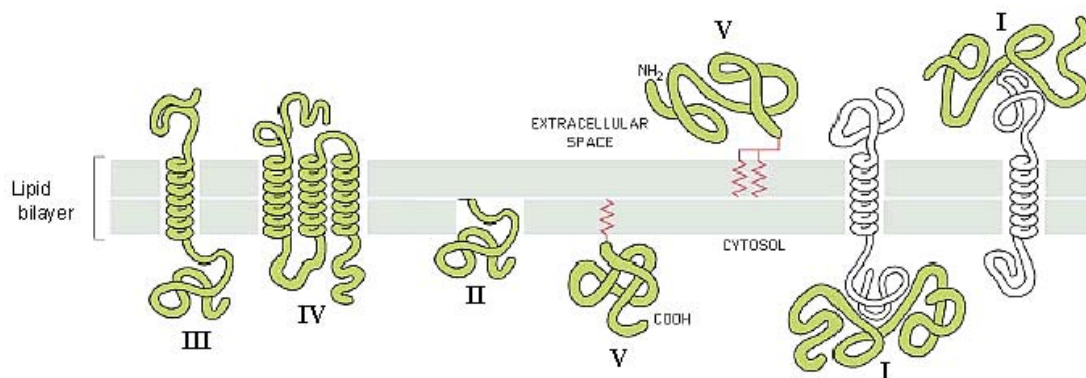


Figure 1.6 Classes of membrane proteins.

I, peripheral proteins; II, proteins partially inserted into lipid bilayer; III, integral proteins with one transmembrane domain; IV, integral proteins with multiple transmembrane domains; V, lipid-anchored peripheral proteins (Evans and Graham, 1991).

Class I Peripheral or extrinsic proteins, such as the F1 subunit of the ATP-synthase and cytochrome *c*. Peripheral proteins are bound mainly by ionic force to polar head groups of phospholipids or to other proteins. Class I proteins can be removed by increasing ionic strength of bacterial medium. Extracellular matrix and cytoskeletal components associated with the external and cytoplasmic membrane faces may exhibit like class I proteins or they may bind to class I proteins.

Class II Proteins are anchored into a part of lipid bilayer by a hydrophobic peptide (Evans and Graham, 1991). However, some toxins, which interfere membrane functions (e.g. mellitin, the bee venom toxin), maybe inserted partially into the extracellular face of the membrane. Subunits of the nucleotide-binding G-protein family also belong to this class.

Classes III and IV Integral or transmembrane proteins. The proteins contain polar amino acid sequences located at the external and cytoplasmic lesion of the membrane. These amino acids usually interact with phospholipid head groups and the extracellular and intracellular environments. They are connected by a single (Class III) or several (Class IV) hydrophobic peptide domains of 20-30 amino acids that span across lipid bilayers. The erythrocyte membrane protein, glycophorin, is an example of a Class III protein. Moreover, many receptors are also members of this class. Some Class IV proteins function as transmembrane channels and ion pumps. Transmembrane proteins have a defined orientation in the membrane and display a functional asymmetry. For example, the K^+ and ouabain-binding sites of the Na^+/K^+ -ATPase are located on the extracellular surface, while the Na^+ -binding and

ATP-hydrolysing sites are located on the cytoplasmic surface. These proteins can only be solubilized by extraction with 8 M urea or 6 M guanidinium chloride or detergents, e.g. SDS.

Class V A peripheral protein domain, which is anchored to the lipid bilayers by covalently attached to glycolipids. Plasma membrane receptors of protozoa and mammalian cells are members of this class. Proteins anchored by a fatty acid via a thio-ester bond are also included in this class. For example, palmitic acid is attached to a cysteine residue, as found in the transferrin receptor and the *ras* oncogene product. Myristic acid is attached to the amino terminus of the *sarc* oncogene product and the α subunit of the nucleotide-binding G-protein.

1.5 Outer membrane of Gram-negative bacteria and porins

The outer membrane of Gram-negative bacteria is peripheral to the periplasmic and peptidoglycan regions (Figure 1.7).

The outer membrane of bacterial cells is covalently attached to the peptidoglycan layer through lipoprotein and helps to preserve shape of the cells. It also provides a protective barrier against the external environment. Under electron microscope, outer and inner membranes are presented as trilaminar (double-track) layers. Chemical analysis shows that the inner and outer membranes are similar in lipid content. Some components of the outer membrane are similar to those of cytoplasmic membrane. But, the outer membrane has an asymmetric bilayer characteristic with the external layer being composed primarily of lipopolysaccharide (LPS) and the inner layer containing phospholipids.

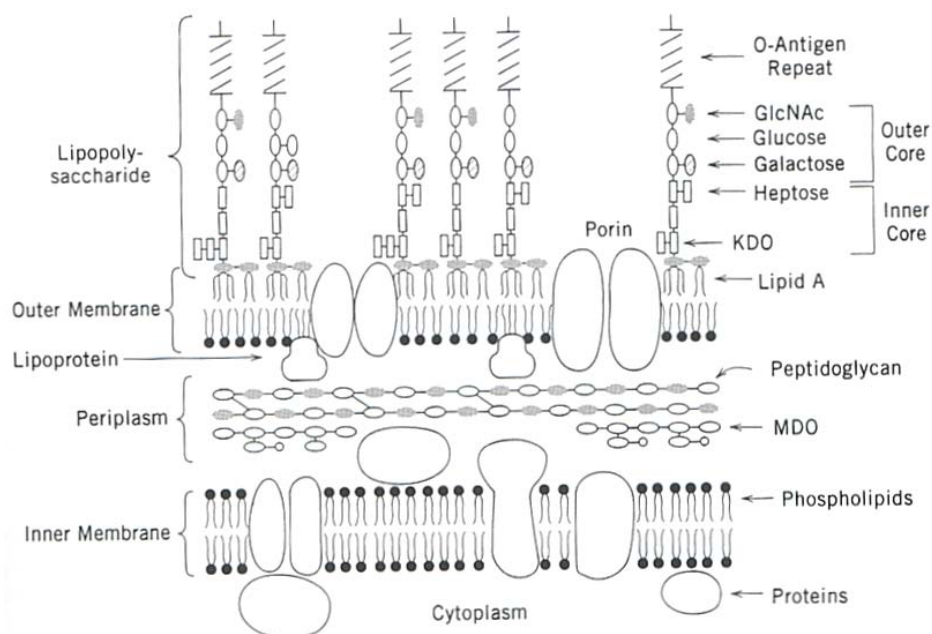


Figure 1.7 Diagram of Gram-negative bacterial cell surface.

Ovals and rectangles represent sugar residues, circles depict the polar head groups of glycerophospholipids (phosphatidylethanolamine and phosphatidylglycerol). MDO is membrane-derived oligosaccharides. The core region of lipopolysaccharide (LPS) is that of *E. coli* K-12, a strain that does not normally contain an O-antigen repeat unless transformed with an appropriate plasmid (Raetz, 1993).

A variety of other outer membrane proteins (Omps) is found in the *Enterobacteriaceae* and other Gram-negative bacteria. As shown in Table 1.1, these Omps play a variety of overlapping roles in physiology of a cell. Some of these proteins facilitate specific metabolites to entry, such as vitamin B₁₂, iron, or maltose. While others, such as OmpC and OmpF, are general porins that allow hydrophilic solutes of less than 600 Da to pass through (Moat and Foster, 1995).

Murein lipoprotein is a major Omp present in a large amount in *E. coli*. Lipoprotein molecules anchor the outer membrane to the peptidoglycan layer. Mutants lacking *lpp*, the structural gene for lipoprotein, and *OmpA*, the structural gene for OmpA, display spherical morphology (Figure 1.8) and the murein layer of these mutants is no longer associated with the outer membrane. These mutants also display an increased growth requirement for Mg²⁺ and Ca²⁺ and are sensitive to hydrophobic antibiotics, such as novobiocin, or to detergents, suggesting a protective function of the outer membrane.

Table 1.1 Outer membrane proteins of Gram-negative bacteria (Moat and Foster, 1995).

Protein	Functions
OmpA	- Stabilization of outer membrane and mating aggregates in F- dependent conjugation. - Receptor for phage TuII.
Murein lipoprotein (Braun's lipoprotein)	- Most abundant surface protein in <i>E. coli</i> and <i>S. typhimurium</i> . - Major structural protein, in conjunction with OmpA, stabilizes cell surface.
OmpB (porin)	- Diffusion channel for various metabolites including maltose.
LamB (maltoporin)	- Specific porin for maltose and maltodextrin. - Receptor for bacteriophage λ .
OmpC (porin)	- Diffusion channel for small molecules. - Receptor for bacteriophages TuIb and T4.
OmpF (porin)	- Diffusion channel for small molecules. - Receptor for phage Tula and T2.
OmpT	- Protease
PhoE (protein E)	- Anion-selective diffusion channels induced under phosphate limitation.
Protein P	- Anion-selective diffusion channel in <i>Pseudomonas aeruginosa</i> ; induced under phosphate limitation.
TolA	- Maintenance of OM integrity. - Activity of group A colicins.
TonA	- Ferrichrome siderophore uptake. - Receptor for phages T1, T5 and 80 colicin M.
TonB	- Siderophore-mediated iron transport - B ₁₂ transport.
Tsx	- Nucleoside-specific channel. - Receptor for T-even phages and colicin K.

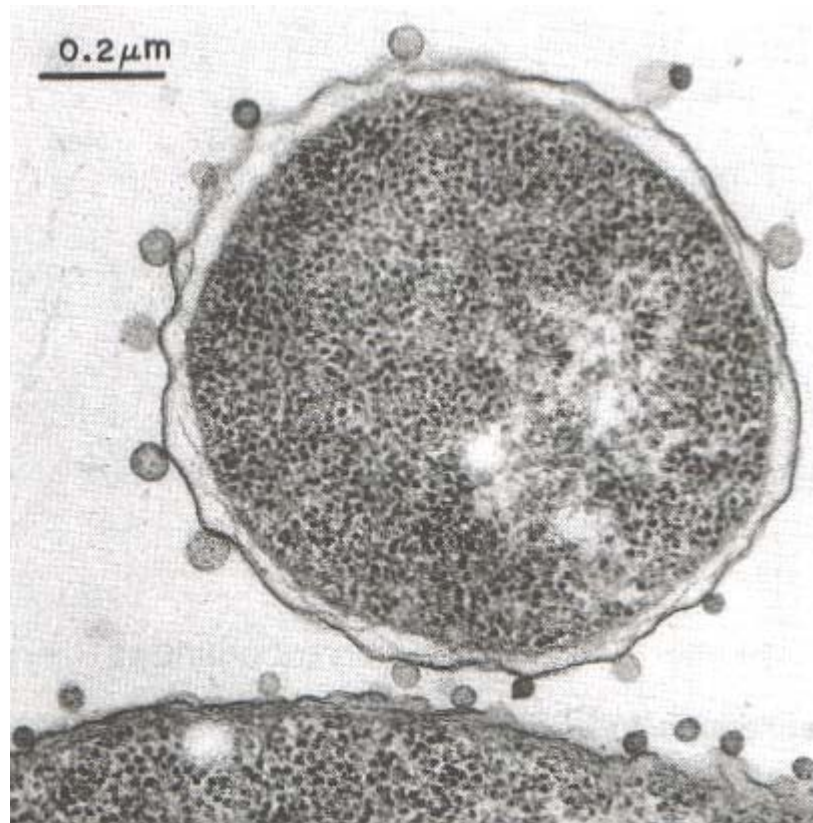


Figure 1.8 Effects of loss of outer membrane lipoprotein (Lpp) and OmpA on the cell envelope and shape of *E. coli* (Moat and Foster, 1995).

Porins are an unusual class of membrane proteins because they form hollow β -barrel structures with a hydrophobic outer surface. The barrel structure is located in the bacterial outer membrane and forms a transmembrane pore with a diameter of 1-2 nm that allows the passive diffusion of solutes across the outer membrane (Moat and Foster, 1995). There are also porin-like proteins found in mitochondria and chloroplasts (Schirmer, 1998). Since porins have different selective properties for the molecules that can pass through, porins have been classified into two classes.

(A) Nonspecific or general porins that show a linear relation between permeation rate and solute concentration gradient and (B) specific porins, which exhibit Michaelis-Menten kinetics for the transport of specific solutes (Nikaido, 1992).

(A) Nonspecific porins

Nonspecific porins allow the passage of hydrophilic solutes up to an exclusion size of approximately 600 Da. The pore properties of the nonspecific porins, e.g. OmpF from *E. coli* (Cowan *et al.*, 1992) and a porin from *Rhodobacter capsulatus* (Weiss and Schulz, 1992) were characterized by measurements of single ion conductance in artificial lipid planar membranes. Current measurements give a rough estimate of the channel size and provide additional insights into electrostatic properties of the pore upon determination of the ratio of cation over anion permeability ($P_{\text{cation}}/P_{\text{anion}}$), i.e. the ion selectivity. The anion selectivity of phosphoporin (PhoE), which is dependent upon phosphate starvation, has been linked to physiological function of the channel in facilitating the import of phosphorylated compounds (Korteland *et al.*, 1982).

Nonspecific porins allow the passage not only of ions, but also of small hydrophilic solutes. The strong transversal electric field at the pore constriction (Weiss *et al.*, 1991) has been implicated with nonspecific binding of dipolar molecules (Karshikoff *et al.*, 1994). Permeation of uncharged solutes can be measured by liposome swelling assays (Saint *et al.*, 1996).

(B) Specific porins

Maltoporin (LamB) was first identified as a specific porin and acted as the receptor for λ -phage in *E. coli* (Randall-Hazelbauer and Schwartz, 1973). This porin

allows the passive diffusion of maltodextrin (α 1-4 linked polyglucose) across the outer membrane. The size exclusion limit of this porin is only about half of the value determined for general porins. The presence of a maltodextrin binding site within the channel has been observed from ion flow inhibition studies (Benz *et al.*, 1987). The block of ion flow also made it possible to probe the kinetics of sugar translocation by analysis of the sugar-induced current noise (Andersen *et al.*, 1995; Jordy *et al.*, 1996). In maltoporin, there are 18 antiparallel β -strands (Figure 1.9) and three internal loops, which constrict the channel to a minimal diameter of only 5 Å. This indicated that maltoporin is a small size channel that allows the specific solute to pass through. When sucrose was diffused into maltoporin crystals, it also revealed ordered binding of sugar hydroxyl groups form a multitude of H-bond with charged protein side chains (Wang *et al.*, 1997). Due to its bulkiness, however, the saccharide is stuck above the channel constriction explaining the low permeability rate (Luckey and Nikaido, 1980). On the other hand, a sucrose specific porin (SrcY) (Schülein *et al.*, 1991) exhibits high sequence homology to maltoporin with a few residues exchanged (Wang *et al.*, 1997).

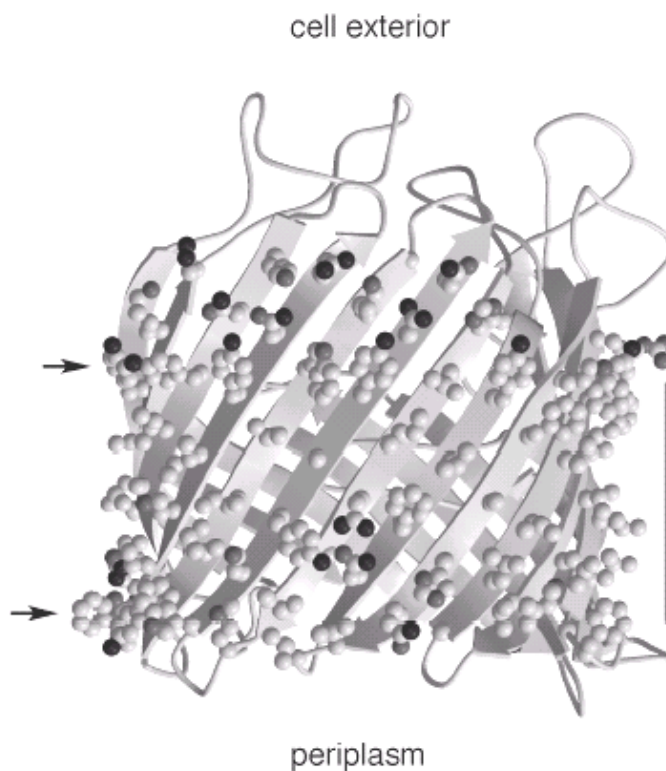


Figure 1.9 View of the membrane exposed surface of maltoporin from *E. coli* (Schirmer *et al.*, 1995).

All external side chains of the β -strands are represented in ball and stick form. Carbon atoms are light gray, nitrogen atoms in medium gray, and oxygen atoms in black. The arrows point to the “aromatic belts” that encircle the trimer at the boundary between hydrophobic and hydrophilic surfaces. The vertical bar (length about 25 Å) indicates the part of the surface that consists of small to medium sized aliphatic side-chains.

Several bacterial porins have been studied and classified into different membrane proteins. Figure 1.10 represents the 3D-structure topology of three different *E. coli* porins, OmpF and PhoE/F and *Pseudomonas aeruginosa* OmpP, all of which are located at the outer membrane of the cell.

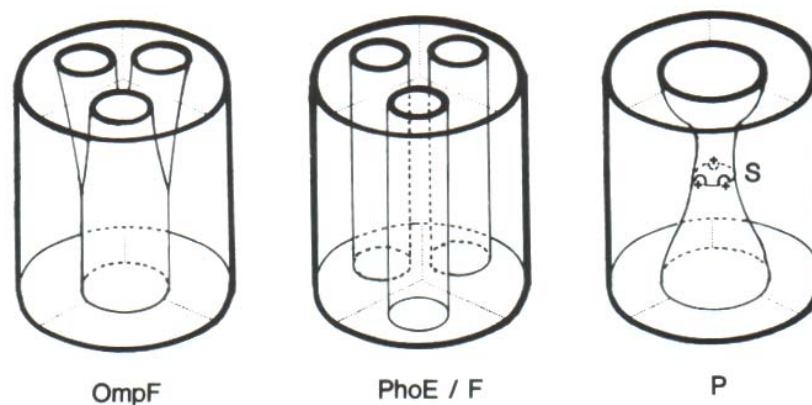


Figure 1.10 Three-dimensional representation of the structure of three different porins.

The proteins are oriented in such a way that the top is the portion exposed to the external environment, whereas the bottom is the portion extending into the periplasmic space. The channels traverse the width of the outer membrane. (Hancock, 1987).

Electron microscopy and image reconstruction techniques were used to explain the structures of three porins shown in Figure 1.10. The result shows that OmpF has three channels on the outer surface converged into a single channel at the periplasmic face (Engel *et al.*, 1985), while the PhoE porin of *E. coli* forms three separate channels that traverse the width of the membrane (Dargent *et al.*, 1986).

On the other hand, OmpP of *Pseudomonas aeruginosa* forms a single, small, highly anion-selective channel, with its permeability related to the presence of a selectivity filter containing three charged lysine residues (+) (Hancock and Benz, 1986).

The 3D structures of *E. coli* OmpF (Cowan *et al.*, 1995), *Klebsiella pneumoniae* OmpK36 (Dutzler *et al.*, 1999) and *Comamonas acidovorans* Omp32 (Zeth *et al.*, 2000) have been determined at high resolution by X-ray crystallography (~ 2-3 Å). A number of porins with related X-ray structures have been studied (Weiss *et al.*, 1991; Cowan *et al.*, 1992; Kreuzsch and Schulz, 1994; Schirmer *et al.*, 1995; Hirsch *et al.*, 1997; Meyer *et al.*, 1997). In most cases, packing of porin trimers in the crystals is mediated by the hydrophilic portions of their surface, leaving the hydrophobic surface fully covered in detergent. Direct apolar protein-protein contacts are found in the trigonal form of OmpF (Cowan *et al.*, 1992).

The typical feature of a porin subunit is shown in Figure 1.11 A. The entire polypeptide contains about 300 to 420 amino acids, which fold into a 16- or 18-stranded antiparallel β -barrel. Porins are usually stabilized by forming the barrels into trimeric molecules (Figure 1.11 B). The trimer is generally dissociated when heated at 95 °C. X-ray crystallography (Weiss and Schulz, 1992; Cowan *et al.*, 1992; PDB entry 2OmpF) and neutron crystallography (Pebay-Peyroula *et al.*, 1995) have demonstrated that a hydrophobic bond encircles the trimer and is in contact with aliphatic detergent tails after solubilization. In vivo, the hydrophobic part is inserted into the core of the outer membrane. In all porins with known 3D structure, the transmembrane pore is constricted by an internal loop or eyelet (Figure 1.11) that folds inwardly and is attached to the inner side of the barrel wall. In maltoporin, the β -strands are connected on the periplasmic side by short loops or turns and on the

extracellular side by long irregular loops. These loops show high sequence variation among homologous porins. The structural variability may have a role of avoiding the cell surface to expose to parts of the molecule when they want to escape from cellular recognitions e.g., antibodies, phages, or proteases (Schirmer, 1998).

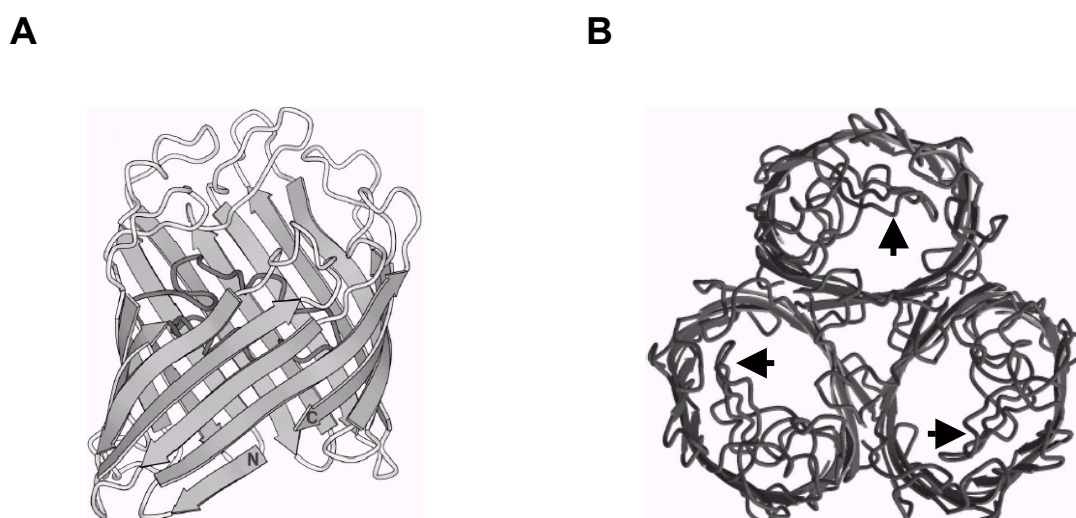


Figure 1.11 A schematic representation of porin subunits.

(A) General fold of a porin monomer, OmpF from *E. coli* (Cowan *et al.*, 1992). The large β -barrel structure is formed by an arrangement of 16 antiparallel β -strands. The strands are connected by short loops or regular turns on the periplasmic edge (bottom), whereas long irregular loops face the cell exterior (top). The internal loop, which connects β -strands 5 and 6 and extends inside the barrel, is darkened. The chain-termini are marked (N and C terminal). The surface closest to the viewer is involved in subunit contacts. (B) Schematic represents the OmpF trimer. The view is from the extracellular space along the molecular threefold symmetry axis. Inside each barrel has the longest loop (arrow), which selects solutes to pass through by setting the size exclusion limit.

Although bacterial porins are usually stable in trimeric form (Schirmer, 1998), some porins are different. For example, an *E. coli* porin OmpG acts as a non-specific channel for mono-, di- and trisaccharides (Behlau *et al.*, 2001). This porin was purified and crystallized in two dimensions. Projection maps of two different crystal forms of OmpG at 6 Å resolution showed that the protein had a β-barrel structure. OmpG is an unusual porin because it appears in monomeric form, unlike most other porins such as OmpF and OmpC. The size of OmpG barrel was estimated to be ~2.5 nm, indicating that the protein is consisted of 14 β-strands. The projection map also suggested that the channel is restricted by internal loops (Behlau *et al.*, 2001).

MspA is a newly discovered porin that provides the main general diffusion pathway for hydrophilic compounds through the outer membrane of *Mycobacterium smegmatis*. The oligomeric porin is composed of four subunits with M_r 20,000 each. Electron microscopy of MspA embedded in the cell walls of *M. smegmatis* showed that the protein formed a tetrameric pore with a central channel of 10 nm in length and an inner diameter of 2.5 nm (Heinz *et al.*, 2003).

1.6 Objectives

An outer membrane protein (OM-1) of *B. pseudomallei*, later designated in this study as Omp38, was initially isolated by Gotoh *et al.* (1994). This peptidoglycan-associated protein contains trimeric subunits with M_r 110,000, which migrates to an M_r 38,000 after heated to 95 °C. According to liposome-swelling assays, Omp38 has been suggested to be a non-specific porin that allows small saccharides with M_r <600 to pass through (Siritapetawee *et al.*, 2004).

This thesis has been focused on isolation, gene cloning and expression of Omp38 from the virulent bacterium, *B. pseudomallei* and the closely related non-virulent bacterium, *B. thailandensis*. Comparative studies of the Omp38 structure and function of the two organisms have been carried out to explain the molecular mechanism of antibiotic resistance of *B. pseudomallei* and to understand the pathogenesis of melioidosis caused by *B. pseudomallei*.

The objectives of this thesis include:

1. Isolation of *B. pseudomallei* Omp38 (*BpsOmp38*) and its homologue from *B. thailandensis* (*BthOmp38*).
2. Production of anti-*BpsOmp38* polyclonal antibodies for gene isolation and protein characterization.
3. Isolation of the genes encoding *BpsOmp38* and *BthOmp38* using a PCR based strategy employing the incomplete *B. pseudomallei* genomic sequence data.
4. Expression of *BpsOmp38* and *BthOmp38* porins in *E.coli*.
5. Functional characterization of the native and refolded Omp38 expressed in *E. coli* using proteoliposome swelling assays.
6. Secondary structure determination and preliminary crystallization of the refolded Omp38 of both organisms.

Chapter II

Materials and Methods

2.1 Materials

2.1.1 Bacterial strains and plasmids

Burkholderia pseudomallei standard type strain ATCC23343, *Escherichia coli* type strain ATCC25922, *Staphylococcus aureus* type strain ATCC25923 and *Pseudomonas aeruginosa* type strain ATCC27853 were gifts from Ms. Worada Samosornsuk, Department of Microbiology, Faculty of Allied Health Science, Thammasat University, Thailand. *B. thailandensis* type strain ATCC700388 was given by Dr. Richard H. Ashley, Department of Biomedical Sciences, University of Edinburgh, UK. *E. coli* strain DH5 α and Origami (DE3) were obtained from Novagen (USA). pGEM[®]-T vector was obtained from Promega (USA), and pET_{23d}(+) expression vector was from Novagen (USA).

2.1.2 Chemicals

Bacteria culture media and bacteriological agar were purchased from Scharlau Chemie (USA) and Difco (USA). Standard antibiotic discs were obtained from Oxoid (UK). Standard antibiotic powders were obtained from Merck (Germany) and Sigma-Aldrich (USA). Dithiothreitol (DTT), iodoacetamide, ammonium hydrogen carbonate, stachyose, *D*-melezitose, *D*-sucrose, *L*-arabinose, *D*-glucose and *D*-mannose were from Acros Organics (USA). GelCode[®] Blue stain reagent and bicinchoninic acid (BCA) kit,

Freund's complete and incomplete adjuvants were obtained from Pierce (USA). GBX developer and GBX fixer for X-ray film were purchased from Kodak (UK). Proteinase K and trypsin (sequencing grade) were from Promega (USA). Sephacryl S-200® HR resin, DEAE Fast Flow HiTrap™ prepacded column, CM Fast Flow HiTrap™ prepacded column and dextran T-40 were from Amersham Pharmacia Biotech (UK). Zwittergent® 3-14 (n-tetradecyl-N, N-dimethyl-3-ammonio-1-propanesulfonate) was from Sigma-Aldrich (USA). Other detergents used for protein preparation were purchased from Carlo Erba Reagenti (Italy). Polyethylene glycol 20,000 (PEG 20,000) was from Fluka (Germany). *Pfu* DNA polymerase and T₄ ligase were purchased from Promega (USA). PCR purification and plasmid preparation kits were purchased from QIAGEN (USA). All restriction endonucleases were from New England Biolabs (USA). All other reagents for general laboratory uses were from Sigma-Aldrich (USA) and Carlo Erba Reagenti (Italy).

2.1.3 PCR primers

Primers for PCR amplification were synthesized by Proligo Singapore Pty Ltd (Singapore). Primers for DNA sequencing were synthesized from Biotechnology Sequencing Unit (BSU, Bangkok, Thailand).

2.2. Methodology

2.2.1 Preparation of peptidoglycan-associated proteins

B. pseudomallei (ATCC₂₃₃₄₃) and *B. thailandensis* (ATCC₇₀₀₃₈₈) were grown in LB broth for 18 h at 37 °C with vigorous shaking. Cells were harvested at late exponential phase by centrifugation at 10,000 x g at 4 °C for 20 min. Crude peptidoglycan was isolated following the method modified from Gotoh *et al.* (1994). Briefly, cells from 2 liters of late exponential culture were washed once and suspended in 10 ml of 10 mM Tris-HCl, pH 8.0 containing 1 mM PMSF and 2 mg hen egg lysozyme. The suspension was sonicated using a Sonopuls ultrasonic sonicator (Germany) with a 6-mm diameter probe (50% duty cycle; amplitude setting 20%; total time 5 min), and large cellular debris and unbroken cells were removed by centrifugation at 10,000 x g for 30 min. Cell membranes were recovered from the lysates by microcentrifugation at 12,000 x g for 1 h, suspended in 10 mM Tris-HCl, pH 8.0 containing 0.5% SDS, and heated at 30 °C for 1 h to solubilize most of the remaining cytoplasmic and membrane proteins. A complex of non-solubilized peptidoglycan sheets (crude peptidoglycan) was then pelleted by microcentrifugation at 12,000 x g for 1 h and heated in 4 ml of 10 mM Tris-HCl, pH 8.0 containing 2% (w/v) SDS and 0.5 M NaCl at 37 °C for 1 h. Solubilized peptidoglycan-associated proteins were then separated from insoluble peptidoglycan by microcentrifugation at 12,000 x g for 1 h.

2.2.2 Purification of native Omp38 protein

Peptidoglycan-associated proteins were purified by gel filtration chromatography. Proteins released from crude peptidoglycan in 10 mM Tris-HCl, pH 8.0, containing 2% (w/v) SDS and 0.5 M NaCl were applied twice to a Sepharacryl S-200 HR (1.5 x 95 cm) column previously equilibrated with 10 mM Tris-HCl, pH 8.0 containing 1% (w/v) SDS and 0.5 M NaCl. The chromatography was carried out at a flow rate of 1 ml min⁻¹, and fractions of 2 ml were collected. Concentrations of eluted proteins were determined by measuring A₂₈₀ and the protein profile was further analyzed on 12% SDS-PAGE (Appendix E). Protein peaks were pooled and precipitated with 50% (v/v) ethanol at -30 °C, overnight (Garavito and Rosenbusch, 1986). The precipitated protein was collected by centrifugation at 20,000 x g for 30 min. The pellet was dissolved in 1 ml of 10 mM Tris-HCl, pH 8.0, containing 2% (w/v) SDS and 0.5 M NaCl. The solubilized protein was dialyzed in 10 mM Tris-HCl, pH 8.0 for 48 h at room temperature with four changes of the same buffer. Final the concentration of protein was determined by bicinchoninic acid (BCA) assay.

2.2.3 Determination of protein concentration

Protein concentrations were estimated using the BCA assay kit (Pierce, USA) in a microplate reader spectrophotometer (Labsystem Oy, Finland). A proper dilution of protein sample in 12.5 µl was mixed with 100 µl of the BCA working reagent. The reaction mixture was incubated at 37°C for 30 min. Absorbance at 540 nm was measured spectrophotometrically using a microplate reader. Bovine serum albumin (BSA) at varied concentrations ranging from 25 µg/ml–2 mg/ml was used to construct a standard calibration curve (Appendix B) and determine protein concentrations of unknown samples.

2.2.4 SDS-PAGE gel electrophoresis

Denaturing polyacrylamide gel electrophoresis was performed according to the method of Laemmli (1970). One part of protein solution was mixed with 4 parts of 5x sample buffer (Appendix E). The protein mixture was boiled at 95 °C for 5 min, then 15 µl was loaded onto a 12% SDS PAGE gel (Appendix E) using a Mini-protein 3 cell apparatus (Bio-RAD, USA), and electrophoresed in Tris-glycine, pH 8.3 containing 0.1% SDS at a constant voltage of 150 V for 1 h. After electrophoresis, the gel was stained with Coomassie Brilliant Blue R 250 for 30 min, then destained with a destaining solution (Appendix E) until protein bands were clear. Relative molecular mass of the protein bands were estimated by comparing with the low molecular weight protein markers (molecular weight ranging from 14-97 kDa) (Amersham Pharmacia Biotech, UK) including phosphorylase b (97 kDa), bovine serum albumin (66 kDa), ovalbumin (45 kDa), bovine carbonic anhydrase (30 kDa), trypsin inhibitor (20 kDa) and bovine α -lactalbumin (14 kDa).

2.2.5 In-gel digestion and peptide mass analysis of Omp₃₈ using MALDI-TOF MS and ESI/MS

2.2.5.1 In-gel digestion

The outer membrane fractions obtained from Sephacryl S-200 HR filtration chromatography were run on SDS-PAGE, then stained with GelCode® Blue stain reagent. In-gel digestion experiments were carried out according to Shevchenko *et al.* (1996). Briefly, the protein band (M_r 38,000) was excised from the gel, cut into small pieces (10 mm x 1.5 mm x 1.5 mm), and washed twice with acetonitrile followed by 100 mM NH_4HCO_3 solution until Coomassie blue was removed, then dried in a vacuum microcentrifuge. Thirty microlitres of 10 mM dithiothreitol (DTT) in 100 mM NH_4HCO_3 was added at 56 °C for 1 h to reduce the protein. After cooling to room temperature, the DTT solution was replaced with the same volume of 55 mM iodoacetamide in 100 mM NH_4HCO_3 . After 45 min of incubation at ambient temperature in the dark with occasional vortexing, the gel pieces were washed twice with 50 - 100 μl of 100 mM NH_4HCO_3 followed by the same volume of acetonitrile. After 10 min of each incubation, the liquid was removed and the gel pieces were finally dried in a vacuum microcentrifuge. The gel pieces were swollen in a digestion buffer containing 50 mM NH_4HCO_3 , 5 mM CaCl_2 and 12.5 ng/ μl trypsin on ice. After 45 min, the supernatant was removed and replaced with 5 – 10 μl of the same buffer without trypsin at 37 °C, overnight to keep the gel pieces wet during enzymatic cleavage. Peptides were extracted

by one change of 20 mM NH_4HCO_3 and three changes of 5% formic acid in 50% acetonitrile (20 min incubation with occasional vortexing for each change at room temperature and dried down in a vacuum microcentrifuge (Shevchenko *et al.*, 1996).

2.2.5.2 Peptide mass analysis and identification of Omp₃₈ by MALDI-TOF MS and ESI/MS

Peptide mass analysis of outer membrane proteins of *B. pseudomallei* and *B. thailandensis* was carried out using the Mass spectrometry facility, of PD. Dr. Heino Prinz's laboratory, Max Planck Institute for Molecular Physiology, Dortmund, Germany. Briefly, a small fraction of the tryptic peptides obtained from Method 2.2.5.1 was analyzed by MALDI-TOF MS (Voyager-DE Pro in reflective mode) in an α -cyano-4-hydroxycinnamic acid matrix for the peptide "mass fingerprinting". The remaining peptides were separated by capillary HPLC using a 0-40% linear gradient of acetonitrile containing 0.1% acetic acid, then detected directly by ESI/MS (Thermo Finnigan LCQ Deca) using the proprietary "triple play" mode for obtaining MS/MS sequence information for the relevant peptides. Data bank searching was performed with "MS-Fit" (<http://prospector.ucsf.edu/>) for MALDI mass fingerprint data, and with "Sequest search" (<http://fields.scripps.edu/sequest/index.html>) for MS/MS data from the HPLC-MS run.

In some experiments, the proteins (not gel pieces) were completely digested with sequencing grade trypsin in a buffer containing 5 mM CaCl₂ and 100 mM NH₄HCO₃, and the resulting peptides were applied to an Agilent 1100 HPLC connected to the LCQ ESI/MS.

Mass spectra of entire proteins were obtained with linear MALDI-TOF 7 (Voyager-DE Pro) using sinapinic acid (3,5-dimethoxy-4-hydroxycinnamic acid) as the matrix.

2.2.6 Production of anti-Omp38 polyclonal antibodies and immunoblot analysis

Production of anti-Omp38 polyclonal antibodies was carried out using in-gel method according to Amero *et al.* (1994). Partially purified *B. pseudomallei* Omp38 (2 µg) was separated by 12% SDS-PAGE. Following electrophoresis, the protein was stained with GelCode® Blue stain reagent. After destaining thoroughly with distilled water, the protein band (M_r 38,000) was excised from the gel. The excised bands (1.5 inches x 3-4 mm x 1.5 mm, each) were homogenized with 200 µl of water, and emulsified with 200 µl of Freund's complete/incomplete adjuvant. The emulsified mixture was injected subcutaneously into a female white rabbit to produce anti-Omp38 antisera. Multiple injections were performed and bleeds were collected as described below:

Day 0: Collection of preimmune serum (10 ml), followed by primary immunization with the Omp38 antigen mixed with the complete Freund's adjuvant.

Day 21: First boosting with the protein antigen mixed with the incomplete Freund's adjuvant.

Day 31: Collection of the first test bleed (10 ml).

Boosting steps were continued three more times with a period of every third week and blood sample was collected 10 days after each boost until the polyclonal antibody titer was tested to be sufficient. The final test bleed was collected from an ear vein of the immunized rabbit. The serum was obtained after centrifugation at 4,500 x g at 4°C for 20 min. The lytic complement activity of the serum was abolished by heating at 56°C for 30 min. After centrifugation, the serum was collected and used for immunoblotting experiments. For long-term storage, the antibodies were aliquoted (100 µl) into microcentrifuge tubes and kept at -30°C until used.

Antisera titres and cross reactivity between *B. pseudomallei* and *B. thailandensis* proteins (5 µg each) were analysed by Western blotting and detected with the enhanced chemiluminescence reagent (ECL, Amersham Pharmacia Biotech, UK). For Western blot analysis, protein samples were mixed with one-fourth volume of the 5x SDS-gel sample buffer and heated at 100°C for 5 min. The protein samples were loaded onto a 12% SDS-PAGE and electrophoresed as described in Method 2.2.4. After electrophoresis, the gel was soaked in a blotting buffer containing 25 mM Tris, 125 mM glycine, 0.25% SDS and 3% methanol. The protein bands were then transferred onto a nitrocellulose membrane (Hybond ECL, Amersham Pharmacia Biotech, UK) using a Semidry

gel blotting system (Bio-Rad, USA). The transferred membrane was washed twice with 10 ml PBS (Appendix E). The membrane was incubated in a blocking solution containing PBS, 5% (w/v) non-fat milk and 0.2% (v/v) Tween 20 (PBS-T) for 1 h at room temperature. The antisera were diluted into different dilutions including 1:2,500; 1:5,00; 1:10,000, and 1:20,000, to test for the appropriate dilution for Western blot analysis. Since the dilution of 1:10,000 gave highest signal intensity, therefore immunoblotting was later carried out by incubating the membrane using a 1:10,000 dilution of anti-*Bps*Omp38 serum in the blocking solution for 2 h. After incubation with the antiserum, the membrane was washed four times with PBS-T, followed by incubation in a 1:5,000 dilution of the secondary antibody (goat anti-rabbit coupled to horse radish peroxidase) in PBS-T for 1 h. The membrane was washed three times with PBS-T, then another time with PBS with 10 min of incubation per wash. Detection using chemiluminescence (ECL, Amersham Pharmacia Biotech, UK) was carried out by incubating the membrane with a small volume of chemiluminescence substrate for 1 minute at room temperature. The membrane was wrapped with Saran wrap, then exposed to an X-ray film (Hyperfilm ECL) in the dark. After the detection step, the nitrocellulose membrane was stained with the Amido Black staining solution for protein detection (Appendix E).

2.2.7 Preparation of genomic DNA from *B. pseudomallei* and *B. thailandensis* (Miniprep protocol)

Five millilitres of *B. pseudomallei* or *B. thailandensis* culture were grown to saturation ($OD_{600} \sim 0.6$) and cells were pelleted by microcentrifugation for 2 min. The cell pellet was resuspended in 567 μ l TE buffer, 30 μ l of 10% SDS

and 3 μ l of 20 mg/ml proteinase K, then incubated 1 h at 37 °C. After incubation, 100 μ l of 5 M NaCl was added and mixed with 80 μ l of CTAB solution (Appendix E) and incubated 10 min at 65 °C. An equal volume of a mixture of chloroform/isoamyl alcohol (24:1 (v/v)) was added into the mixture, and microcentrifuged for 4 to 5 min. The supernatant was transferred to a fresh tube, an equal volume of phenol/chloroform/isoamyl alcohol (25:24:1 (v/v/v)) was added, mixed, and then microcentrifuged for 5 min, and supernatant was transferred to a fresh tube. Genomic DNA was precipitated by adding 0.6 volume of isopropanol. The precipitated DNA was picked using a sealed Pasteur pipette then transferred to 1 ml of 70% ethanol and microcentrifuged for 5 min. Supernatant was discarded, the DNA pellet was then resuspended in 100 μ l of 10 mM Tris-HCl, pH 8.5 (Ausubel *et al.*, 1999). After that, the DNA solution was subjected to 0.7% agarose gel electrophoresis. DNA bands were stained with 0.5 μ g/ml ethidium bromide and visualized under UV light. Concentrations of the prepared genomic DNA were measured spectrometrically at A_{260} .

2.2.8 DNA analysis by agarose gel electrophoresis

Genomic DNA were analyzed by 0.7 or 1% agarose gel electrophoresis in 1x TAE buffer (Appendix E), as described by Sambrook *et al.* (1989). The agarose gel (molecular biology grade) was prepared using the Gel Electrophoresis Apparatus GNA-100 (Amersham Pharmacia Biotech, UK). DNA sample was prepared by mixing five parts of DNA sample with one part of 6x DNA loading buffer (Appendix E) and applied into gel wells. Electrophoresis was performed at a constant voltage of 95 V for 45-50 min.

After electrophoresis, the gel was stained with 0.5 µg/ml ethidium bromide for 5-10 min, then destained with distilled water. The DNA band was visualized under UV light using a Fluor-S™ MultiImager (Bio-RAD Laboratories, USA). Sizes of DNA fragments were estimated by comparing with the migration of the standard 1-kb DNA ladder marker (New England Biolabs, USA).

2.2.9 Quantitation of DNA

DNA solution (2 µl) was mixed with 998 µl distilled water, then A_{260} and A_{280} were measured. The A_{260}/A_{280} ratio was calculated using a Lambda Bio20 UV/VIS Spectrometer (Perkin Elmer, USA). Normally, the A_{260}/A_{280} ratio of approximately 1.8-2.0 indicates good purity of DNA. The DNA content was calculated using the A_{260} value of double stranded DNA with the following equation:

$$\begin{aligned}\mu\text{g/ml of DNA} &= (A_{260} \times \text{dilution factor} \times 50 \mu\text{g/ml}) \\ &= (A_{260} \times 200 \times 50 \mu\text{g/ml})\end{aligned}$$

One A_{260} unit equals 50 µg of double stranded DNA/ml (Sambrook *et al.*, 1989).

2.2.10 Gene isolation, cloning and sequencing

2.2.10.1 Primers and PCR conditions

Based on peptide mass analysis obtained from MALDI-TOF MS and ESI/MS, an open reading frame (gln-Sanger_28450/bpsmalle_Contiq836) corresponding to Omp38 was identified from the incomplete *B. pseudomallei* genomic database (http://www.ncbi.nlm.nih.gov/sutils/genome_table.cgi). PCR was used to isolate the gene that encodes Omp38. The genomic DNA of

B. pseudomallei was used as PCR template. A set of primers flanking between the 3' and 5' ends of the identified open reading frame were designed as follows:

Sense primer: 3'-ATGAACAAGACTCTGATTGTTGCA-5',

Antisense primer: 3'-GAAGCGGTGACGCAGACCAA-5'

This primer set was later used to isolate the Omp38 homologue from *B. thailandensis*. The PCR reaction comprised 250 ng of genomic DNA, 1x PCR buffer, 1.5 mM MgCl₂, 200 μM dNTP mix, 0.3 μM primer, and 1 unit of *Taq* DNA polymerase. Reaction mixtures were amplified in a GeneAmp® PCR System 9700 thermocycler (PE Applied Biosystems, USA). The DNA template was denatured for 3min at 95 °C, then subjected to 30 cycles of 95 °C for 1 min, 60 °C for 30 s and 72 °C for 1.5 min, followed by a final extension for 7 min at 72 °C. PCR products were resolved on 1% agarose gel and stained with ethidium bromide and visualized under UV light. The DNA band of expected size (1.122 kb) was excised and purified using the QIAGEN gel extraction kit as described later in Method 2.2.11.

2.2.10.2 Ligation of PCR product into the pGEM®-T vector

Ligation reactions were carried out according to the Promega manufacturer's instruction. The purified PCR products were cloned into the pGEM®-T cloning vector (Appendix C) with the ratio of 3 inserts : 1 vector. The amounts of insert were calculated as follows:

$$\frac{(\text{ng of vector} \times \text{kb size of insert})}{\text{kb size of vector}} \times (\text{insert} : \text{vector molar ratio}) = \text{ng of insert}$$

Ligation reactions comprised 1x T4 DNA ligase buffer, 50 ng of pGEM®-T vector (3 kb), 56 ng of PCR product (1.122 kb) and 0.3 unit of T4 DNA ligase.

Deionized water was added to bring a final volume to 10 μ l. The reaction mixture was incubated overnight at 16 °C.

2.2.10.3 Transformation, selection and nucleotide sequence analysis

Transformation reactions were done as described by Sambrook *et al.* (1989). A 50- μ l aliquot of frozen DH5 α *E. coli* competent cells (Appendix D) was thawed on ice for 5 min. The vector or recombinant plasmids (10-100 ng) or 5 μ l of the ligation reaction was added to the thawed competent cells (Appendix D), mixed gently by swirling the tube and incubated on ice for 30 min. The cells were heated shock at 42 °C for 90 s, then immediately chilled on ice for 1 min. The transformed cells were grown in 450 μ l of SOC medium or LB broth by shaking at 200 rpm for 45 min. For blue-white colony selection of the recombinant pGEM®-T vector, 200 μ l of cell culture was spread on an LB plate (Appendix E) containing 100 μ g/ml of ampicillin, which was pre-spread with 25 μ l of 50 mg/ml X-gal and 50 μ l of 0.1 M IPTG. After spreading, the plate was air-dried at room temperature for 15-20 min, then inverted and incubated at 37 °C overnight (16-18 h). Using blue-white color screening, white colonies, which carried the plasmid containing insert, were subjected to boiling miniprep and run on 1% agarose gel electrophoresis (see Method 2.2.12). Positive colonies, designated pGEM®-T-*Omp38*, were then grown in LB broth containing ampicillin (100 μ g/ml) and the recombinant plasmid was prepared using the QIAGEN plasmid miniprep kit (Method 2.2.13). The DNA insert was sequenced in both

directions using an automated sequencer by the Bioservice Unit (BSU, Bangkok, Thailand).

2.2.11 Purification of PCR products from an agarose gel

PCR products from an agarose gel were purified using the QIAQuick gel purification kit (QIAGEN, USA), according to the manufacture's protocol. The PCR products (100 μ l) were separated on 1% TAE agarose gel. The DNA bands (~1.1 kb) was excised, placed in a clean 1.5 ml microtube, and the gel pieces were washed once with distilled water. Three volumes of QG buffer were added to 1 volume of gel and the tube was incubated at 50 °C for 10 min with vortexing every 2-3 min. One gel volume of isopropanol was added to the sample and mixed (this step was used with the DNA fragments with sizes of <500 bp or >4 kb to increase the yield of DNA fragments). The sample was applied to the QIA Quick column and centrifuged for 1 min at 13,000 x g, and the flow through was discarded. Seven hundred fifty microliters of PE buffer was added to the column, then the column was allowed to stand for 2–5 min and centrifuged at 13,000 x g for 1 min. Flow through was discarded and the column was centrifuged for an additional 1 min. The column was placed in a clean 1.5 ml microtube, and the plasmid DNA was eluted from the column with 50 μ l EB buffer (10 mM Tris-HCl, pH 8.5) by centrifugation at 13,000 x g for 1 min. The DNA solution was stored at -30°C.

2.2.12 Analysis of DNA inserts by boiling miniprep

Preparation of recombinant plasmids for preliminary analysis was done using the boiling miniprep method (Sambrook *et al.*, 1989). Single colonies were picked with a sterile needle, restreaked on LB plate containing 100 µg/ml of ampicillin and grown at 37°C overnight. Single colonies grown on a freshly prepared LB agar plate were inoculated in 5 ml LB broth containing 100 µg/ml of ampicillin and grown overnight at 37°C with 200 rpm shaking. The cells were pelleted in a microtube by centrifugation at 10,000 x g for 1 min. The cell pellet was resuspended in 350 µl STET buffer (Appendix E) and mixed with 20 µl of freshly prepared lysozyme (10 mg/ml). The suspension was boiled at 95°C for 1 min to break the cells. The broken cells were precipitated by centrifugation at 12,000 x g for 10 min at room temperature, and the cell pellet was removed with a sterile toothpick and discarded. To precipitate the plasmids in the supernatant, 400 µl isopropanol was added and the tube was incubated at room temperature for 5 min, then centrifuged at 12,000 x g for 5 min at 4°C to pellet the plasmids. The pellet was washed with 500 µl 75% ethyl alcohol and dried for 15-20 min. The pellets was resuspended in 50 µl 10 mM Tris-HCl, pH 8.0 containing 0.1 mg/ml RNase A, and incubated at 37°C for 30 min to degrade contaminating RNA. The purified plasmids were run on 1% agarose and DNA bands were compared to the plasmids without insert. The plasmids containing insert was stored at -30°C.

2.2.13 QIAGEN plasmid miniprep

The QIA prep spin miniprep plasmid extraction kit (QIAGEN, USA) was used to purify recombinant plasmids following manufacture's instruction. A single colony was inoculated in 5 ml LB broth with 100 µg/ml of ampicillin and the cells were grown by shaking at 200 rpm at 37°C for 12-16 h. The cultured cells were pelleted by centrifugation at 10,000 x g for 1 min at room temperature. The cell pellets were resuspended in 250 µl P1 buffer containing RNase A. Two hundred fifty microliters of P2 buffer was added to the resuspended cells, and mixed by inverting the tube gently (to avoid genomic DNA shearing) 4-6 times until the solution became viscous and slightly clear. Three hundred fifty microliters of N3 buffer was added and mixed immediately (to avoid localized precipitation) by inverting the tube gently for 4-6 times. The tube was centrifuged at 13,000 x g for 10 min to compact the white pellet. The supernatant was applied to a QIA prep column, then centrifuged at 13,000 x g for 1 min, and the flow through was discarded. The column was washed with 0.75 ml PE buffer and centrifuged at 13,000 x g for 1 min. The flow through was discarded, and the column was centrifuged for an additional 1 min. The column was placed in a new 1.5 ml microtube and 50 µl 10 mM Tris-HCl, pH 8.5, was added to the center of column. The column was allowed to stand for 1 min, and centrifuged at 13,000 x g for 1 min to elute the plasmid DNA. The DNA was stored at -30°C.

2.2.14 DNA sequencing and amino acid sequence analysis

Nucleotide sequences of *BpsOmp38* and *BthOmp38* were obtained in both directions from a DNA automated sequencer (see Method 2.2.10.3). The complete DNA sequences were assembled using SeqManTM II program in the DNASTAR package (DNASTAR Inc., USA). The full length of *Omp38* sequence was translated to a deduced amino acid sequence by DNASTAR EditSeqTM program. The amino acid sequences of *Omp38* were subjected to RPS-BLAST search to identify protein conserved domains using (<http://www.ncbi.nlm.nih.gov/BLAST>). Protein sequences were aligned using Clustal W (<http://www.ebi.ac.uk/clustalw/>). Signal peptide cleavage sites were predicted using SignalP V1.1 (<http://www.cbs.dtu.dk/services/SignalP/>). The DNA sequences of *BpsOmp38* and *BthOmp38* were deposited in the GenBank database under accession numbers; AY312416 and AY312417, respectively.

2.2.15 Subcloning of *Omp38* inserts into an expression vector

2.2.15.1 Primer and PCR conditions

A set of primers designed from the *BpsOmp38* gene lacking a signal peptide sequence was synthesized. The sense primer sequence containing the *NcoI* restriction site was 5'-CATGCCATGGCTCAAAGCAGCGTCACGC-3'. The antisense primer sequence containing the *XhoI* restriction site was 5'-CCGCTCGAGTTAGAAGCGGTGACGCAGACC-3'. The same set of primers was also used to amplify the *BthOmp38* fragment lacking a signal peptide sequence. The DNA templates used for PCR amplification were

pGEM®-T-*BpsOmp38* and pGEM®-T-*BthOmp38*. The PCR reaction comprised 1 ng of the recombinant plasmid, 1x *Pfu* buffer, 1.5 mM MgCl₂, 200 μM dNTP mix, 0.1 μM primer, and 1 unit of *Pfu* DNA polymerase. Reaction mixtures were subjected to GeneAmp® PCR System 9700 thermocycler (PE Applied Biosystems, USA). Amplification conditions were began with denaturation for 3min at 95 °C, followed by 30 cycles of 95 °C for 1 min, reannealing at 60 °C for 30 s and extension at 72 °C for 1.5 min. The final extension cycle was 7 min at 72 °C. PCR products were resolved on a 1% agarose gel, then the electrophoresed gel was stained with ethidium bromide and visualized under UV light. The DNA band (1.1 kb) was excised and purified with the QIAGEN gel extraction kit, as described in Method 2.2.11.

2.2.15.2 Insert and vector preparation for restriction enzyme digestion

The purified PCR products obtained from Method 2.2.11 and pET23d(+) vector (Appendix C) were digested with the restriction enzymes *XhoI* and *NcoI* to obtain cohesive-end ligation. Digestion reaction comprised 10 μg target DNA, 1x compatible buffer, 10 units of *XhoI/NcoI*. Sterile distilled water was added to bring the final volume to 20 μl. The reaction mixture was incubated at 37°C for 6 h. The digested reaction products were separated on 1% agarose gel and purified by the QiaQuick gel extraction kit as previously described in Method 2.2.11.

2.2.15.3 Ligation of the *Omp38* fragments to an expression vector

The reaction mixture was consisted of 4 μ l 5x ligation buffer, 50 ng purified pET23d(+) vector digested with *Nco*I and *Xho*I, 45 ng purified PCR product also digested with *Nco*I and *Xho*I, 1 unit of T4 DNA ligase, and sterile distilled water to bring the volume up to 20 μ l. The reaction mixture was incubated at 16°C overnight. The total reaction mixture was transformed into *E. coli* strain DH5 α host cells. The transformed cells were grown in LB broth containing ampicillin (Method 2.2.10.3) and the recombinant plasmid was isolated using the QIAprep Spin Miniprep kit (QIAGEN, USA), as described in Methods 2.2.13.

2.2.15.4 Transformation of the recombinant plasmids into the expression *E. coli* host cells

The recombinant plasmids, pET23d(+)-*BpsOmp38* and pET23d(+)-*BthOmp38*, isolated from *E. coli* DH5 α were transformed into *E. coli* strain Origami(DE3) (Appendix D). The plasmid (100 ng) was mixed with 50 μ l competent cells (see Method 2.2.10.3) and spread on a LB agar plate containing 100 μ g/ml ampicillin. Clones carrying the DNA insert were identified by colony PCR method (Method 2.2.15.5).

2.2.15.5 Colony PCR

Single colonies were picked with sterile toothpicks, restreaked on LB plate containing 100 µg/ml ampicillin, and grown at 37°C overnight. The freshly grown colonies were inoculated in 1 ml LB broth containing 100 µg/ml ampicillin and grown overnight with 200 rpm shaking at 37°C. The cell culture was pelleted in a microtube by centrifugation at 3,000x g for 3 min. The cell pellets were resuspended in 100 µl deionized water and boiled at 100°C for 1 min to break the cells. The broken cells were precipitated by centrifugation at 12,000 x g for 10 min at room temperature, and 1 µl of supernatant was subjected to PCR as described in Method 2.2.15.1. The *E. coli* cells carrying pET23d(+) without an insert was used as a negative control.

2.2.16 Expression of *BpsOmp38* and *BthOmp38* and preparation of inclusion bodies

About 100 ng of pET23d(+)-*BpsOmp38* or pET23d(+)-*BthOmp38* plasmid was freshly transformed into the *E. coli* Origami (DE3) (Method 2.2.15.4), and a single colony was inoculated into 50 ml LB medium containing ampicillin (100 µg/ml) and 1% glucose. Glucose was added into the culture medium to stabilize the plasmids (Pullen, 1995). After incubation for 8 h at 37 °C, the culture (10 ml) was transferred to 4x 1,000-ml flasks, each containing 500 ml of the same medium. Incubation was continued in a shaking incubator at 37 °C, until an OD₆₀₀ of ~0.6 was reached. At this point, IPTG was added to a final concentration of 0.4 mM. After shaking at 37 °C for 90 min, cells were harvested by centrifugation at 10,000 x g for 30 min at 4°C, then resuspended in 10 ml of 50 mM Tris-HCl buffer, pH 8.0 containing 1mM

EDTA and 100 mM NaCl (TEN buffer) per g (wet weight) of cells. The cell suspension was added with 1 mM PMSF and 2 mg lysozyme per g (wet weight) of cells (QI *et al.*, 1994). The mixture was sonicated using a Sonopuls ultrasonic sonicator using a 6 mm diameter probe with 50% duty cycle; amplitude setting 20%; total time 5 min. Large cellular debris and unbroken cells were removed by centrifugation at 10,000 x g for 30 min, while the cell lysate was pelleted at 20,000 x g at 4 °C for 30 min. The resulting insoluble fraction was washed once with 10 ml of 2 M urea containing 0.05% Tween-20 in 10 mM Tris-HCl, pH 8.0, then further centrifuged at 20,000 x g at room temperature for 30 min (modified from Conlan *et al.*, 2000). The white pellet containing inclusion bodies were further purified and subsequently subjected to refolding experiments.

2.1.17 Western blotting analysis

To confirm Omp₃₈ expression, the whole cell lysates obtained from IPTG-induced and without IPTG-induced *E. coli* Origami(DE₃) were analyzed on 12% SDS-PAGE followed by Western blotting using a 1:10,000 dilution of the anti-*Bps*Omp₃₈ antiserum in PBS, pH 7.4 containing 0.2% Tween 20 and 5% (w/v) non-fat dried milk (Method 2.2.6). The purified native *Bps*Omp₃₈ and *Bth*Omp₃₈ were used as positive controls of Western blot analysis.

2.1.18 Purification and refolding of Omp₃₈ expressed in *E. coli* cells

The fraction containing inclusion bodies obtained from Method 2.2.16 was resuspended in 10 ml of a denaturation buffer containing 25 mM sodium acetate buffer, pH 5.0 and 8 M urea, then centrifuged at 20,000 x g at room temperature for 2 h. The clear supernatant (5 ml) was applied onto a SP Fast Flow HiTrapTm (1.5 cm x 3 cm) column (Amersham Pharmacia Biotech, UK) previously equilibrated with 25 mM sodium acetate buffer, pH 5.0, containing 8 M urea. Bound proteins were eluted with a 0-0.3 M step gradient of NaCl in 25 mM sodium acetate buffer, pH 5.0 containing 8 M urea at a flow rate of 1 ml min⁻¹. Eluted proteins were initially detected by measuring A₂₈₀, then analysed on a 12% SDS-PAGE. Fractions containing a 38-kDa band were pooled and precipitated with 50% (v/v) final concentration of ethanol at -20 °C, overnight (modified from Garavito and Rosenbusch, 1986). The precipitated protein was pelleted by centrifugation at 20,000 x g for 20 min and re-dissolved to 5 ml with 8 M urea in 20 mM Tris-HCl, pH 7.0, then further applied onto a DEAE Fast Flow HiTrapTm (1.5 cm x 3 cm) column (Amersham Pharmacia Biotech, UK) previously equilibrated with 20 mM Tris-HCl buffer, pH 7.0 containing 8 M urea. Proteins were eluted with a 0-0.3 M step gradient of NaCl in 20 mM Tris-HCl, pH 7.0, and 8 M urea with an applied flow rate of 1 ml min⁻¹. Eluted fractions were detected by measuring A₂₈₀ and analysed on 12% SDS-PAGE. Fractions containing a highly purified 38-kDa band, which was later proven to be Omp₃₈, were pooled and precipitated again using ethanol

as described earlier, pelleted by centrifugation at 20,000 x g for 20 min and re-dissolved with 2 ml of 8 M urea in 20 mM Tris-HCl, pH 8.0. Protein concentrations of the purified Omp₃₈ were determined using bicinchoninic acid (BCA) kit (Pierce, USA). With regard to refolding experiments, a protein concentration of the purified Omp₃₈ fraction was adjusted to less than 10 mg/ml with Tris-HCl-urea solution. Then, the protein solution was diluted 1:1 with a refolding solution (20 mM Tris-HCl, pH 7.0 containing with 10% (w/v) Zwittergent® 3-14, 200 mM NaCl, 20 mM CaCl₂, 10 mM EDTA and 0.02% NaN₃), then heated at 95 °C for 5 min and left standing overnight at room temperature. The protein solution was loaded onto a Sephacryl S-200 HR (1.5 x 95 cm) column previously equilibrated with 20 mM Tris-HCl, pH 7.0, containing 0.05% Zwittergent® 3-14. A flow rate of 1.0 ml.min⁻¹ was applied and fractions of 2 ml were collected. A₂₈₀ of each fraction was measured, then SDS-PAGE analysis was performed with protein-containing fractions (Modified from Qi *et al.*, 1994 and Pullen *et al.*, 1995). The protein fractions were pooled and concentrated to 1 ml in a dialysis bag using PEG 20,000. The clear protein solution was further dialyzed against a buffer system comprising 20 mM Tris-HCl, pH 7.0 and 0.05% Zwittergent® 3-14 at room temperature for 2 days. The final concentration of refolded Omp₃₈ was measured again using BCA assay. The purified refolded Omp₃₈ was stored at -20 °C until used.

2.2.19 Protein identification and peptide mass analysis by MALDI-TOF

MS and ESI/MS

The purified unfolded Omp₃₈ (5 µg) obtained after SP Fast Flow HiTrap[™] following DEAE Fast Flow HiTrap[™] purification steps, was run on 12% SDS-PAGE and the protein band (M_r 38,000) was excised, then subjected to in-gel digestion with trypsin as described in Method 2.2.5.1. The digested peptide masses analyzed using MALDI-TOF MS (Method 2.2.5.2) were compared with the putative tryptic peptide masses predicted by “PAWS” program (ProteoMetrics LLC., USA).

2.2.20 Antibiotic susceptibility tests and functional study of Omp₃₈

2.2.20.1 Antibiotic susceptibility tests

Fifteen antimicrobial agents were used for antibiotic susceptibility testing by the disc diffusion technique (Woods and Washington, 1995). A list of antibiotics and their concentrations is shown on Table 2.1. Briefly, freshly cultured bacteria grown in tryptic soy broth were diluted with a normal saline solution into McFarland standard no. 0.5 (Appendix A) (A_{625} was between 0.08-0.10 equal to 10^6 CFU/ml). The cells were then spread on a Mueller-Hinton agar plate (plate diameter 90 mm.). Four standard diffusion discs containing selected antimicrobial agents (Oxoid, UK) (Table 2.1) were distributed on the surface of the cell-spread agar plate. The plate was incubated at 37 °C for 16 to 18 h. A diameter of inhibition zones were measured and compared with the standard diameter of inhibition zones tested with *E. coli* ATCC25922, *Staphylococcus aureus* ATCC25923 and *Pseudomonas aeruginosa* ATCC27853 (NCCLS, 2001).

Table 2.1 A list of antibiotics used in agar disc diffusion method.

Antimicrobial agent	Disc content (µg)
Antibiotics that inhibit cell wall synthesis	
<ul style="list-style-type: none"> • Aminoglycosides <ul style="list-style-type: none"> - Amikacin - Gentamicin • Carbapenems <ul style="list-style-type: none"> - Imipenem - Meropenem • Cephems <ul style="list-style-type: none"> - Cefepime - Ceftazidime - Cefotaxime • β-Lactam / β-Lactamase inhibitor combinations <ul style="list-style-type: none"> - Amoxicillin / Clavulanic acid • Lincosamides <ul style="list-style-type: none"> - Clindamycin • Macrolides <ul style="list-style-type: none"> - Erythromycin • Phenicol <ul style="list-style-type: none"> - Chloramphenicol • Tetracyclines <ul style="list-style-type: none"> - Tetracycline 	<p style="text-align: right;">30 10 10 10 30 30 30 20 / 10 2 15 30 30</p>
Antibiotics that effect nucleic acids	
<ul style="list-style-type: none"> • Fluoroquinolones <ul style="list-style-type: none"> - Ciprofloxacin • Ansamycins <ul style="list-style-type: none"> - Rifampin 	<p style="text-align: right;">5 5</p>
Antimetabolites	
<ul style="list-style-type: none"> • Folate pathway inhibitors <ul style="list-style-type: none"> - Trimethoprim / Sulfamethoxazole 	<p style="text-align: right;">1.25 / 3.75</p>

2.2.20.2 Proteoliposome-swelling assays

Pore-forming activities of the purified native (Method 2.2.2) and refolded Omp₃₈ (Method 2.2.18) were assessed by liposome-swelling technique. Preparation of proteoliposomes and determination of diffusion rates were based on the methods described previously (Gotoh *et al.*, 1994; Nikaido and Rosenberg, 1983; Odou *et al.*, 2001; Yoshimura *et al.*, 1983). Briefly, a mixture of 2.4 μ mol phosphatidylcholine (Sigma-Aldrich, USA) and 0.2 μ mol dicetylphosphate (Sigma-Aldrich, USA) (12:1 molar ratio of phosphatidylcholine:dicetylphosphate) in chloroform was dried by vacuum centrifugation and the phospholipid films were resuspended in 0.2 ml distilled water and mixed with 50 μ g of the purified Omp₃₈. The lipid mixture was sonicated at 20°C for 7 min in a water bath, then dried overnight by vacuum centrifugation. Proteoliposomes were formed when the dried phospholipids were resuspended in 0.2 ml of 10 mM Tris-HCl, pH 8.0 containing 15% (w/v) dextran T-40. The proteoliposomes were diluted to 0.6 ml with an isoosmotic solution (40 mM saccharide solution in 10 mM Tris-HCl, pH 8.0 or 20 mM an antibiotic in a proper diluent) as described in Appendix E. Changes in A_{400} were monitored continuously for 60 s using a Spectronic® GenesysTM 5 (Spectronic Instrument Inc., New York). Initial diffusion rates were recorded immediately after the addition of the liposomes. Permeability rates of sugar molecules through the Omp₃₈ reconstituted liposomes were calculated to

be proportional to the initial swelling rate, which is also proportional to $d[1/OD]/dt$ as follows:

$$d[1/OD]/dt = [1/(OD)^2] \times [d(OD)/dt]$$

Where OD is the initial turbidity of the suspension, and $d(OD)/dt$ (Nitzan *et al.*, 1999) is the initial slope of the OD versus time interval. Each experiment was repeated at least three times and liposomes without any protein or bovine serum albumin were used as negative controls.

2.2.20.3 Effects of anti-*Bps*Omp₃₈ antibodies on permeability of Omp₃₈

Anti-*Bps*Omp₃₈ polyclonal antibodies at various dilutions: 1:10; 1:100; 1:1,000; 1:10,000; and 1:100,000 were mixed with 50 µg of the purified native or refolded Omp₃₈, then incubated at 37 °C for 2 h. The antigen-antibody complex was subjected to liposome-swelling assays as described in Method 2.2.20.2. BSA and various dilutions of the antibodies added in the proteoliposome mixture without Omp₃₈ were used as negative controls.

2.2.21 Secondary structure determination

Secondary structure of Omp₃₈ was analyzed using either FTIR or CD spectroscopy.

2.2.21.1 Fourier Transform Infrared (FTIR) spectroscopy

FTIR determination was kindly done by Prof. Dieter Naumann, Robert-Koch Institute, Berlin, Germany. Briefly, FTIR measurements were carried out using a Bruker IFS-66 FTIR spectrometer equipped with a DTGS detector. The purified porins were measured in homemade demountable

equipped cells with CaF_2 windows. Aliquots of the protein solutions (5 μl , 10 mg/ml) were first dried in a vacuum centrifuge for 5 min with $^2\text{H}_2\text{O}$ (5 μl). To compensate for $^2\text{H}_2\text{O}$ absorption, buffer solutions were subtracted using the same cells. The path length was about 50 μm . FTIR spectra of the protein solutions were recorded using identical scanning parameters. Typically, the nominal physical resolution was 4 cm^{-1} using a Happ-Genzel apodisation function for Fourier transformation and a zerofilling factor of 4 to yield a data encoding interval of 1 data point per wavenumber and 32 scans were accumulated before performing the Fourier-transform analysis to optimize the signal-to-noise ratio. The protein spectrum was obtained after subtracting the buffer spectrum from the spectrum of the protein solution measured under the same conditions. To eliminate spectral contributions due to atmospheric water vapor, the instrument was continuously purged with dry air. Spectral contributions from residual water vapor were eliminated using water vapor spectra measured under identical conditions. The absorption region 1000 to 4000 cm^{-1} was primarily monitored. However, to obtain secondary structure information on the proteins, the amide I and II absorption regions between 1300 to 1800 cm^{-1} were specifically acquired for second derivative plots.

2.2.21.2 Circular Dichroism (CD) spectroscopy

Secondary structure composition indicating unfolded and folded states of the expressed *BpsOmp38* and *BthOmp38* was determined with a Jasco J-715 spectropolarimeter (Japan Spectroscopic Co., Japan). The purified Omp38 (0.5

mg/ml) was used and CD spectral data were acquired at both far UV (180-250) and near UV (250-320 nm) regions. CD measurements were performed at 25 °C with a scan speed of 20 nm/min, 2 nm bandwidth, 100 mdeg sensitivity, an average response time of 2 s and an optical path length of 0.2 mm. A minimum of three consecutive scans was accumulated, and the average spectra were stored. The baseline buffer for the native proteins was 10 mM Tris-HCl, pH 8.0. The buffer baseline for the unfolded proteins was 8 M urea in 20 mM Tris-HCl, pH 7.0. The baseline buffer for the refolded proteins was 20 mM Tris-HCl, pH 7.0 containing 0.05% Zwittergent® 3-14. The baseline for each buffer was measured and subtracted from the corresponding spectrum. The raw data were transformed to mean residue molar ellipticity (MRE) using the following equation:

$$[\theta] = (73.33 m^\circ) / ([\text{prot}]_{\text{mM}} l_{\text{cm}} n)$$

Where $[\theta]$ is the MRE in $\text{deg cm}^2 \text{dmole}^{-1}$, n is the number of amino acids in the polypeptide chain, m° is the measured ellipticity, and l is the path length in centrimeters.

The intensity of JASCO standard CSA (nonhygroscopic ammonium (+)-10-camphorsulfonate) at wavelength 290 nm was around 45 units. Therefore, the conversion factor was calculated to be 3,300/CSA intensity at 290 nm or 73.33 using the equation described above. The number of amino acids per Omp38 monomer was estimated to be 354 with the calculated molecular weight of 37,163.5 Da.

2.2.22 Molecular weight determination of Omp38

Gel filtration chromatography on a Sephacry S-200 HR column was used to determine the molecular weight of Omp38 at different states (native, unfolded and folded). The molecular weight markers (Sigma) including lysozyme (14 kDa), ovalblumin (45 kDa), albumin (66 kDa), alcohol dehydrogenase (150 kDa) were used to estimate the native and unfolded molecular weights of Omp38. A (1.5 x 95 cm) Sephacryl S-200 HR column was pre-equilibrated with 20 mM Tris-HCl, pH 7.0. To determine the void volume (V_0), 0.5 ml of blue dextran (4 mg/ml) in the equilibration buffer was applied to the column. The column was eluted with the equilibration buffer at a flow rate of 1.0 ml min⁻¹. Fractions of 1 ml were collected and their absorbance at 280 nm was measured. To determine the elution volume (V_e), each protein was dissolved in an elution buffer containing 1% SDS and 0.5 M NaCl in 10 mM Tris-HCl, pH 8.0. Standard protein concentrations used to determine the molecular weight of unknown samples is shown in Table 2.2. Each protein sample (0.5 ml) was applied to the column separately and eluted under the same condition as used for blue dextran. In the case of the refolded Omp38, the column was previously equilibrated with 0.05% Zwittergent® 3-14 in 20 mM Tris-HCl, pH 7.0. The protein was eluted with the same buffer condition. The unfolded Omp38 was applied to the column, which was equilibrated and eluted with 8 M urea in 20 mM Tris-HCl, pH 7.0. Concentrations of the eluted proteins were estimated by measuring A_{280} . To determine the molecular weight of Omp38, the ratio of V_e/V_0 for each standard protein was plotted against its molecular weight on a semi logarithmic scale.

Table 2.2 Concentrations of standard proteins and blue dextran used for gel filtration chromatography.

Protein sample	M_r	Concentration (mg/ml)
Blue dextran	2,000	4
Alcohol dehydrogenase	150	8
Albumin, Bovine	66	10
Ovalbumin, hen egg white	45	10
Lysozyme	14	10
Native Omp38 or refolding Omp38	-	2
Unfolded Omp38 in 8 M Urea	-	2

2.2.23 Membrane topology and 3D structural predictions

The membrane topology of Omp38 was predicted by the method of Diederichs *et al.* (1998) (http://strucbio.biologie.uni-konstanz.de/~kay/om_topo_predict2a.html). Transmembrane domains were obtained using the PSORT program by prediction of the protein localization sites (<http://psort.ims.u-tokyo-ac.jp/cgi-bin/okumura.pl>).

A potential 3D-structural model of Omp38 was constructed using 3D-PSSM (<http://www.sbg.bio.ic.ac.uk/~3dssm>), 123D+ search (<http://123d.ncifcrf.gov>), and Swiss-Model analysis (<http://www.expasy.org/swissmod>). The structural prediction was performed based on the primary sequence and 3D structure of anion-selective porin,

Omp32, of *Comamonas acidovorans* (accession number 1E54_A, PDB 1E54) (Zeth *et al.*, 2000).

2.2.24 Preliminary crystallization studies of the expressed and refolding Omp38

The sitting drop vapor diffusion method was used for crystallization of the refolded Omp38 (Garavito and Rosenbusch, 1986). One ml of each MembFac reagent was added into a reservoir of a 24-wells sitting drop plate. The MembFac precipitant reagents obtained from the crystallization screen kit (Hampton Research, USA) are shown in Appendix F. The protein concentration of approximate 3 mg/ml in 20 mM Tris-HCl, pH7.0 containing 0.05% Zwittergent® 3-14 (5 µl) were mixed with an equal volume of each precipitant (Figure 2.1). Crystal plates were covered with a clear film and incubated at room temperature. Crystals were observed under a stereomicroscope (Appendix G) every second day after incubation. The crystallization set up is shown in Figure 2.1. To confirm that the obtained crystals were Omp38, a single crystal was fished using a crystal loop and mounted on a glass slide, then washed with the precipitant that was used in crystallization set up, followed by a small volume of distilled water in a 1.5-ml microtube. The dissolved crystal was mixed with 5x SDS sample buffer, then heated at 95 °C for 5 min and applied to a 12% SDS-PAGE.

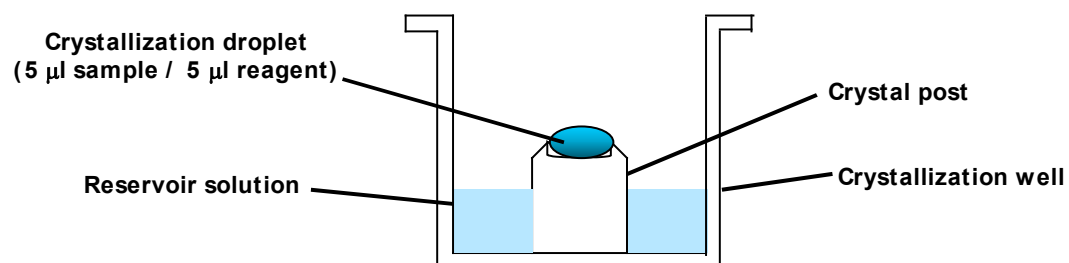


Figure 2.1 Crystallization setting by the sitting drop method.

Chapter III

Results

3.1 Isolation and purification of outer membrane proteins from *B. pseudomallei* and *B. thailandensis*

Outer membrane proteins were isolated from *B. pseudomallei* type strain ATCC23343 and *B. thailandensis* type strain ATCC700388. The bacteria were grown for 18 h at 37 °C and the cells were collected by centrifugation (see Method 2.2.1). After the bacterial whole cells were broken by sonication, cell debris was removed and total membranes were separated from the whole cell lysates by centrifugation. Supernatants containing non-outer membrane fraction were discarded and total membrane proteins were subjected to SDS extractions. Peptidoglycan-associated proteins were solubilized by 2% SDS and 0.5 M NaCl, and further purified using Sephacryl S-200 HR filtration chromatography (see Method 2.2.2). Figures 3.1 and 3.2 show SDS-PAGE analysis of the outer membrane protein fractions isolated from *B. pseudomallei* and *B. thailandensis*, respectively SDS-PAGE analysis of the purified outer membrane proteins, designated in *Materials and Methods* as *BpsOmp38* and *BthOmp38*, obtained after the final purification step is presented in Figure 3.3. The SDS-PAGE compared under heated (Figures 3.1 and 3.2, lanes 1, 3 and 5) and unheated (Figures 3.1 and 3.2, lanes 2, 4, and 6) conditions showed similar protein patterns for both *B. pseudomallei* and *B. thailandensis*. When the protein samples were heated at 95 °C for 5 min, the peptidoglycan-associated fractions

obtained after 0.5% SDS following 2% SDS and 0.5 M NaCl extractions gave two major protein bands. The high molecular weight band migrated at 110 kDa, (Figure 3.1 and 3.2, lane 6), whereas the low molecular weight band migrated at 38 kDa (Figures 3.1 and 3.2, lane 5). However, when the protein samples were not heated prior to subjecting to SDS-PAGE, the 38-kDa band seemed to disappear and only the 110-kDa was detectable (Figures 3.1 and 3.2, lane6). Figure 3.3 shows SDS-PAGE analysis of *BpsOmp38* and *BthOmp38* obtained after Sephacryl S-200 HR filtration chromatography. Similar results were observed where the 110-kDa band (lanes 2 and 4) was dissociated to the 38-kDa band when the protein samples were heated at 95 °C for 5 min (lanes 1 and 3). Western blot analysis later confirmed that the 38-kDa band was monomeric subunits of the 110-kDa Omp38.

Purification of Omp38 from *B. pseudomallei* and *B. thailandensis* is shown in Table 3.1. The results showed that the total crude proteins obtained from a 2-liter culture were 492 mg for *B. pseudomallei* and 296 mg for *B. thailandensis*. The total membranes isolated from total crude proteins by microcentrifugation at 12,000 x g were 175.4 mg, giving 36% yield of *BpsOmp38* and 107.4 mg, giving 36% yield of *BthOmp38*. Further purification was performed using SDS extractions, followed by Sephacryl S-200 HR filtration chromatography (see Methods 2.2.1 and 2.2.2). The total proteins of *Bpsomp38* and *BthOmp38* obtained from Sephacryl S-200 HR filtration step were 0.8 mg (equal to 0.2% yield) and 0.6 mg (equal to 0.2% yield), respectively. These purified *BpsOmp38* and *BthOmp38* were further used for structural determination and functional study.

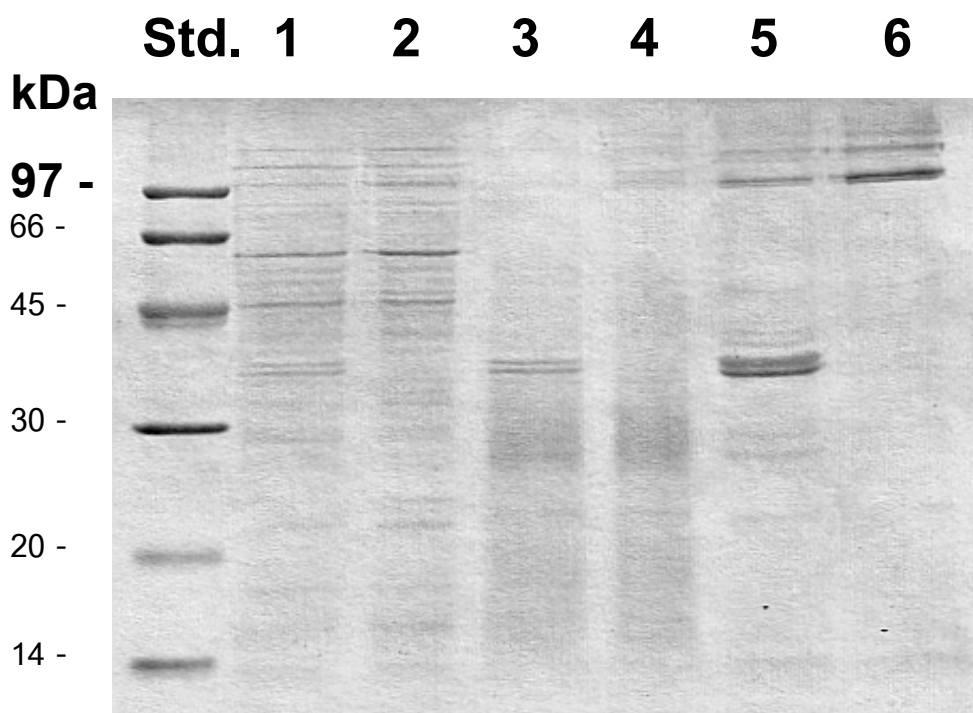


Figure 3.1 SDS-PAGE of peptidoglycan-associated proteins from *B. pseudomallei* ATCC23343.

Non-membrane fractions after the bacterial cells were broken (lanes 1 and 2). SDS-soluble materials when total membranes were extracted with 0.5% SDS (lanes 3 and 4). The peptidoglycan-associated protein fractions after 2% SDS and 0.5 M NaCl extraction (lanes 5 and 6). Samples (10 μ g) were solubilized in SDS sample buffer either heated at 95 °C (lanes 1, 3 and 5) or unheated (lanes 2, 4 and 6). Std is standard protein molecular weight markers.

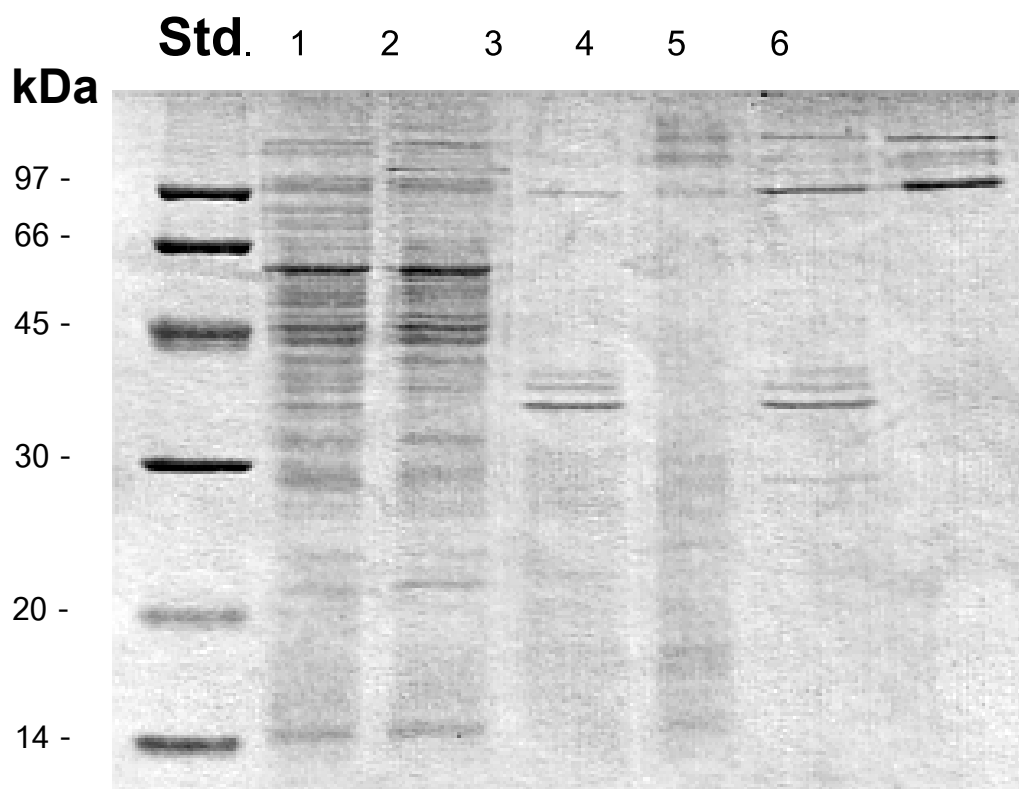


Figure 3.2 SDS-PAGE of peptidoglycan-associated proteins from *B. thailandensis* ATCC700388.

Non-membrane fractions after the bacterial cells were broken (lanes 1 and 2). SDS-soluble materials when total membranes were extracted with 0.5% SDS (lanes 3 and 4). The peptidoglycan-associated protein fractions after 2% SDS and 0.5 M NaCl extraction (lanes 5 and 6). Samples (10 μ g) were solubilized in SDS sample buffer either heated at 95 °C (lanes 1, 3 and 5) or unheated (lanes 2, 4 and 6). Std is standard protein molecular weight markers.

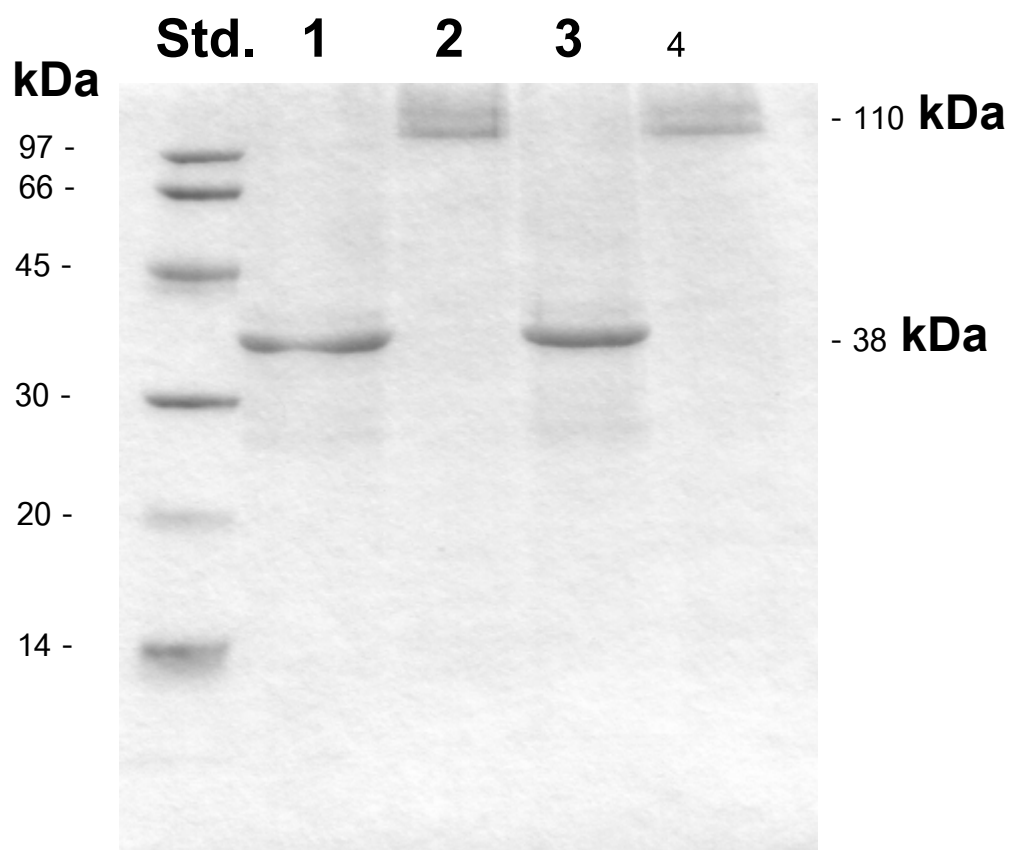


Figure 3.3 SDS-PAGE of Omp38 purified from *B. pseudomallei* and *B. thailandensis* by Sephacryl S-200 HR filtration chromatography.

Samples (5 μ g) were solubilized in 5x SDS sample buffer either heated *Bps*Omp38 (lanes 1) and *Bth*Omp38 (lane 3) or unheated *Bps*Omp38 (lane 2) and *Bth*Omp38 (lane 4) at 95 °C for 5 min. Std is standard molecular weight of protein markers.

Table 3.1 Purification of Omp38 from a 2-liter culture of *B. pseudomallei* and *B. thailandensis*. The results are the average values of two separate experiments for each protein.

Purification step	<i>Bps</i>-proteins (mg)	Yield (%)	<i>Bth</i>-proteins (mg)	Yield (%)
1. Total crude protein	492.0	100	296.0	100
2. Total membrane proteins	175.4	36	107.4	36
3. Peptidoglycan-associated fraction				
- 0.5% (w/v) SDS extraction	5.4	1.1	3.4	1.1
- 2% SDS (w/v) and 0.5 M NaCl extraction	5.0	1.0	3.0	1.0
4. Sephacryl S200 HR filtration chromatography and dialysis	0.8	0.2	0.6	0.2

3.2 Antibody production and Western blot analysis

After the Omp38 proteins were isolated from the outer membrane of *B. pseudomallei* and *B. thailandensis* and purified using Sephacryl S-200 HR filtration chromatography, *BpsOmp38* was separated on SDS-PAGE and the 38-kDa band was excised from a gel and used to raise polyclonal antiserum (Method 2.2.6). Initially, the antiserum was diluted to various dilutions: 1:2,500; 1:5,00; 1:10,000, and 1:20,000, to determine the appropriate dilution for Western blot analysis. The proper dilution of antibodies, which gave a clear signal of antigen-antibody complex with less nonspecific background was found to be 1:10,000 (Figure 3.4). Therefore, this dilution was used for identification of *BpsOmp38* and determination of cross-reactivity of *BthOmp38* by immunoblotting. SDS-PAGE following Western blot analysis of the purified Omp38 (Figure 3.5) shows that the antibodies strongly reacted with the protein bands of 110 kDa (trimeric) (Figure 3.5 A and B, lanes 1 and 2) and 38 kDa (Figure 3.5 C and D, lanes 1 and 2). Moreover, the antibodies also recognized a ~110-kDa protein (Figure 3.5 A and B, lane 3) and a 39-kDa protein (Figure 3.5, C and D, lane 3) from *E. coli* BL21(DE3)pLysS outer membrane fraction. In addition, the antibodies also strongly recognized the protein band corresponding to OpcPO (81 kDa), the monomeric protein bands corresponding to OpcP1 (36 kDa) and OpcP2 (27 kDa), as well as a non-identified 18 kDa of *B. cepacia* OM crude fraction. None of these proteins was recognized by rabbit pre-immune serum.

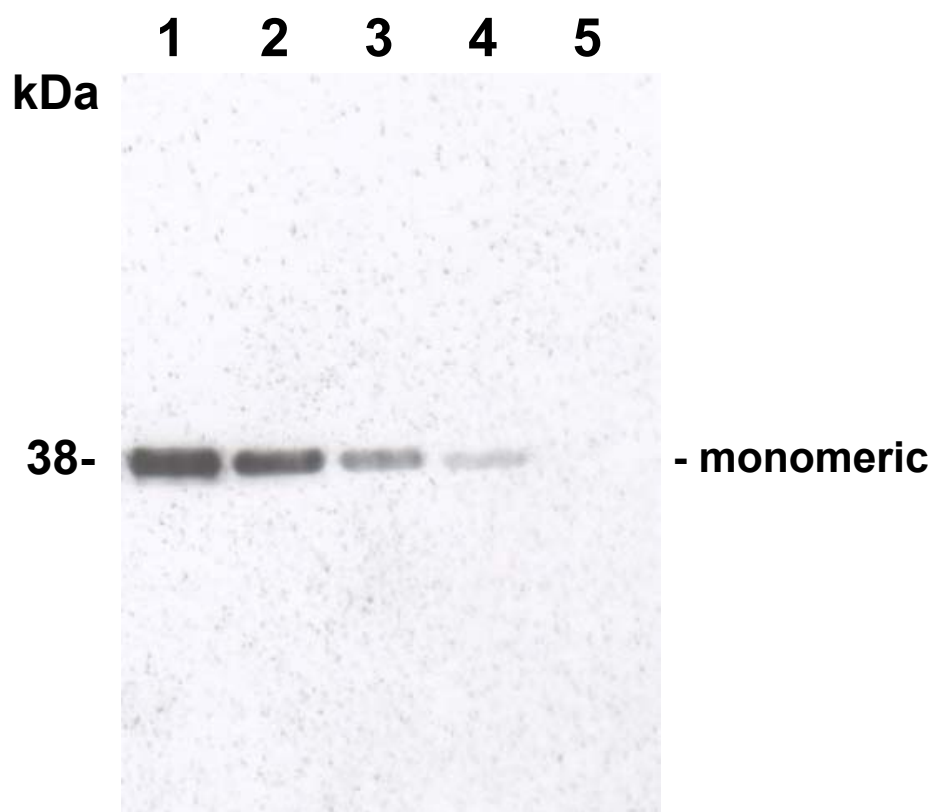


Figure 3.4 Determination of the proper dilution of anti-*BpsOmp38* polyclonal antibodies for Western blot analysis.

The rabbit antiserum was diluted to various dilutions (lanes: 1, 1:2,500; 2, 1: 5,000; 3, 1:10,000; 4, 1: 20,000) and used to determine the appropriated dilution for Western blot analysis. Lane 5 is the pre-immune serum.

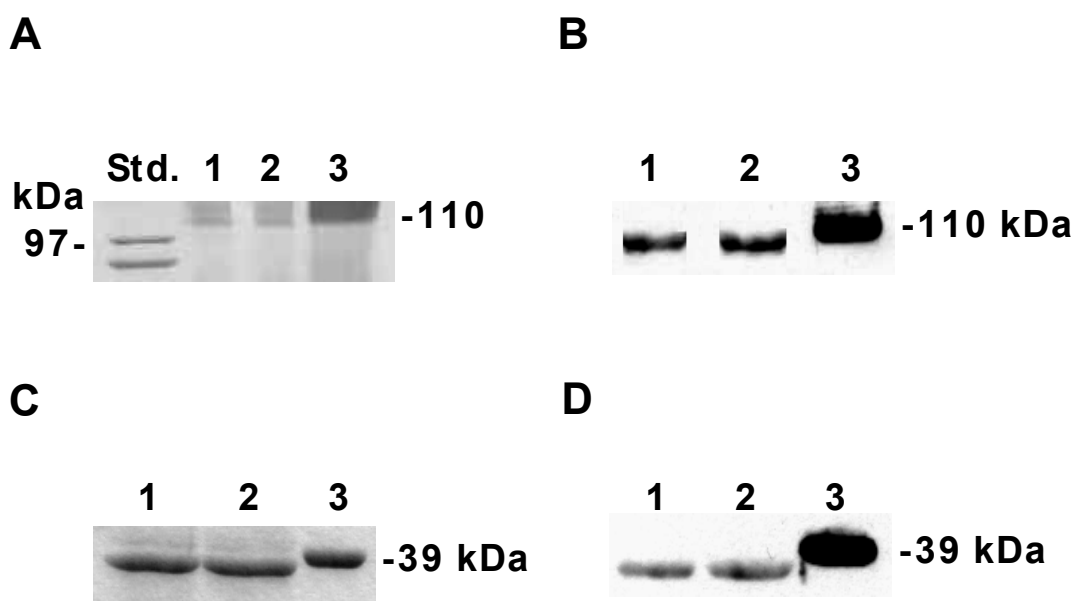


Figure 3.5 Immunoblots of *BpsOmp38*, *BthOmp38* and *Escherichia coli* BL21(DE3)pLysS porin.

(A) Unheated protein before SDS-PAGE analysis and (B) The corresponding immunoblot using anti-*BpsOmp38* polyclonal antibodies (C) Heated sample before SDS-PAGE analysis and (D) The corresponding immunoblot. Std is molecular weight of protein markers. Lanes:1, *BpsOmp38*; 2, *BthOmp38*; 3, *E. coli* BL21(DE3)pLysS.

3.3 Pore-forming activity of the native Omp38

Pore-forming activities of *BpsOmp38* and *BthOmp38* were determined using liposome-swelling assays. Accordingly, the purified proteins isolated from *B. pseudomallei* and *B. thailandensis* were reconstituted into proteoliposomes prepared as described in Method 2.2.20.2. In principle, diffusion of solutes through the protein pores will cause the liposomes to swell, leading to a decrease in optical density at wavelength 400 nm. The results in Figures 3.6 and 3.7 reveal that L-arabinose (M_r 150), which is the smallest sugar tested in this experiment, gave highest diffusion rate, followed by the diffusion rates obtained for D-glucose (M_r 180), D-mannose (M_r 180), D-galactose (M_r 180), N-acetylglucosamine (M_r 221), D-sucrose (M_r 342) and D-melezitose (M_r 522). On the other hand, stachyose gave slowest diffusion rate as it has the highest M_r (M_r 667) compared to other sugar molecules. The results obtained from both *BpsOmp38* and *BthOmp38* were similar. The results suggested that Omp38 proteins act as a porin-like channel and the permeation rates of solutes that passed through the Omp38 channels decreased with an increase in M_r of sugar molecules indicated the general diffusion characteristic of the channels.

Figures 3.8 and 3.9 represent the diffusion rates of the sugars through the Omp38 pores relatively to the diffusion rate of L-arabinose. Similarly, as shown in Figures 3.8 and 3.9, the relative diffusion rate of sugar solutes through Omp38 decreased when the size of sugar increased, where the relative permeability corresponding to D-glucose (M_r 180) showed highest relative diffusion rate, followed by N-acetylglucosamine (M_r 221), D-sucrose (M_r 342), D-melezitose (M_r 522) and stachyose (M_r 667), respectively. A “limiting” M_r that can pass through

the Omp38 channels was estimated to be ~650 (defined as the value corresponding to 5% relative permeability) (Figure 3.10). The results obtained for *Bps*Omp38 and *Bth*Omp38 were found to be similar.

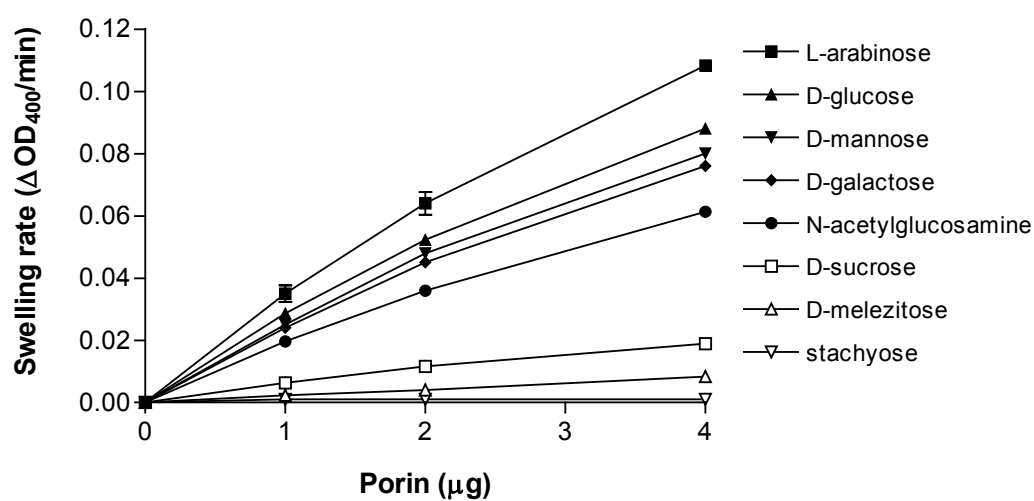


Figure 3.6 Liposome-swelling assays of *Bps*Omp38.

Diffusion rates of neutral saccharides were determined by liposome-swelling assays using proteoliposomes reconstituted with various amounts of the purified *Bps*Omp38 isolated from *B. pseudomallei* ATCC23343.

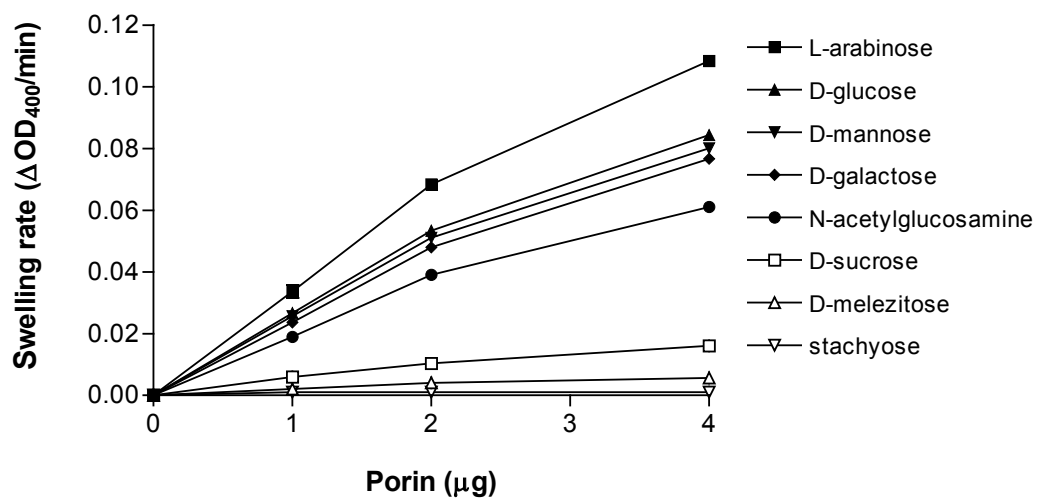


Figure 3.7 Liposome-swelling assays of *BthOmp38*.

Diffusion rates of neutral saccharides were determined by liposome-swelling assays using proteoliposomes reconstituted with various amounts of the purified *BthOmp38* isolated from *B. thailandensis* ATCC700388.

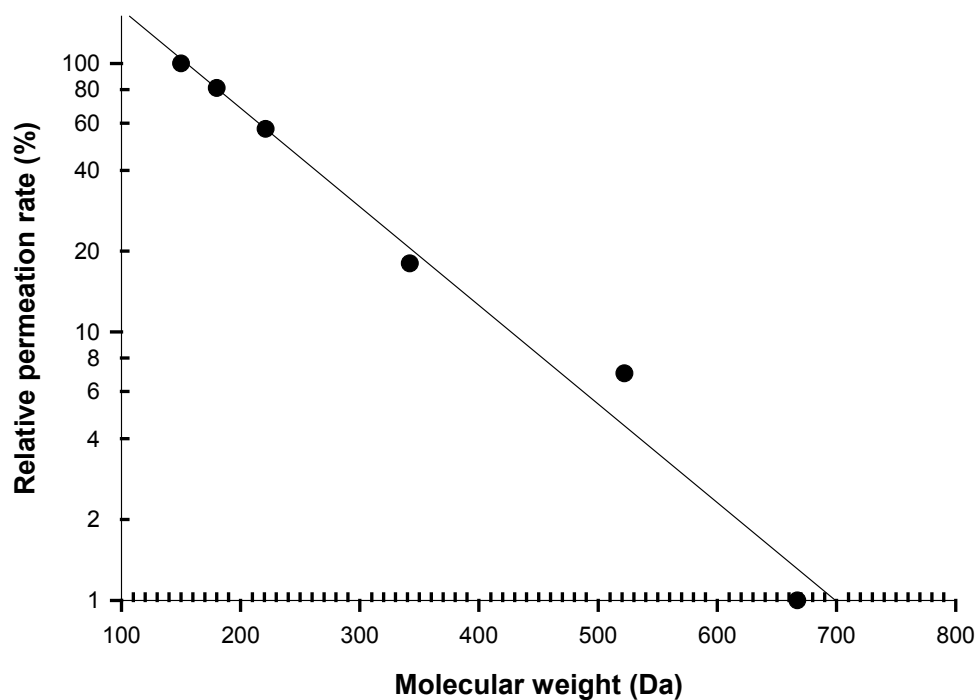


Figure 3.8 Relative permeation rates of neutral sugars through liposomes reconstituted with the purified *BpsOmp38*.

The permeation rates of neutral sugars through the reconstituted proteoliposomes were prepared according to Method 2.2.20.2. The values are normalized to the permeation rate of L-arabinose and plotted on a logarithmic scale. The sugars used are: L-arabinose (M_r 150), D-glucose (M_r 180), N-acetylglucosamine (M_r 221), D-sucrose (M_r 342), D-melzitose (M_r 522) and stachyose (M_r 667).

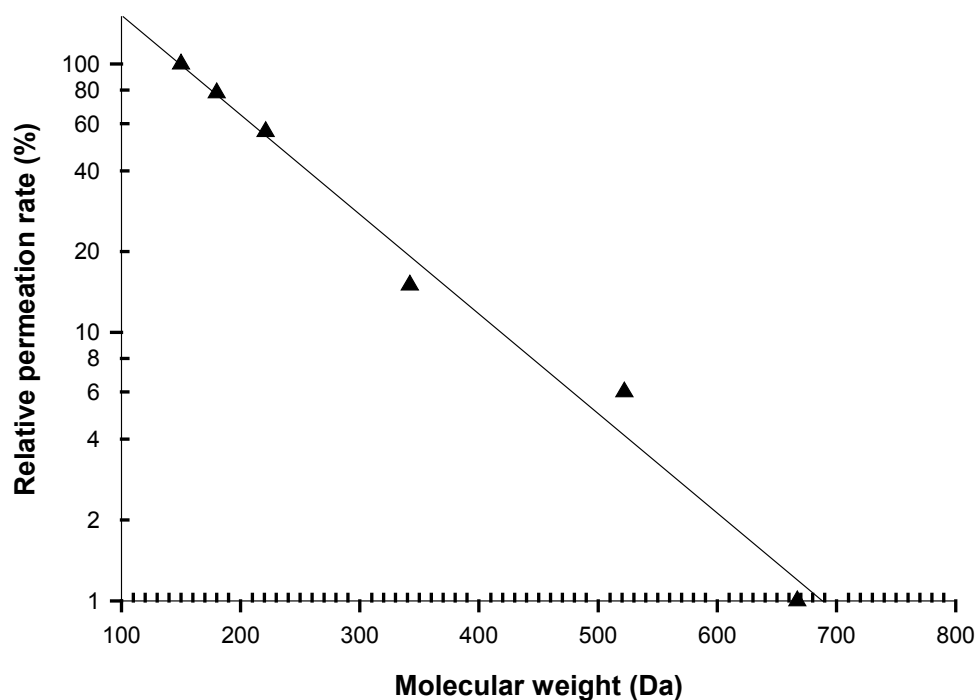


Figure 3.9 Relative permeation rates of neutral sugar through liposomes reconstituted with the purified *BthOmp38*.

The permeation rates of neutral sugars through the reconstituted proteoliposomes were prepared according to Method 2.2.20.2. The values are normalized to the permeation rate of L-arabinose and plotted on a logarithmic scale. The sugars used are: L-arabinose (M_r 150), D-glucose (M_r 180), N-acetylglucosamine (M_r 221), D-sucrose (M_r 342), D-melizitose (M_r 522) and stachyose (M_r 667).

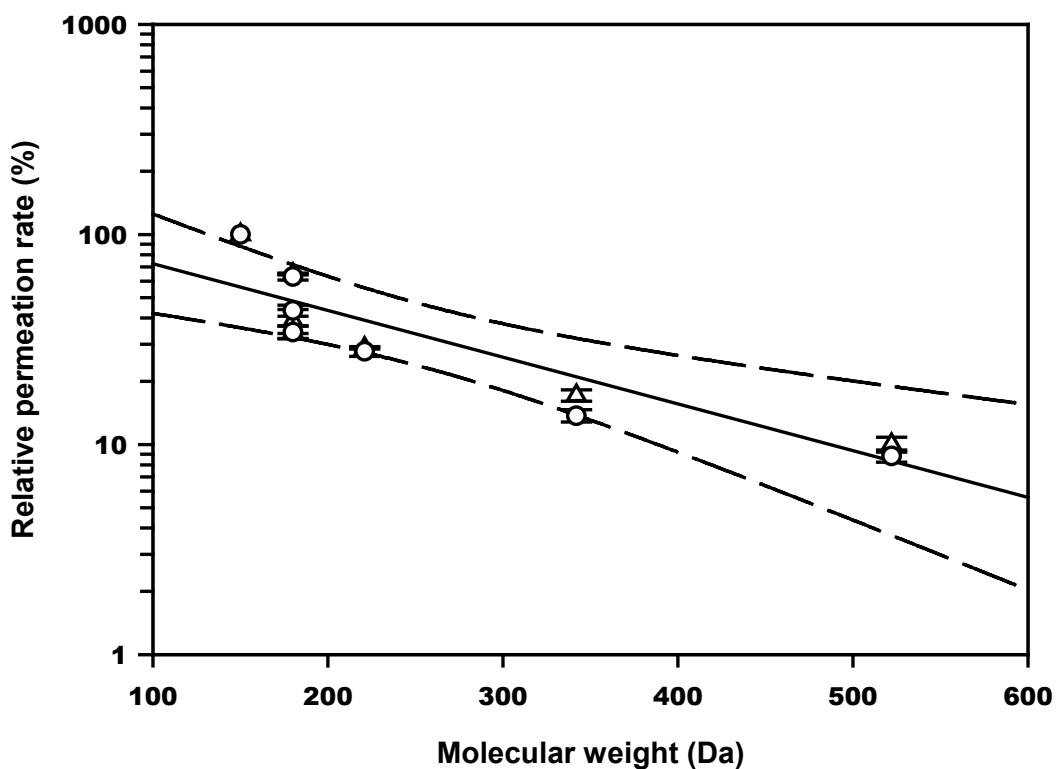


Figure 3.10 Relative permeability rates and the size exclusion limit of *BpsOmp38* and *BthOmp38*.

Initial relative swelling rates for liposomes reconstituted with the purified *BpsOmp38* (Δ) and *BthOmp38* (o) porins plotted on a logarithmic scale against the molecular weight of the solute-dependent permeation. Data are shown as means \pm SEM ($n = 3$ triplicate measurements in a single experiment for each protein, swelling rate for arabinose is 100%). The size-dependent swelling rates for the two porins are indistinguishable, and the straight line is a regression fit to all the data. The dashed lines indicate the 95% confidence limits of the fit. The near-limiting M_r defined as 5% relative permeability through both *Burkholderia* porins is ~ 650 .

3.4 Secondary structure determination using Fourier Transform Infrared (FTIR) spectroscopy

The secondary structure of the purified *BpsOmp38* and *BthOmp38* were determined by FTIR, as described in Method 2.2.21.1. The second derivative spectra (Figure 3.11) gained from FTIR measurements at the amide I region revealed extensive secondary structure similarity between *BpsOmp38* and *BthOmp38*. Their spectra could almost be directly superimposed apart from differences in the ester carbonyl stretching regions (signals at $1,727\text{ cm}^{-1}$ and $1,740\text{ cm}^{-1}$), which most probably originate from residual lipopolysaccharide tightly bound to the porin (Mäntele and Fabian, 2002). These indicated that *BpsOmp38* contained more associated LPS than *BthOmp38*. The secondary derivative plots in the amide I ($1,600$ to $1,700\text{ cm}^{-1}$) region showed that both proteins contained predominantly β -sheet, as indicated by the two distinct peaks at 1626 cm^{-1} and 1696 cm^{-1} , which is typical for the antiparallel β -pleated sheets of porins (Mäntele and Fabian, 2002; Abrecht *et al.*, 2000). Minor contributions at 1652 cm^{-1} and 1674 cm^{-1} were tentatively assigned to be loop and turn structures.

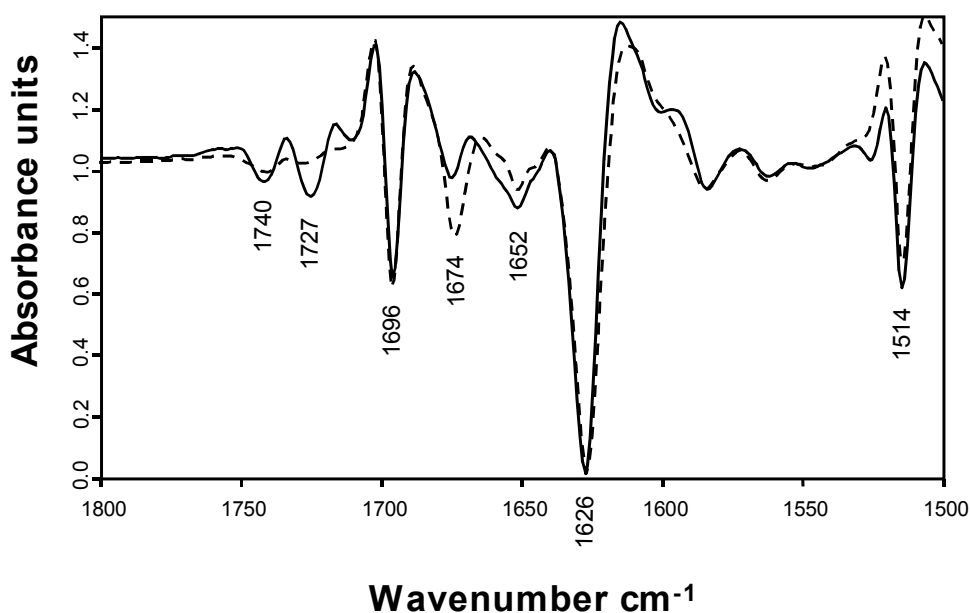


Figure 3.11 FTIR spectra of native *BpsOmp38* and *BthOmp38*.

FTIR spectra of the purified *BpsOmp38* (—) and *BthOmp38* (---) between 1,300-1,800 cm^{-1} were normalized using the IR band of Tyr (1,514 cm^{-1}) and superimposed. Signals at amid I region: 1,626 cm^{-1} represents β -sheet; 1,652 cm^{-1} and 1,674 cm^{-1} represent turns and loops; 1,696 cm^{-1} represents antiparallel β -pleated sheets; 1,740 cm^{-1} represent lipopolysaccharide.

3.5 Peptide mass analysis by MALDI-TOF MS and ESI/MS

Native *BpsOmp38* and *BthOmp38* were isolated and purified as described in Methods 2.2.1 and 2.2.2, respectively. The proteins were separated on SDS-PAGE, then the protein band (M_r 38,000) was subjected to in-gel digestion as described in

Method 2.2.5. Tryptic peptide masses were determined using MALDI-TOF MS and capillary HPLC/MS. MALDI mass fingerprints of the tryptic digests revealed almost identical peptide ensembles. When these peptides were separated on a capillary HPLC, then subjected to partial fragmentation using ESI-MS/MS, eight *BpsOmp38* peptides were identified including:

- 1) TDVYAQAVYQR, 2) GSEDLGGGLK, 3) SLWSVGAGVDQSR,
- 4) LNTNGDVAVNNTVK, 5) AYSAGASYQFQGLK,
- 6) QAFVGLSSNYGTVTLGR, 7) AIFTLESGFNIGNGR, and
- 8) NANASIYNGDLSTPFSTSINQTAATVGLR

and four identical *BthOmp38* peptides including:

- 1) GSEDLGGGLK, 2) SLWSVGAGVDQSR, 3) QAFVGLSSNYGTVTLGR, and
- 4) AIFTLESGFNIGNGR).

Sequest search of these identified fragments obtained from the available protein databases gave an unambiguous match to the outer membrane porin, OpcP₁, of *Burkholderia cepacia*. The corresponding nucleotide OpcP₁ sequence was found to be well aligned with a single predicted ORF in contig 836 of the incomplete *B. pseudomallei* genome (http://www.ncbi.nlm.nih.gov/sutils/genom_table.cgi).

The entire masses of *BpsOmp38* and *BthOmp38* were also determined by MALDI-TOF MS (Method 2.2.5.2). The average molecular masses of *BpsOmp38* and *BthOmp38* were $37,159 \pm 55$ Da (Figure 3.12 A) and $37,108 \pm 55$ Da (Figure 3.12 B), respectively.

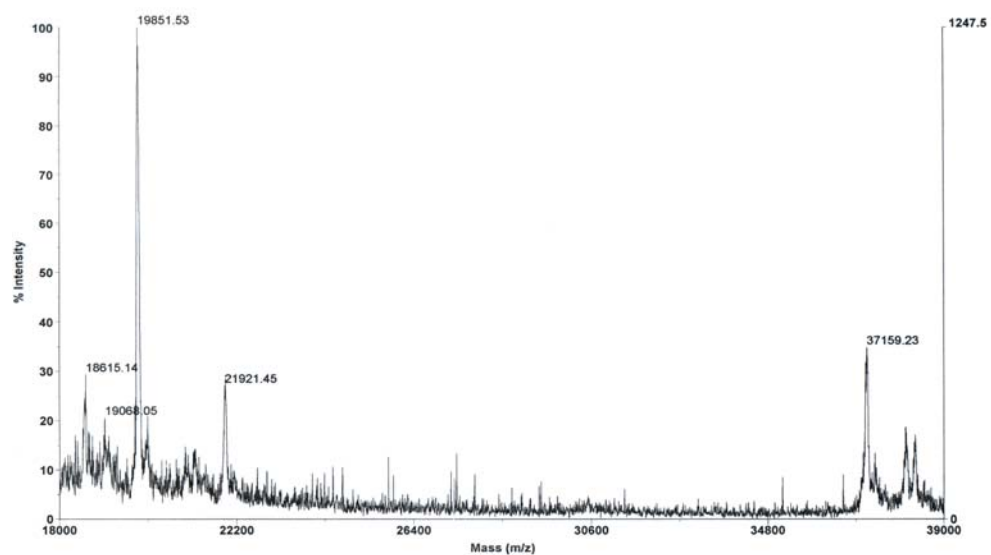
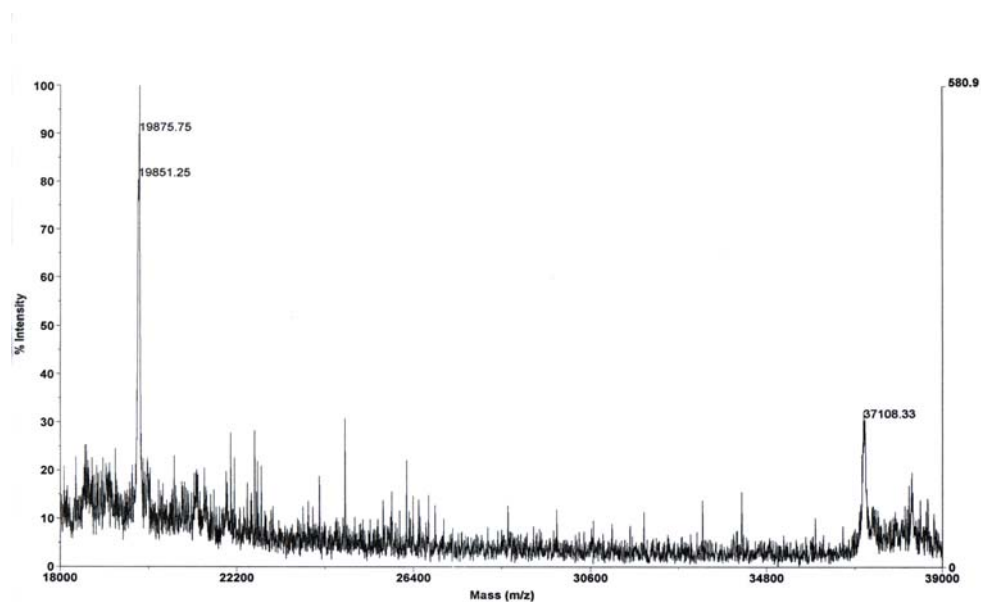
A**B**

Figure 3.12 Determination of the M_r of native Omp38 using MALD-TOF MS.

The average M_r of *Bps*Omp38 (A) and *Bth*Omp38 (B).

3.6 Gene isolation, nucleotide and amino acid sequence analysis

3.6.1 Gene isolation and nucleotide sequencing

As mentioned earlier, the peptide mass fingerprints of *BpsOmp38* and *BthOmp38* identified from MALDI-TOF MS and ESI-MS/MS matched with OpcP₁ of *B. cepacia* (see Result 3.5) and the nucleotide sequence that encodes OpcP₁ was well aligned with a predicted single ORF in contig 836 of the incomplete *B. pseudomallei* genome. A PCR-based strategy was therefore employed to amplify the full-length *BpsOmp38* and *BthOmp38* DNAs using the sense primer: 3'-ATGAACAAGACTCTGATTGTTGCA-5', and antisense primer: 3'-GAAGCGGTGACGCAGACCAA-5' (Figure 3.13). PCR reactions were carried out under the conditions described in Method 2.2.10.1 using the genomic DNA of *B. pseudomallei* and *B. thailandensis* as DNA templates. The PCR products of identical size (1.1 kb) are shown in Figure 3.14 (lane 1 for *BpsOmp38*) and (lane 4 for *BthOmp38*). DNA fragments containing *BpsOmp38* and *BthOmp38* genes were cloned into the pGEM®-T cloning vector (Promega) and transformed into the *E. coli* host strain DH5 α as described in Methods 2.2.10.2 and 2.2.10.3. The recombinant plasmids carrying *BpsOmp38* and *BthOmp38* DNA fragments, designated pGEM®-T-*BpsOmp38* and pGEM®-T-*BthOmp38* respectively, were identical in size (4.112 kb). Their supercoiled DNA migrated to approx. 3.0 kb on 1% agarose gel (Figures 3.14, lanes 2 and 5). The success of cloning of the *Omp38* DNA into the pGEM®-T vector was

confirmed by PCR amplification (Figure 3.14, lane 3 for pGEM®T-*BpsOmp38* and lane 6 for pGEM®T-*BthOmp38*). Nucleotide sequences of both inserts were determined automatically in both directions and have been deposited in the GenBank database under GenBank accession numbers AY312416 and AY312417 for *BpsOmp38* and *BthOmp38*, respectively. The nucleotide sequences of the full-length *BpsOmp38* and *BthOmp38* were determined to be 98% identical.

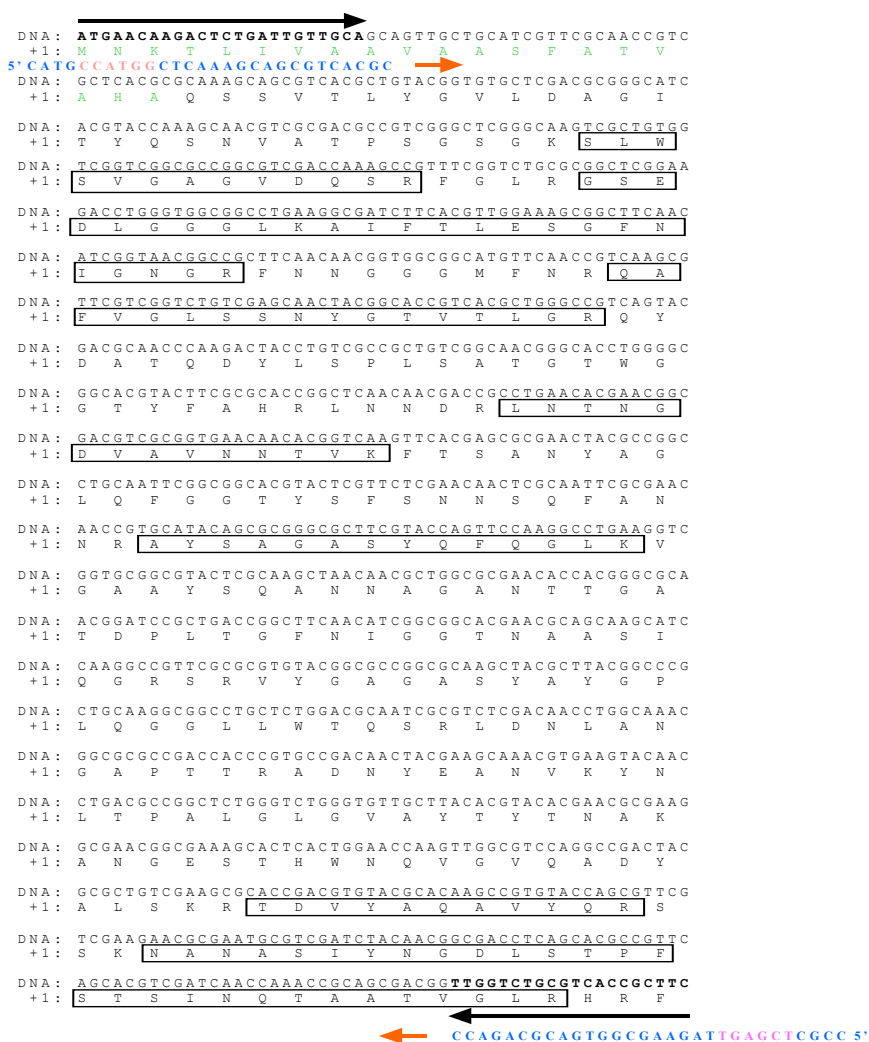


Figure 3.13 Identification of the *Omp38* gene in contig 836 of the incomplete

B. pseudomallei genome.

Black Arrows represent the set of primers used for amplifying the full-length *Omp38* DNAs. Blue letters are the flanking sequences containing endonuclease restriction sites for *NcoI* (orange) and *XhoI* (pink). The predicted signal peptide for *Omp38* is shown in green.

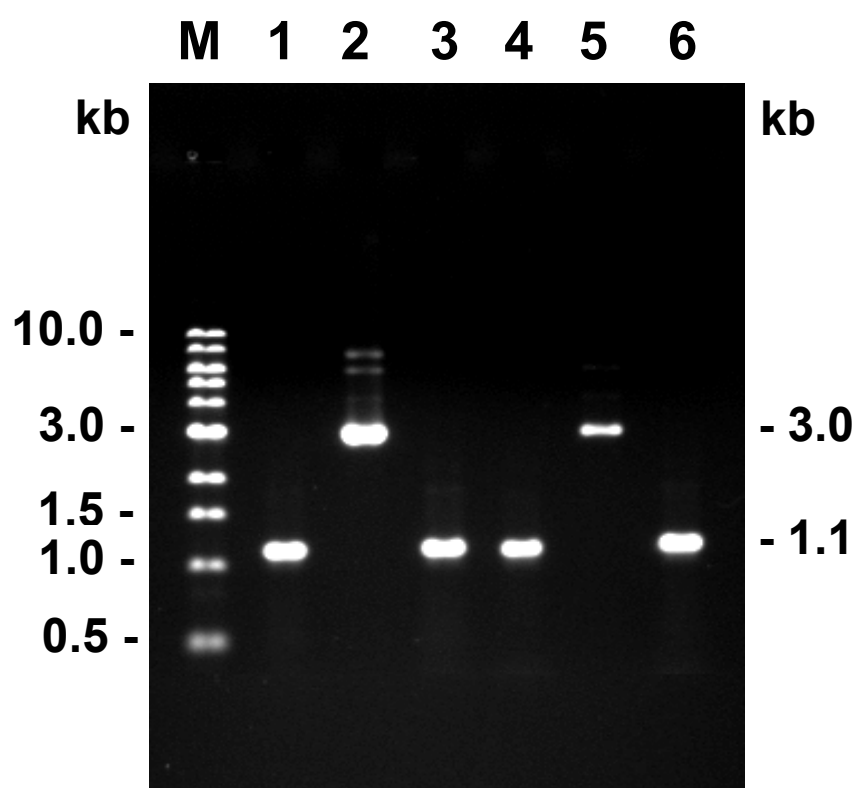


Figure 3.14 PCR amplification from genomic DNA of *B. pseudomallei* and *B. thailandensis*.

The PCR products were electrophoresed on 1% agarose gel. Lanes: M, 1 kb DNA ladder marker; 1, PCR products of *BpsOmp38*; 2, supercoiled plasmids of pGEM®T-*Bpsomp38*; 3, PCR products of *BpsOmp38*; lane 4 PCR products of *BthOmp38*; 5, supercoiled plasmids of pGEM®T-*Bthomp38*; 6, PCR products of *BthOmp38*.

3.6.2 Amino acid sequence analysis

After the genes encoding *BpsOmp38* and *BthOmp38* were isolated, their nucleotide sequences were subsequently determined. Result 3.6.1 shows that the DNA sequences of *BpsOmp38* and *BthOmp38* were 98% identical. SignalP V1.1 program obtained from <http://www.cbs.dtu.dk/services/SignalP> predicted the signal peptide sequence of Omp38 to be Met¹→Ala²⁰. The putative amino acid sequences of the two polypeptides translated from the corresponding nucleotide sequences were almost identical (99.7%) with the exception that the second *N*-terminal residue, asparagine, in the *BpsOmp38* sequence was replaced by aspartic acid in the *BthOmp38* sequence (Figure 3.15). However, the peptide composition as analyzed by MALDI-TOF MS and capillary HPLC-MS was identical for both mature proteins. The determined M_r of *BpsOmp38* ($37,159 \pm 55$) (see Result 3.5) was almost identical to the predicted M_r of the mature Omp38 ($37,163.5$), which was back translated from its corresponding nucleotide sequence obtained from Protparam tool program (http://us.expasy.org/cgi_bin/protparam). Moreover, the theoretical pI of Omp38 predicted by the same program was 9.30.

RPS-BLAST search (<http://www.ncbi.nlm.nih.gov/BLAST>) showed that Omp38 contained only one conserved domain, which matched with other 847 amino acid sequences of Gram-negative bacterial porins in the protein databases (Figure 3.16). This suggested that Omp38 belongs to the “porin” superfamily. The putative sequences of *BpsOmp38* and *BthOmp38* were further analyzed and found to be highly similar with that of OpcP1 of *B. cepacia* but had low similarity to other Gram-

negative bacterial porins as shown in Figure 3.17. By comparison with other porins with known 3D structure, especially *E. coli* OmpF (Cowan et al., 1995) and *Comamonas acidovorans* Omp32 (Zeth et al., 2000), the secondary structures of *BpsOmp38* and *BthOmp38* were predicted to contain 16- β strands, 8 loops, 8 turns and a short α helix (Tyr¹¹⁹→Lue¹²⁶) near the longest loop 3 (Ser¹²⁷→Asp¹⁵⁴) (Figure 3.17).

```

BpsOmp38 : MNKTLIVAAVAASFATVAHAQSSVTLYGVLDAGITYQSNVATPSGSGKSLWSVGAGVDQSR : 61
BthOmp38 : MDKTLIVAAVAASFATVAHAQSSVTLYGVLDAGITYQSNVATPSGSGKSLWSVGAGVDQSR : 61
M KTLIVAAVAASFATVAHAQSSVTLYGVLDAGITYQSNVATPSGSGKSLWSVGAGVDQSR

BpsOmp38 : EGLRGSSEDLGGGLKAIFTLESGFNIGNGRFNNGGGMFNROAFVGLSSNYGTVTLGRQYDAT : 122
BthOmp38 : EGLRGSSEDLGGGLKAIFTLESGFNIGNGRFNNGGGMFNROAFVGLSSNYGTVTLGRQYDAT : 122
EGLRGSSEDLGGGLKAIFTLESGFNIGNGRFNNGGGMFNROAFVGLSSNYGTVTLGRQYDAT

BpsOmp38 : QDYLSPLSATGTWGGTYFAHPLNNDRLNTNGDVAVNNTVKFTSANYAGLQFGGTYSF SNNS : 183
BthOmp38 : QDYLSPLSATGTWGGTYFAHPLNNDRLNTNGDVAVNNTVKFTSANYAGLQFGGTYSF SNNS : 183
QDYLSPLSATGTWGGTYFAHPLNNDRLNTNGDVAVNNTVKFTSANYAGLQFGGTYSF SNNS

BpsOmp38 : QFANNRAYSAGASYQFQGLKVGAAYSQANNAGANTTGATDPLTGFNIGGTNAASIQGRSRV : 244
BthOmp38 : QFANNRAYSAGASYQFQGLKVGAAYSQANNAGANTTGATDPLTGFNIGGTNAASIQGRSRV : 244
QFANNRAYSAGASYQFQGLKVGAAYSQANNAGANTTGATDPLTGFNIGGTNAASIQGRSRV

BpsOmp38 : YGAGASYAYGPLQGGLLWTQSRLDNLANGAPTIRADNYEANVKYNLTPALGLGVAYTYTNA : 305
BthOmp38 : YGAGASYAYGPLQGGLLWTQSRLDNLANGAPTIRADNYEANVKYNLTPALGLGVAYTYTNA : 305
YGAGASYAYGPLQGGLLWTQSRLDNLANGAPTIRADNYEANVKYNLTPALGLGVAYTYTNA

BpsOmp38 : KANGESTHWNQVGQADYALSKRTDVYAQAVYQRS SKNANASIYNGDLSTPFST SINQTAA : 366
BthOmp38 : KANGESTHWNQVGQADYALSKRTDVYAQAVYQRS SKNANASIYNGDLSTPFST SINQTAA : 366
KANGESTHWNQVGQADYALSKRTDVYAQAVYQRS SKNANASIYNGDLSTPFST SINQTAA

BpsOmp38 : TVGLRHRF : 374
BthOmp38 : TVGLRHRF : 374
TVGLRHRF

```

Figure 3.15 The amino acid sequence alignment of Omp38.

The putative amino acid sequences of *BpsOmp38* and *BthOmp38* were aligned using ClustalW and displayed by Genedoc program. The signal peptides of both proteins are given in an open box.

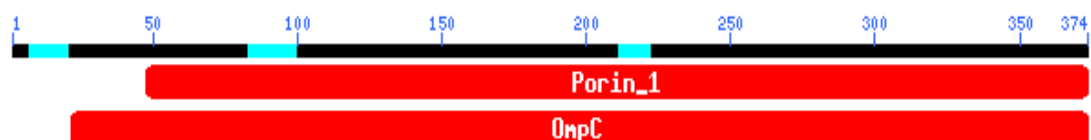


Figure 3.16 Identification of conserved domains and protein family of Omp38. RPS-BLAST indicated that the Omp38 proteins contained one conserved domain, which is classified as a bacterial porin superfamily.

3.7 Subcloning of *Omp38* DNA fragments into the pET23d(+) expression vector

After the putative signal peptides of *BpsOmp38* and *BthOmp38* were identified using SignalP as described in Result 3.6.2. A set of primers containing the restriction sites for *NcoI* and *XhoI* were designed for amplification of the *Omp38* fragment encoding the protein lacking its signal peptide (Figure 3.13). Moreover, the initiation codon (ATG) followed by two nucleotides (GC) were included in the sense primer sequence to ensure that the *Omp38* inserts were inframe. The stop codon (TAA) was also included in the antisense primer. As a result, the expressed proteins were expected to contain two additional amino acid residues including Met¹ and Ala² at the *N*-terminal end. PCR products of ~1.1 kb (Figure 3.18, lane 1 for *BpsOmp38* and lane 2 for *BthOmp38*) were cloned into the pET23d(+) vector at the *NcoI* and *XhoI* sites. The recombinant plasmids, designated pET23d(+)-*BpsOmp38* (Figure 3.19, lane 2) and pET23d(+)-*BthOmp38* (Figure 3.19, lane 3), were shown to migrate less slowly than the pET23d(+) plasmid without insert (Figure 3.19, lane 1). The pET23d(+)-*BpsOmp38* and pET23d(+)-*BthOmp38* were subsequently transformed into the *E. coli* DH5 α cells.

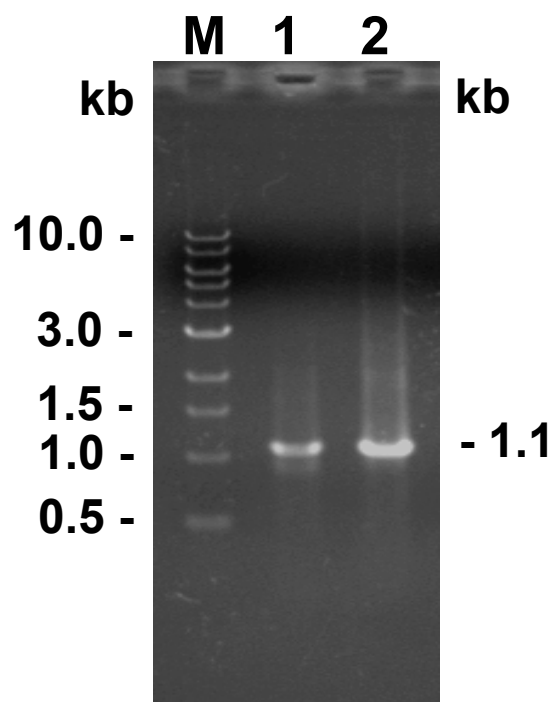


Figure 3.18 PCR amplification of *Omp38* DNA fragments lacking a signal peptide sequence.

The PCR products were analyzed on 1% agarose gel. Lanes: M, 1 kb DNA ladder marker; 1, *BpsOmp38* PCR product; 2, *BthOmp38* PCR product.

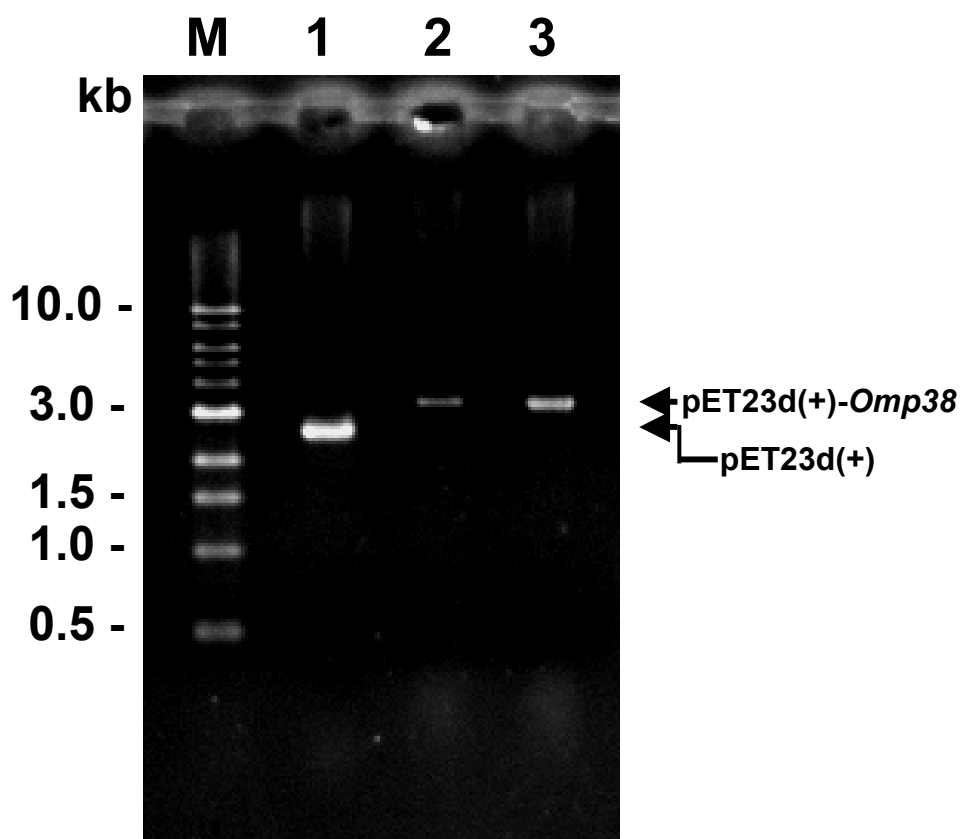


Figure 3.19 Subcloning of *Omp38* fragments into the pET23d(+) plasmid.

Lanes: M is 1 kb DNA ladder marker; 1, pET23d(+) plasmid vector; 2, pET23d(+)-*BpsOmp38* ; 3, pET23d(+)-*BthOmp38*.

3.8 Expression of Omp38 in *E. coli*

The recombinant plasmids, pET23d(+)-*BpsOmp38* and pET23d(+)-*BthOmp38*, were purified from *E. coli* DH5 α cells and transformed into *E. coli* Origami(DE3) cells for a large-scale production. When the cells were grown to log phase (OD₆₀₀ ~0.6), Omp38 expression were induced by adding IPTG (0.4 mM) at 37 °C for 1.5 h. Figure 3.20 A shows the whole-cell lysate of *E. coli* expressing *BpsOmp38* (lane 2) and *BthOmp38* (lane 4). Western blot analysis using anti-*BpsOmp38* polyclonal antibodies reacted with a protein band corresponding to 38 kDa (lanes 2 and 4), while no signal was detected with the whole cell lysate without IPTG induction (lanes 1 and 3). This suggested that the expressed proteins were *BpsOmp38* and *BthOmp38* (Figure 3.20 B). The native *BpsOmp38* (lane 5) and native *BthOmp38* (lane 6) were included as positive controls (Figure 3.20 A and B).

The Omp38 proteins were expressed in *E. coli* Origami(DE3) as insoluble inclusion bodies. After the induced cells were broken by sonication and the inclusion bodies were pelleted by centrifugation, the inclusion bodies were solubilized in 10 ml of freshly prepared 8 M urea. The soluble proteins were subsequently purified by a strong cation exchange (SP Fast Flow HiTrap[™]) column, followed by a weak anion exchange (DEAE Fast Flow HiTrap[™]) column chromatography (see Method 2.2.18). The highly purified monomeric proteins were confirmed on SDS-PAGE as shown in Figure 3.21.

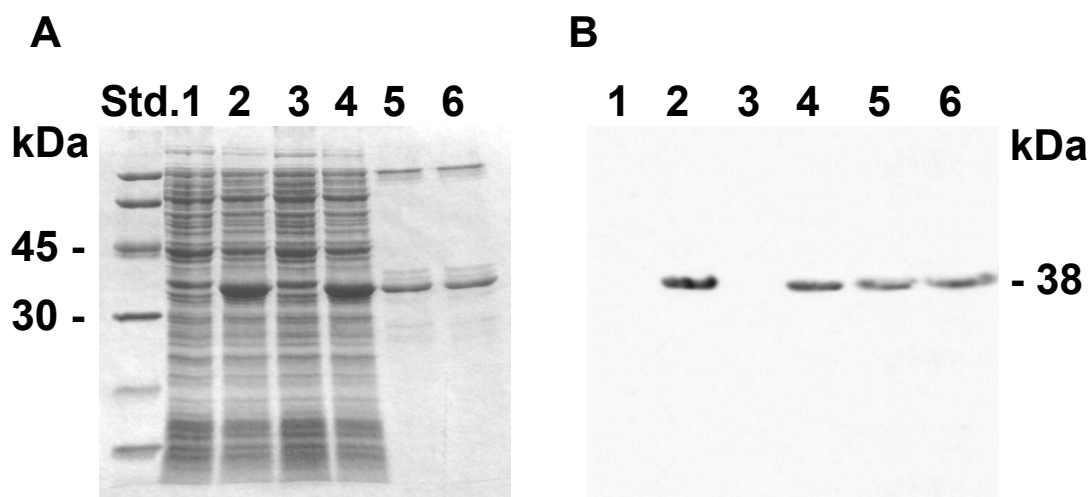


Figure 3.20 Expression of Omp38 in *E. coli* Origami(DE3).

The whole cell lysate with IPTG induction or without IPTG induction of *E. coli* carrying the recombinant plasmids pET23d(+)-*BpsOmp38* or pET23d(+)-*BthOmp38* were subjected to (A) SDS-PAGE following Coomassie stain and (B) Immunoblot analysis using anti-*BpsOmp38* antiserum. Lanes: Std, standard molecular weight of protein markers; 1, *E. coli* Origami(DE3) carrying pET23d(+)-*BpsOmp38* without IPTG induction; 2, IPTG induced *E. coli* Origami(DE3) carrying pET23d(+)-*BpsOmp38*; 3, *E. coli* Origami(DE3) carrying pET23d(+)-*BthOmp38* without IPTG; 4, IPTG induced *E. coli* Origami(DE3) carrying pET23d(+)-*BthOmp38*; 5 native *BpsOmp38*; 6, native *BthOmp38*.

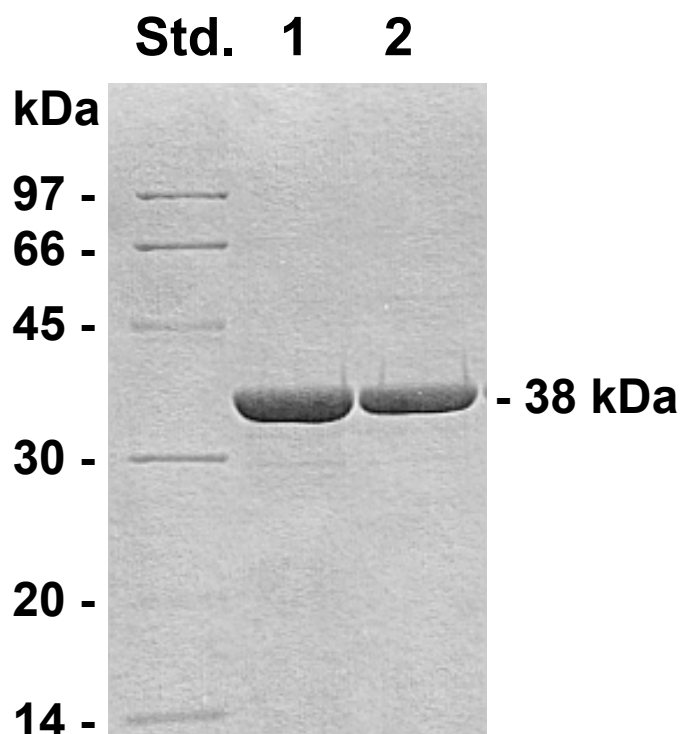


Figure 3.21 SDS-PAGE analysis of the expressed Omp38 after DEAE Fast Flow HiTrap[™] column chromatography.

Lanes: Std, standard molecular weight of protein markers; 1, purified expressed *Bps*Omp38; 2, purified expressed *Bth*Omp38.

3.9 Mass analysis and refolding of the expressed Omp38

3.9.1 Mass analysis by MALDI-TOF mass spectrometry.

The purified monomeric *Bps*Omp38 and *Bth*Omp38 in 20 mM Tris-HCl, pH 7.0 containing 8 M urea (Results 3.8) were resolved by SDS-PAGE. The protein band (38 kDa) was subjected to in-gel digestion using trypsin. The peptide masses were identified using MALDI-TOF MS. The identified peptides, designated

3.9.2 Refolding of the expressed Omp38

The purified monomer of expressed *Bps*Omp38 and *Bth*Omp38 in 20 mM Tris-HCl, pH 7.0, containing 8 M urea (described in Result 3.8) were refolded by diluting with an equal volume of a refolding solution (20 mM Tris-HCl, pH 7.0 containing with 10% (w/v) Zwittergent® 3-14, 200 mM NaCl, 20 mM CaCl₂, 10 mM EDTA and 0.02% NaN₃) (see Method 2.2.18). Folding states of the expressed Omp38 were analyzed on SDS-PAGE (Figure 3.23). After the proteins were allowed to fold slowly overnight at room temperature, almost complete refolding was detected. Under the given conditions the protein band corresponding to the dimer (M_r ~76,000) of *Bps*Omp38 (lane 2) and *Bth*Omp38 (lane 5) were still observed on 12% SDS-PAGE (Figure 3.23). However, the monomeric Omp38 was completely refolded into trimeric form (M_r 110,000) when the protein mixtures were subsequently heated at 95 °C for 5 min (lanes 3 and 6 in Figure 3.23). After refolding, the refolding reagent was removed by Sephacryl S-200 HR filtration chromatography. After gel filtration, the 10% Zwittergent® 3,14 detergent was reduced to 0.05% and all salts were removed. The purified refolded proteins were analyzed on SDS-PAGE (Figure 3.24, lanes 1 and 3) and further used for determination of pore-forming activity and secondary structure. It was also found that the trimer of both refolded Omp38 (solubilized with 0.05% Zwittergent® 3,14) and native proteins were dissociated into monomers when they were subsequently heated at 95 °C for 5 min (Figure 3.24, lanes 2 and 4).

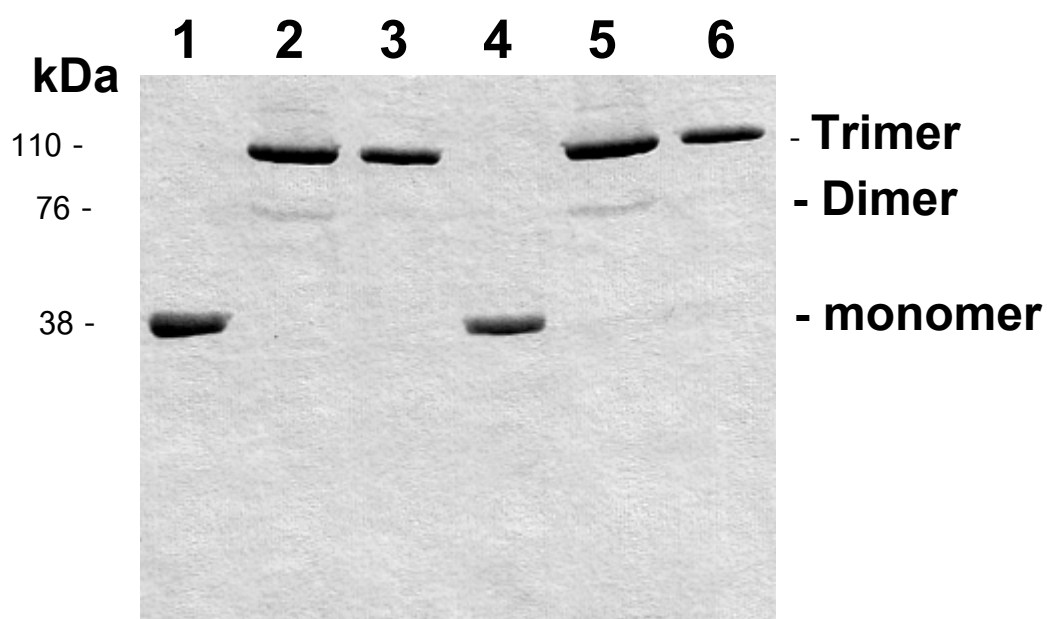


Figure 3.23 SDS-PAGE analysis of refolded Omp38.

The purified monomer of the expressed *Bps*Omp38 and *Bth*Omp38 in 20 mM Tris-HCl, pH 7.0 containing 8 M urea was subjected to refold using 20 mM Tris-HCl, pH 7.0 containing with 10% (w/v) Zwittergent® 3-14, 200 mM NaCl, 20 mM CaCl₂, 10 mM EDTA and 0.02% NaN₃. Lanes: 1, unfolded expressed *Bps*Omp38; 2, incompletely refolded expressed *Bps*Omp38; 3, completely refolded expressed *Bps*Omp38; 4, Unfolded expressed *Bth*Omp38; 5, incompletely refolded expressed *Bth*Omp38; 6, completely refolded expressed *Bth*Omp38.

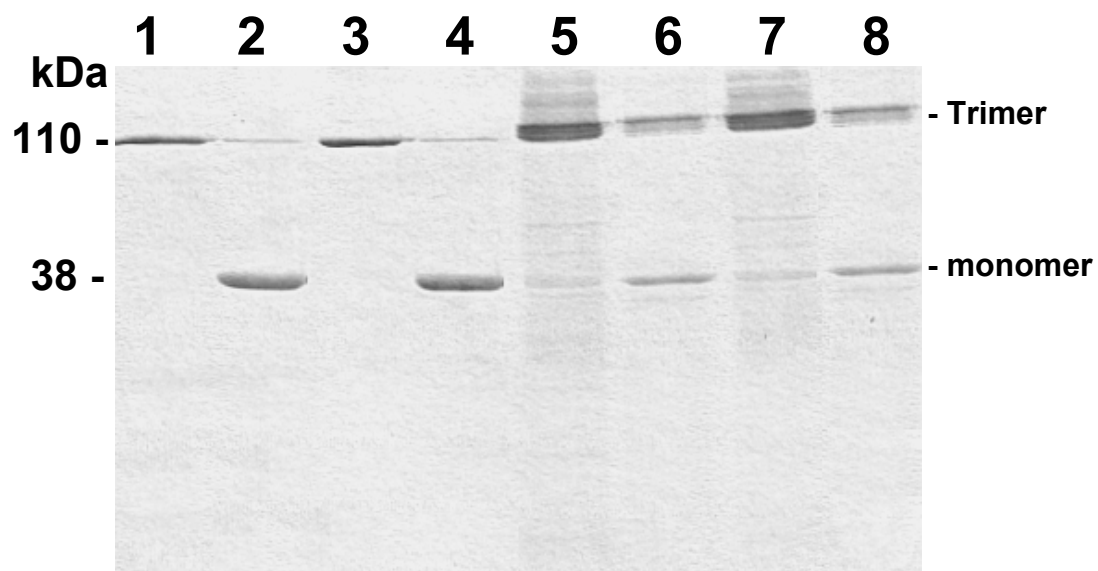


Figure 3.24 SDS-PAGE of refolded and native Omp38.

Lanes: 1-2, refolded *Bps*Omp38; 3-4, refolded *Bth*Omp38; 5-6, native *Bps*Omp38; 7-8, native *Bth*Omp38. Unheated samples before SDS-PAGE are in lanes 1, 3, 5 and 7. Samples were solubilized in SDS sample buffer and heated at 95 °C for 5 min (lanes 2, 4, 6 and 8).

3.10 Drug susceptibility test of *B. pseudomallei* and *B. thailandensis*

Antibiotic susceptibility tests were carried out using the disc diffusion technique as described in Method 2.2.20.1. Various groups of antibiotics that have been reported to be potential candidates for melioidosis treatment were tested. These antibiotics included aminoglycosides (amikacin and gentamicin), carbapenems (imipenem and meropenem), cepheems (cefepime, ceftazidime, and cefotaxime), β -lactam/ β -lactamase inhibitor combinations (amoxicillin/clavulanic acid), lincosamides (clindamycin), macrolides (erythromycin), phenicol (chloramphenicol), tetracyclines, fluoroquinolones (ciprofloxacin), ansamycin (rifampin), and folate pathway inhibitors (trimethoprim/sulfamethoxazole). According to the National Committee for Clinical Laboratory Standards recommendations (NCCLS), resistance of *B. pseudomallei* ATCC23343 and *B. thailandensis* ATCC70088 to antibiotics were judged from the size of inhibition zone produced on the antibiotic disc comparing with the standard size of inhibition zones produced from the control bacterial strains, including *E. coli* ATCC25922, *Staphylococcus aureus* ATCC25923 and *Pseudomonas aeruginosa* ATCC27853. The results on Table 3.2 do not show significant differences between *B. pseudomallei* and *B. thailandensis*, where both bacteria appeared to be susceptible to most of the tested antibiotics and both bacteria appeared to be resistant to gentamicin, clindamycin and erythromycin. On the other hand, *B. thailandensis* seemed to resist to amikacin and rifampin, while *B. pseudomallei* did not.

Table 3.2 Susceptibility tests of bacteria to various antibiotics.

Antimicrobial agent	Disc content (µg)	Zone diameter interpretive standards, nearest whole mm			Microorganism			
					<i>B. pseudomallei</i> ATCC23343		<i>B. thailandensis</i> ATCC700388	
		R	I	S	Zone Diameter (mm)	R / S	Zone Diameter (mm)	R / S
Antibiotics that inhibit cell wall synthesis								
• Aminoglycosides								
- Amikacin	30	≤14	15-16	≥17	20	S	14	R
- Gentamicin	10	≤12	13-14	≥15	12	R	6	R
• Carbapenems								
- Imipenem	10	≤13	14-15	≥16	40	S	38	S
- Meropenem	10	≤13	14-15	≥16	35	S	32	S
• Cephems								
- Cefepime	30	≤14	15-17	≥18	35	S	32	S
- Ceftazidime	30	≤14	15-17	≥18	29	S	23	S
- Cefotaxime	30	≤14	15-22	≥23	32	S	26	S
• β-Lactam / β-Lactamase inhibitor combinations								
- Amoxicillin / Clavulanic acid	20 / 10	≤19	-	≥20	31	S	23	S
• Lincosamides								
- Clindamycin	2	≤14	15-20	≥21	6	R	6	R
• Macrolides								
- Erythromycin	15	≤13	14-22	≥23	13	R	6	R
• Phenicol								
- Chloramphenicol	30	≤12	13-17	≥18	30	S	28	S
• Tetracyclines								
- Tetracycline	30	≤14	15-18	≥19	33	S	23	S
Antibiotics that effect nucleic acids								
• Fluoroquinolones								
- Ciprofloxacin	5	≤15	16-20	≥21	25	S	26	S
• Ansamycins								
- Rifampin	5	≤16	17-19	≥20	20	S	6	R
Antimetabolites								
• Folate pathway inhibitors								
- Trimethoprim / Sulfamethoxazole	1.25 / 23.75	≤10	11-15	≥16	16	S	23	S

3.11 Pore-forming activity of the refolded Omp38

3.11.1 Penetration of neutral sugars through the refolded Omp38

Pore-forming activity of the refolded Omp38 was determined using liposome-swelling assays as described for the native Omp38 (see Method 2.2.20.2). Accordingly, the purified proteins were reconstituted into liposomes and permeability rates of the same set of sugars were measured. The results shown in Figures 3.25 and 3.26 revealed that L-arabinose (M_r 150), which is the smallest sugar tested in this experiment gave highest diffusion rate, followed by the diffusion rates of D-glucose (M_r 180), D-mannose (M_r 180), D-galactose (M_r 180), N-acetylglucosamine (M_r 221), D-sucrose (M_r 342) and D-melezitose (M_r 522). On the other hand, stachyose (M_r 667) relatively gave slowest diffusion rate as it has the highest molecular weight. The results were similar to the native proteins as previously described in Figures 3.6 and 3.7.

Figures 3.27 and 3.28 represent diffusion rates of the tested sugars through *Bps*Omp38 and *Bth*Omp38 pores relatively to the diffusion rate of L-arabinose. The molecular weight of sugar plotted against relative permeation rates (%) was used to measure the relative permeability rates of the tested sugars or antibiotics. Similarly, as shown in Figures 3.27 and 3.28 the relative diffusion rates of D-glucose, D-mannose, D-galactose, N-acetylglucosamine, D-sucrose, D-melezitose and stachyose through the refolded Omp38 decreased when the size of sugar increased. The relative diffusion rates through refolded *Bps*Omp38 and *Bth*Omp38 porins were insignificantly different.

The relative permeation rates of neutral sugars molecule passing through the refolded Omp38 were compared with the native proteins as shown in Table 3.3.

It clearly shows that the relative permeation rate of the refolded Omp38 were also similar to those of the native proteins.

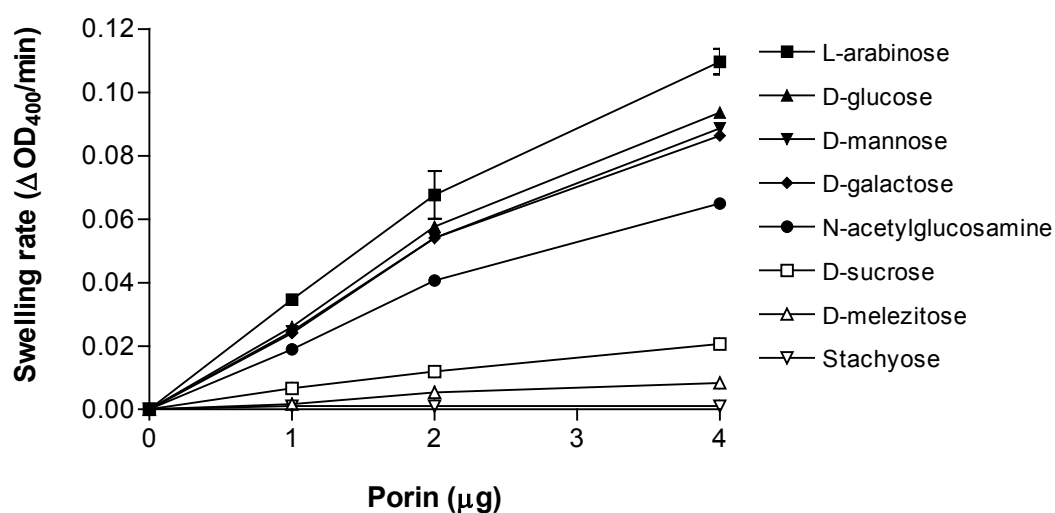


Figure 3.25 Liposome-swelling assays of refolded *BpsOmp38*.

Diffusion rates for neutral saccharides were determined by liposome-swelling assay using proteoliposomes reconstituted with various amounts of refolded *BpsOmp38* expressed from *E. coli*.

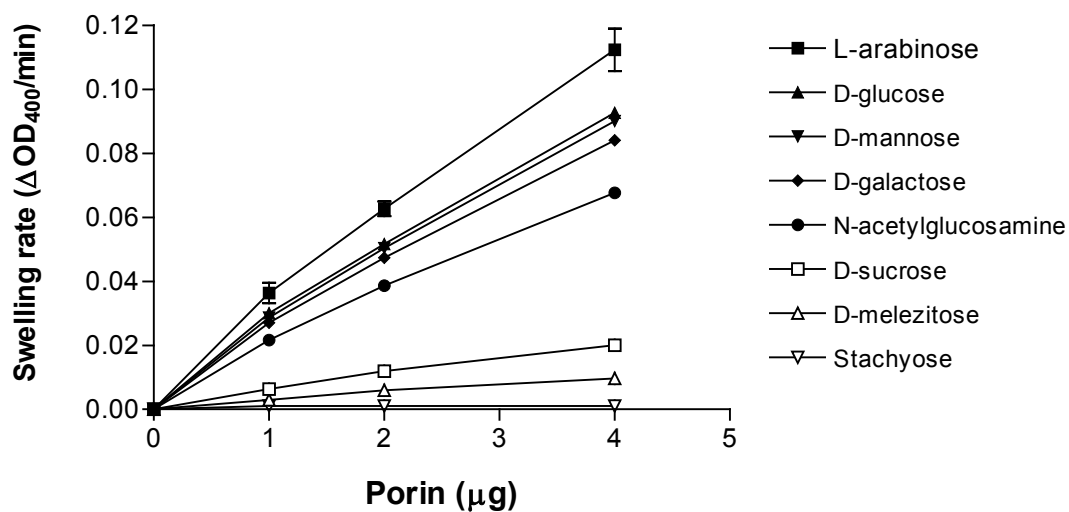


Figure 3.26 Liposome-swelling assays of refolded *BthOmp38*.

Diffusion rates for neutral saccharides were determined by liposome-swelling assay, using proteoliposomes reconstituted with various amounts of refolded *BthOmp38* expressed from *E. coli*.

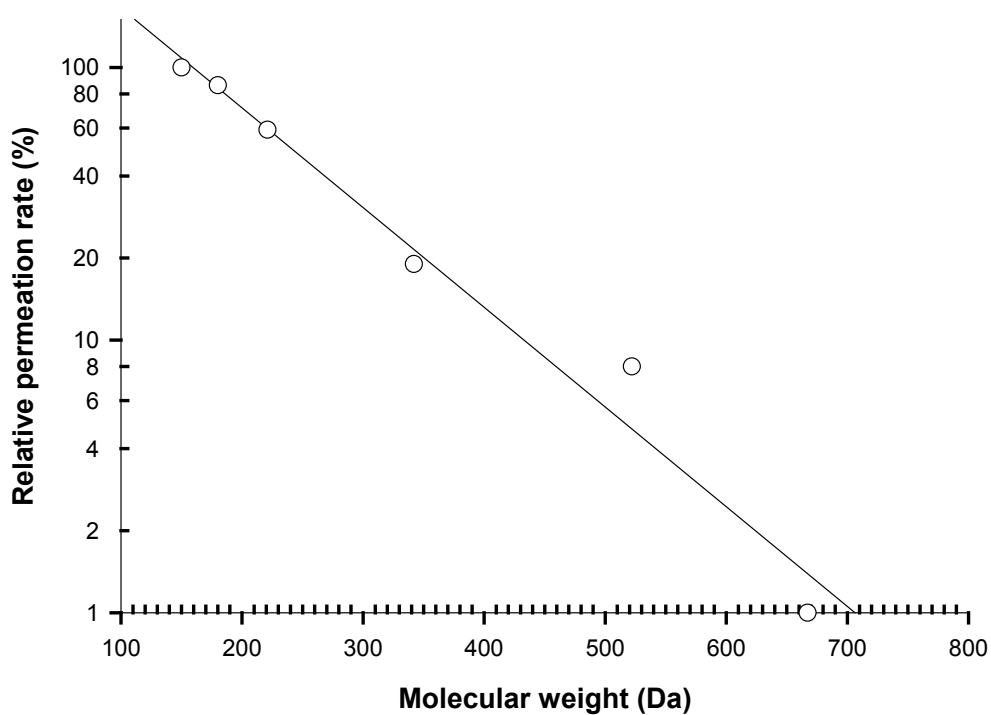


Figure 3.27 Relative permeation rates of sugar solutes through liposomes incorporated with refolded *BpsOmp38*.

The values are normalized to the permeation rate of L-arabinose and plotted on a logarithmic scale. The sugars used are: L-arabinose (M_r 150), D-glucose (M_r 180), N-acetylglucosamine (M_r 221), D-sucrose (M_r 342), D-melzitose (M_r 522) and stachyose (M_r 667).

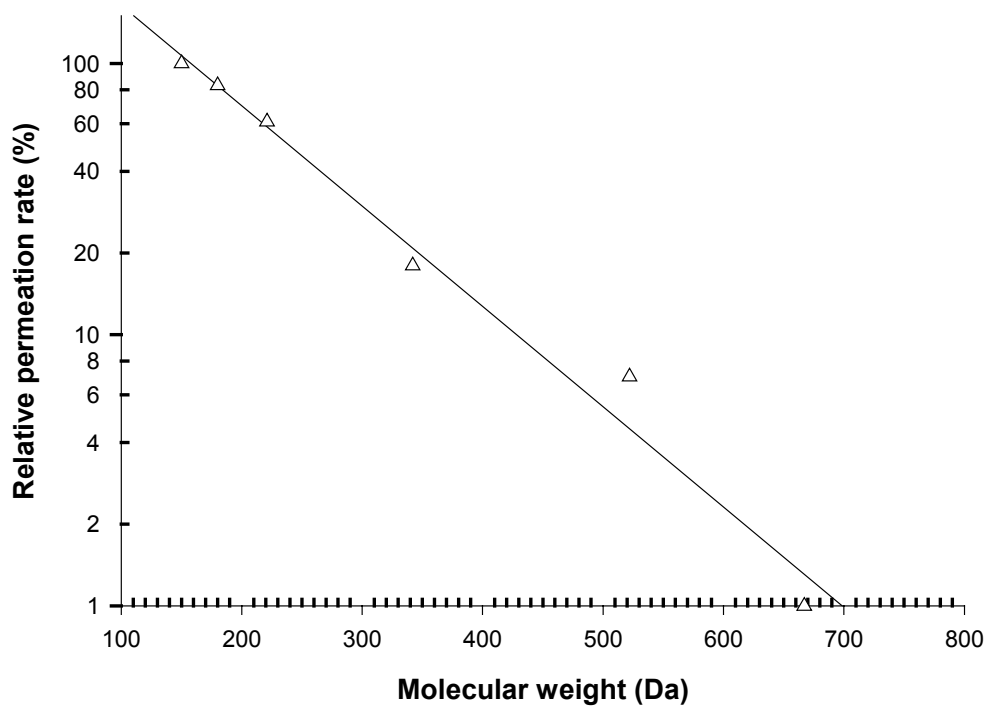


Figure 3.28 Relative permeation rates of sugar solutes through liposomes incorporated with refolded *BthOmp38*.

The values are normalized to the permeation rate of L-arabinose and plotted on a logarithmic scale. The sugars used are: L-arabinose (M_r 150), D-glucose (M_r 180), N-acetylglucosamine (M_r 221), D-sucrose (M_r 342), D-melizitose (M_r 522) and stachyose (M_r 667).

Table 3.3 Relative permeation rates of neutral sugars through native and refolded Omp38.

Neutral sugar	M_r	Relative permeation rate (%)			
		Native	Native	Refolded	Refolded
		<i>BpsOmp38</i>	<i>BthOmp38</i>	<i>BpsOmp38</i>	<i>BthOmp38</i>
L-arabinose	150	100	100	100	100
D-glucose	180	81	78	86	83
D-mannose	180	71	74	81	80
D-galactose	180	70	71	78	75
N-acetylglucosamine	221	57	56	59	61
D-sucrose	342	18	15	19	18
D-melezitose	522	7	6	8	7
Stachyose	667	1	1	1	1

3.11.2 Permeation of antibiotics through native and refolded Omp38 porins

Liposome-swelling assays were used to study the penetration of eight antibiotics through the native and refolded Omp38. These antibiotics included aminoglycosides (amikacin and gentamicin), carbapenems (meropenem), cepheims (cefepime, ceftazidime and cefotaxime), fluoroquinolones (ciprofloxacin), and lincosamides (clindamycin) (Tables 3.4 A and B). These antibiotics were selected since they were well solubilised in water or phosphate buffer. The permeation rates of the antibiotic were determined using liposome-swelling assays as described in Method 2.2.20.2. The relative permeability rates of antibiotics through each porin were calculated by comparing with the penetration rate of L-arabinose (indicated as “Observed” on Tables 3.4 A and B), and the estimated relative permeability rate from its molecular weight on the log-curve from (Figures 3.8, 3.9, 3.27, and 3.28) and indicated as “Estimated” on Table 3.4 A and B). Control experiments were set up using bovine serum albumin reconstituted liposomes. No diffusion of antibiotics was observed with the control reactions. Table 3.4 A (for native and refolded *Bps*Omp38) and Table 3.4 B (for native and refolded *Bth*Omp38), demonstrate that the permeability of the antibiotics through the Omp38 pores depended solely on size of the antibiotics with permeability decreased with an increase in the M_r of the antibiotics. Though *B. pseudomallei* is inhibited by gentamicin (M_r 782) but not by amikacin (M_r 709), both antibiotics could not entirely pass through the Omp38 pores as their molecular weights were too large (Result 3.10). On the other hand, clindamycin, which inhibits the growth of *B. pseudomallei* and *B. thailandensis*, could pass through the Omp38 channels as its molecular weight was relatively small

compared to the calculated pore size of Omp38. This implies that susceptibility or resistance of the bacteria to these antibiotics may not be associated with the permeation of antibiotics through the Omp38 channels. The same results were also observed with the refolded Omp38 expressed from *E. coli*.

Table 3.4 A Relative permeability rates of antibiotics through native and refolded *Bps*Omp38 porins.

Antibiotics	M_r	<i>B. pseudomallei</i> ATCC 23343						
		Antibiotics susceptibility test	Native <i>Bps</i> Omp38			Refolded <i>Bps</i> Omp38		
			Estimated (%)	Observed (%)	Ratio	Estimated (%)	Observed (%)	Ratio
• Aminoglycosides - Amikacin - Gentamicin	782	S	<1	0	-	<1	0	-
	709	R	<1	0	-	<1	0	-
• Carbapenems - Meropenem	383	S	18	20	1.11	18	20	1.11
• Cephems - Cefepime - Ceftazidime - Cefotaxime	572	S	3	4	1.33	3	5	1.00
	637	S	2	1	0.50	2	1	0.50
	477	S	6	8	1.33	7	11	1.11
• Fluoroquinones - Ciprofloxacin	421	S	11	15	0.73	11	15	1.36
• Lincosamides - Clindamycin	505	R	5	8	1.60	5	8	1.60

Table 3.4 B Relative permeability rates of antibiotics through native and refolded *BthOmp38* porins.

Antibiotics	M_r	<i>B. thailandensis</i> ATCC 700388						
		Antibiotics susceptibility test	Native <i>BthOmp38</i>			Recombinant <i>BthOmp38</i>		
			Estimated (%)	Observed (%)	Ratio	Estimated (%)	Observed (%)	Ratio
• Aminoglycosides -Amikacin -Gentamicin	782	R	<1	0	-	<1	0	-
	709	R	<1	0	-	<1	0	-
• Carbapenems - Meropenem	383	S	16	19	1.19	15	18	1.00
• Cephems - Cefepime - Ceftazidime - Cefotaxime	572	S	3	4	1.33	3	5	1.20
	637	S	2	1	0.50	2	1	0.5
	477	S	6	7	1.17	7	10	1.11
• Fluoroquinones - Ciprofloxacin	421	S	10	10	1.00	12	16	1.07
• Lincosamides - Clindamycin	505	R	5	5	1.00	5	7	1.00

3.11.3 Effects of anti-*Bps*Omp38 antibodies on pore-forming activity of the Omp38

Proteoliposome-swelling assays were used to determine effects of anti-*Bps*Omp38 antibodies on channel activity of both native and refolded Omp38. The native Omp38 proteins were prepared according to Method 2.2.2 and the refolded Omp38 were prepared according to Method 2.2.18. The purified proteins were incubated at 37 °C for 2 h with various dilutions of anti-*Bps*Omp38 polyclonal antibodies, then subsequently reconstituted into liposomes and tested with isoosmotic sugars as described in Method 2.2.20.2. The polyclonal antibodies incubated with liposomes were used in control experiments. Figures 3.29, 3.30, 3.31 and 3.32, reveal inhibitory effects of the antibodies on pore forming activity of Omp38. The results showed that the diffusion rates of the tested sugars decreased with increasing concentrations of the antibodies, whereas the control reactions using BSA, BSA-antibodies or antibodies alone did not give significant swelling rate of all sugars. Again, the diffusion rates decreased with an increase in size of the sugar molecule.

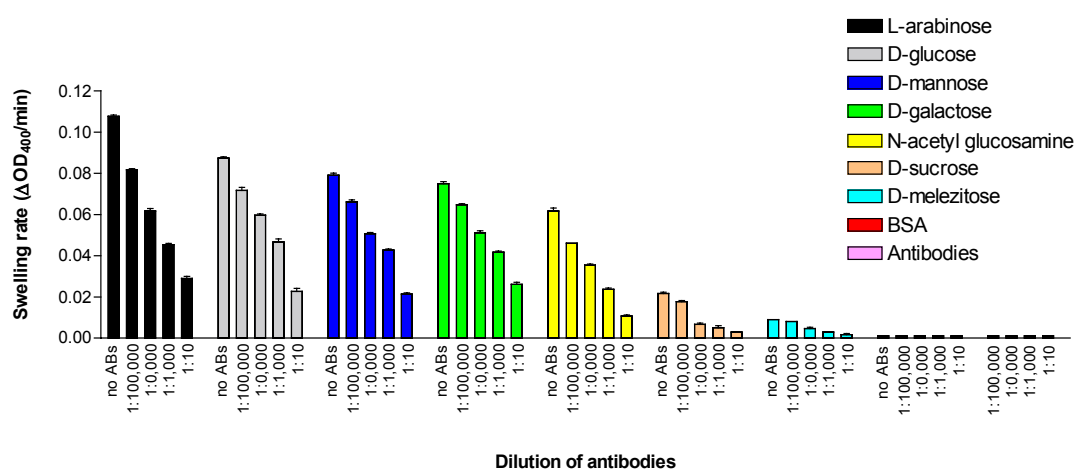


Figure 3.29 Effects of anti-*BpsOmp38* polyclonal antibodies on native *BpsOmp38* channel activity.

Various dilutions of antibodies were incubated with 50 μg of native *BpsOmp38* in a final volume of 200 μl . After that, the reaction mixtures were mixed with liposomes and the permeability rates of the tested sugars were determined. Each experiment was repeated three times using BSA, BSA-antibodies and antibodies as control tests.

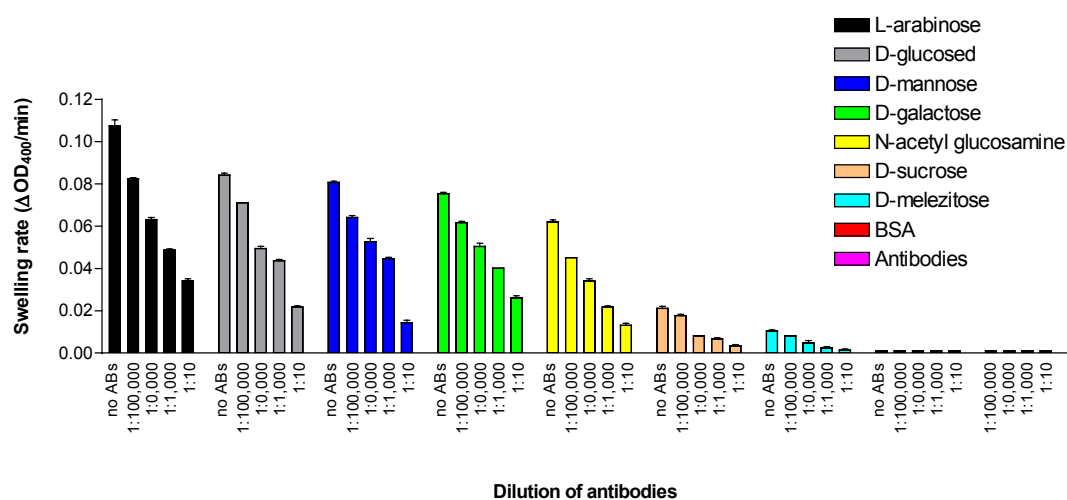


Figure 3.30 Effects of anti-*BpsOmp38* polyclonal antibodies on native *BthOmp38* channel activity.

Various dilutions of antibodies were incubated with 50 μg of native *BthOmp38* in a final volume of 200 μl . After that, the reaction mixtures were mixed with liposomes and the permeability rates of the tested sugars were determined. Each experiment was repeated three times using BSA, BSA-antibodies and antibodies as control tests.

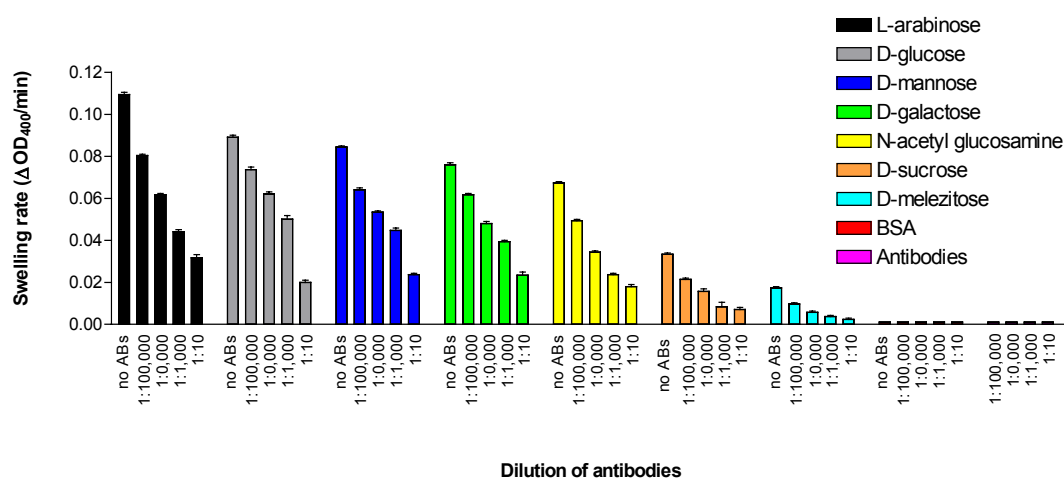


Figure 3.31 Effects of anti-*BpsOmp38* polyclonal antibodies on refolded *BpsOmp38* channel activity.

Various dilutions of antibodies were incubated with 50 μg of refolded *BpsOmp38* in a final volume of 200 μl . After that, the reaction mixtures were mixed with liposomes and the permeability rates of the tested sugars were determined. Each experiment was repeated three times using BSA, BSA-antibodies and antibodies as control tests.

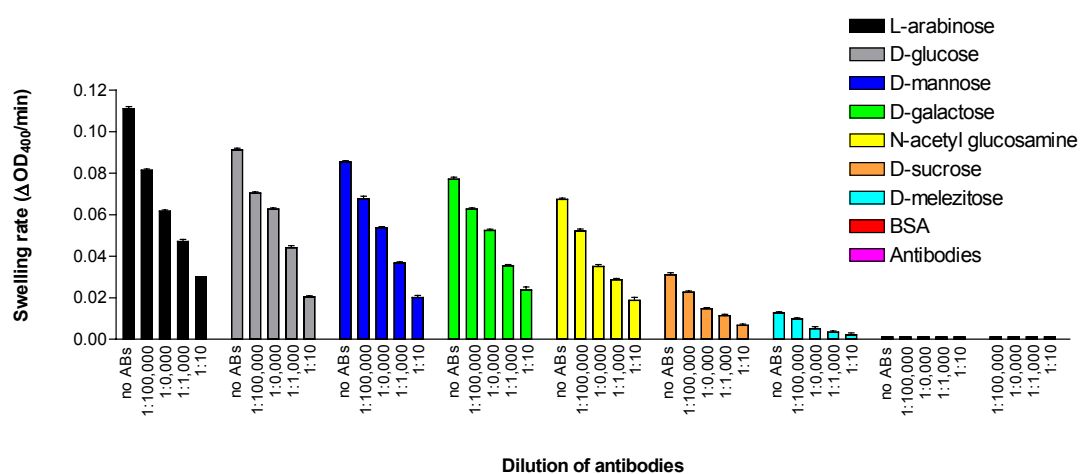


Figure 3.32 Effects of anti-*BpsOmp38* polyclonal antibodies on refolded *BthOmp38* channel activity.

Various dilutions of antibodies were incubated with 50 μg of refolded *BthOmp38* in a final volume of 200 μl . After that, the reaction mixtures were mixed with liposomes and the permeability rates of the tested sugars were determined. Each experiment was repeated three times using BSA, BSA-antibodies and antibodies as control tests.

3.12 Secondary structure determination using Circular Dichroism (CD) spectroscopy

Circular Dichroism spectroscopy was employed to investigate whether or not the Omp38 proteins expressed from *E. coli* were properly folded after the proteins have been subjected to denaturing-refolding processes. Basically, their CD spectra giving the secondary structure information were compared with the spectra of the native proteins. Figure 3.33 illustrates the CD spectra obtained for native Omp38. Identification of the CD spectra obtained from the corresponding CD patterns has been assessed based on the previously reported spectra described for OmpA porin (Bulieris *et al.*, 2003). Figure 3.33 shows that the spectra obtained from the two proteins were almost completely superimposed. In addition, both spectra gave a minus peak near to 215 nm, suggesting that the Omp38 contained a predominant β -sheet structure. These results were in good agreement with the secondary structure information previously determined for native Omp38 by FTIR (see Result 3.4).

In the case of Omp38 expressed in *E. coli*, inclusion bodies of *Bps*Omp38 and *Bth*Omp38 were solubilized with 20 mM Tris-HCl, pH 7.0 containing 8 M urea to completely denature the proteins and the CD spectra of their unfolded proteins are shown in Figures 3.34 and 3.35. The unfolded structures were identified to be random coil as the spectra of denatured proteins gave a minus peak at 205 nm were very similar to the spectra obtained for the urea-denatured OmpA porin from *E. coli* previously determined by Bulieris *et al.* (2003).

The urea-denatured Omp38 porins were subsequently refolded by addition of 10% Zwittergent® 3-14 detergent and high salts solution. To reduce concentration of

the detergent in the protein samples to 0.05% Zwittergent® 3-14 and to further purify the proteins, the protein samples were applied onto a Sephacryl S-200 HR filtration column. The CD spectra of the refolded proteins showed high abundance of β -sheet structure, which were similar to the spectra of the native conformation of Omp38 (Figures 3.34 and 3.35). Complete superimposition of the secondary structures of the refolded Omp38, as shown in Figure 3.36, clearly indicated that the expressed Omp38 had identical secondary structure to the structure of the native Omp38.

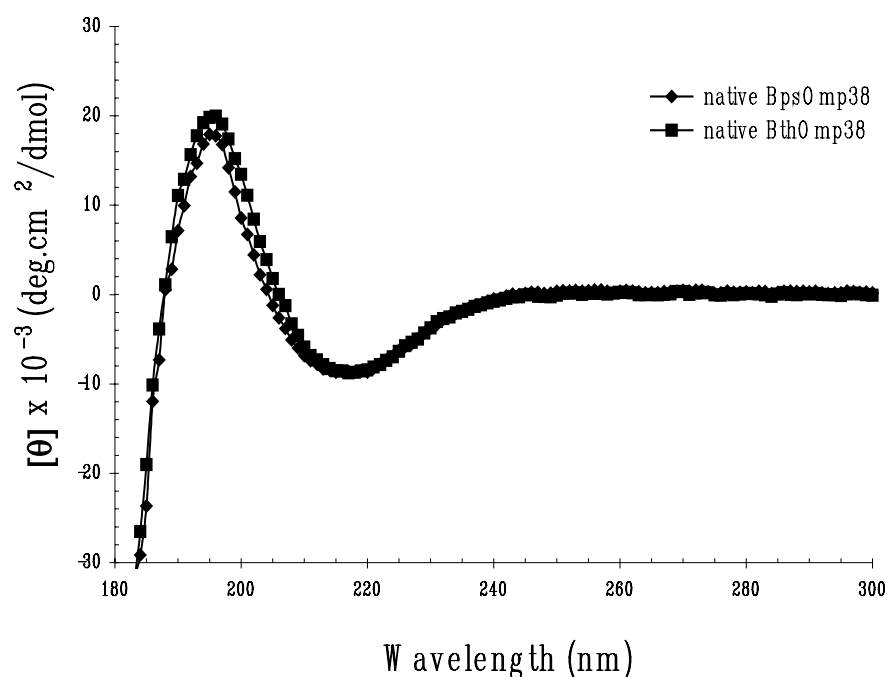


Figure 3.33 CD spectra of native Omp38.

The native proteins were prepared using SDS extraction, followed by gel filtration on a Sephacryl S-200 HR column. SDS was removed from the protein solution by extensive dialysis. The spectra were obtained with a Jasco J-715 spectropolarimeter and the spectral backgrounds were corrected with the spectra of 10 mM Tris-HCl, pH 8.0.

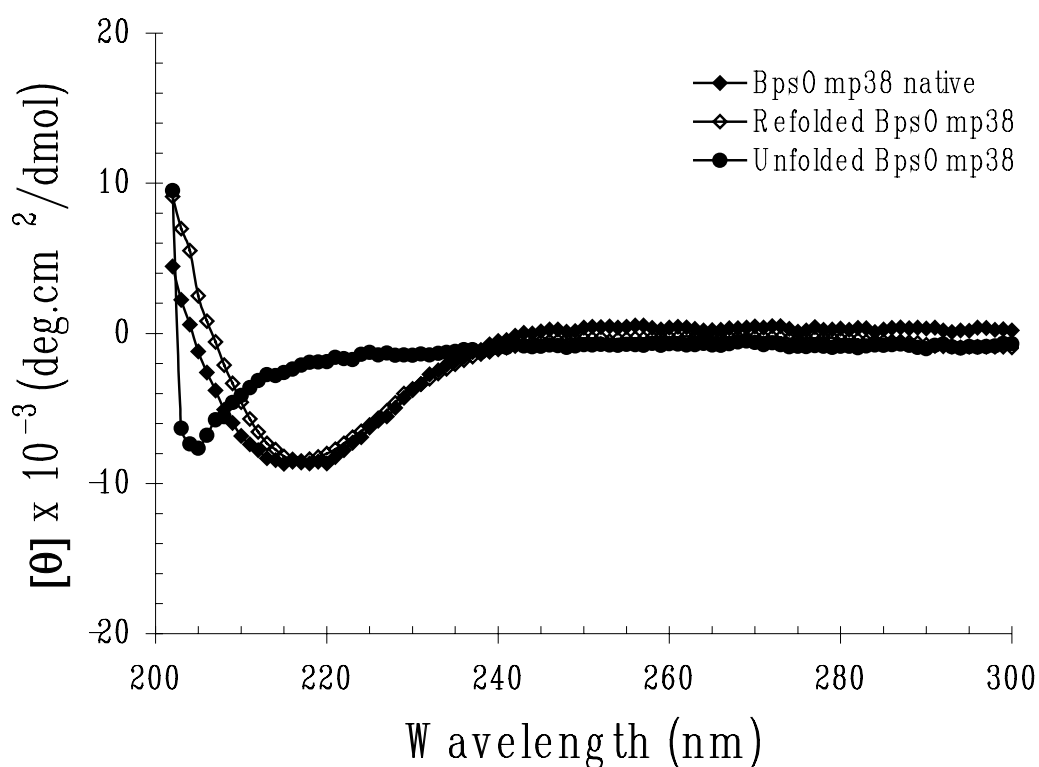


Figure 3.34 CD spectra of native, refolded and unfolded *BpsOmp38*.

The native protein was prepared by SDS extraction followed by gel filtration. The purified native protein was dialyzed extensively to remove SDS. The unfolded protein was solubilized in 20 mM Tris-HCl, pH 7.0 containing 8 M urea and the unfolded protein was refolded and finally solubilized in 0.05% Zwittergent® 3-14 in 20 mM Tris-HCl, pH 7.0. Spectra were obtained with a Jasco J-715 spectropolarimeter. The 20 mM Tris-HCl, pH 7.0 containing 0.05 % Zwittergent® or 8 M urea solutions were used for background subtraction.

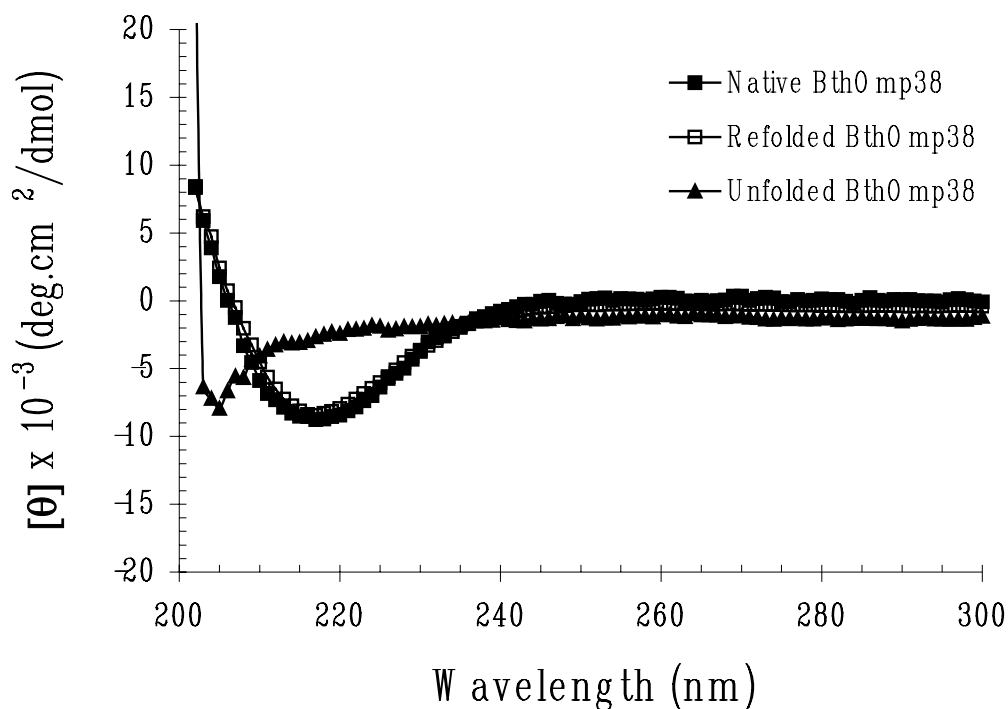


Figure 3.35 CD spectra of native, refolded and unfolded *BthOmp38*.

The native protein was prepared by SDS extraction followed by gel filtration, then dialyzed to remove SDS. The unfolded protein was solubilized in 20 mM Tris-HCl, pH 7.0 containing 8 M urea and the unfolded protein was refolded and finally solubilized in 0.05% Zwittergent® 3-14 in 20 mM Tris-HCl, pH 7.0. Spectra were obtained with a Jasco J-715 spectropolarimeter. The 20 mM Tris-HCl, pH 7.0 containing 0.05 % Zwittergent® or 8 M urea solutions were used for background subtraction.

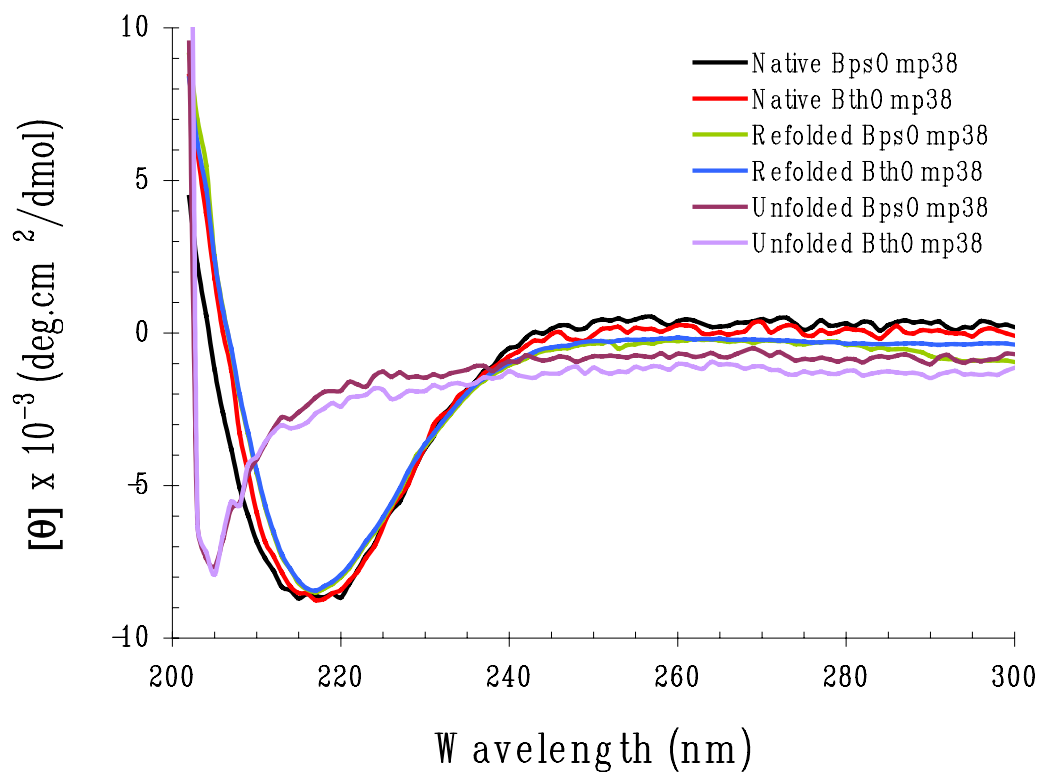


Figure 3.36 Superimposition of the CD spectra of Omp38 obtained from a Jasco J-715 spectropolarimeter.

3.13 The M_r determination using Sephacryl S-200 HR filtration chromatography

Gel filtration chromatography on a Sephacryl S-200 HR column was used to determine the M_r of the native and refolded Omp38 (see Method 2.2.22). As shown in Figure 3.34, the trimeric form of native and refolded Omp38 had M_r of 110,000, whereas the monomeric Omp38 had M_r of 38,000. The results corresponded with the

data obtained from SDS-PAGE (Figures 3.3 and 3.24) and the chromatographic profiles of both *Bth*Omp38 and *Bps*Omp38 were identical.

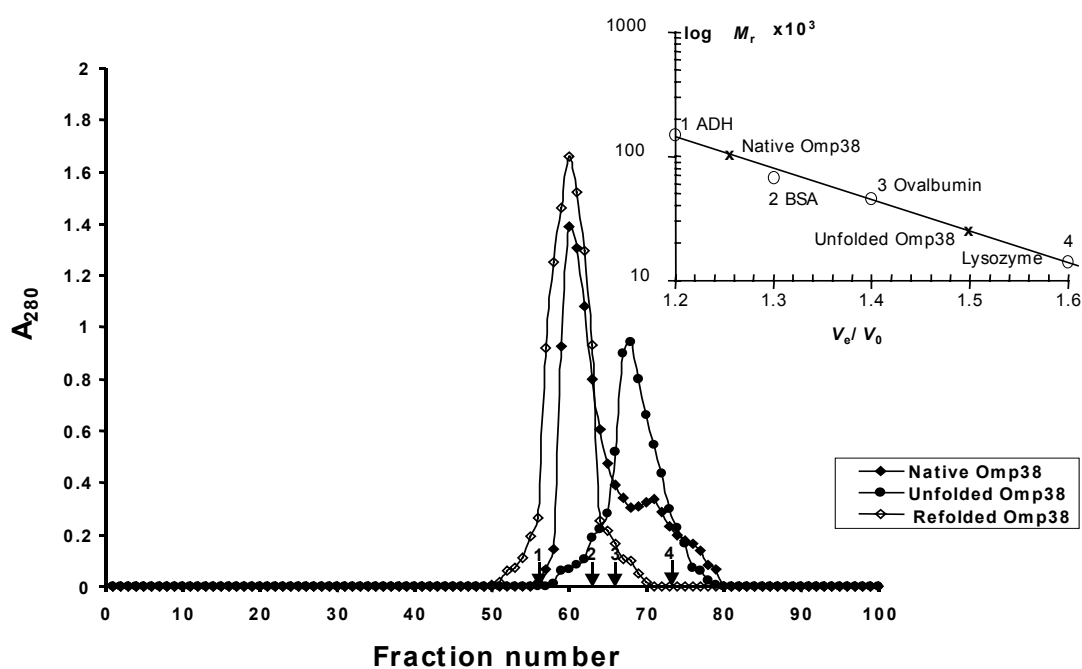


Figure 3.36 Determination of the M_r of Omp38.

The purified native, refolded or unfolded Omp38 proteins were applied on a Sephacryl S-200 HR (1.5 x 95 cm) column. The column was run at a flow rate of 1 ml min^{-1} , and fractions of 2 ml were collected and protein concentrations of eluted fractions were determined by measuring A_{280} . The logarithmic plot displays a calibration curve determining the M_r of native, refolded and unfolded Omp38.

3.14 Membrane topology and 3D structural predictions

Membrane topology of *BpsOmp38* and *BthOmp38* were predicted by the method of Diederichs *et al.* (1998) and PSORT program as described in Method 2.2.23. The topology of both proteins was predicted to be identical. The predicted topology plot identified 16 transmembrane domains, 8 short periplasmic turns and 8 external loops designated as L1 to L8 (Figure 3.38).

The 3D structure of *BpsOmp38* and *BthOmp38* porins was analyzed using 123D+, 3D-PSSM and Swiss-Model. The prediction was carried out using the most highly related structure, the anion selective porin Omp32, from *Comamonas acidovorans* (PDB 1e54a) (35.8% identity) as template. The predicted 3D structure of monomeric Omp38 is shown in Figure 3.39 and the predicted structure of trimeric Omp38 was displayed by Cn3D version 4.1 available from <http://www.ncbi.nlm.nih.gov/> (Figure 3.40). Figure 3.39 shows that the monomeric protein was composed of a 16-stranded antiparallel β barrel, 8 periplasmic turns and 8 external loops. The longest loop, designated Loop 3 (L3), contained 28 amino acid residues (Ser¹²⁷ \rightarrow Asp¹⁵⁴) and had two short antiparallel β strands at the very beginning and the end. A short right-handed α helix (Tyr¹¹⁹ \rightarrow Lue¹²⁶) was found in front of L3. Loop 3 is a typical characteristic for many porins and identified to be a constriction loop responsible for molecular size selectivity of porin channels (Zeth *et al.*, 2000; Breden *et al.*, 2002). Loop 8 (L8), the second longest loop in the Omp38, appeared to fold into the barrel interior and was suggested to assist L3 to control the size exclusion limit of the Omp38 pore. The *N*-terminal amino acid residues of monomeric Omp38 was apparently exposed to the periplasm and did not fold back towards the *C*-terminal phenylalanine (Phe³⁷⁴). In addition, the predicted structure

also revealed that the contact regions of monomer subunits involved the amino acid residues Glu⁶⁸ → Ala⁷⁶ and Ser³²⁶ → Thr³²⁹, which contained Turn1 and Turn7 as shown in Figure 3.17.

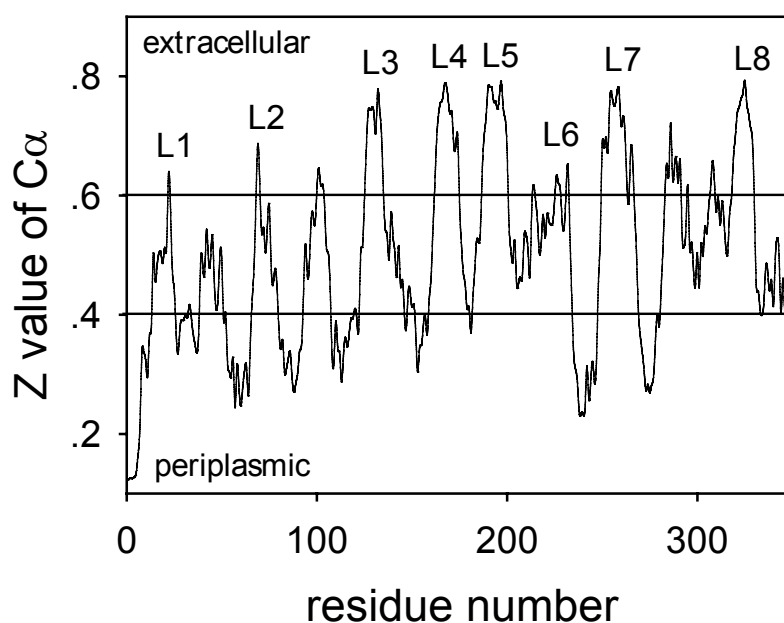


Figure 3.38 Predicted transmembrane topology of *BpsOmp38* and *BthOmp38*.

The succession of C_{α} carbons plotted against residue number for the identical prediction of *B. pseudomallei* and *B. thailandensis* porins (Diederichs *et al.*, 1998). The Z value (scaled from 0-1) corresponds to the predicted position of each C_{α} carbon relative to the plane of the membrane. Values <0.4 represent positions in periplasmic turns, values between 0.4-0.6 are predicted to be in transmembrane crossings, and values >0.6 represent extracellular loops. Putative membrane crossings are defined as bounding by periplasmic and extracellular domains. The 16 transmembrane domains were identified, and the corresponding external loops are labeled L1-L8.

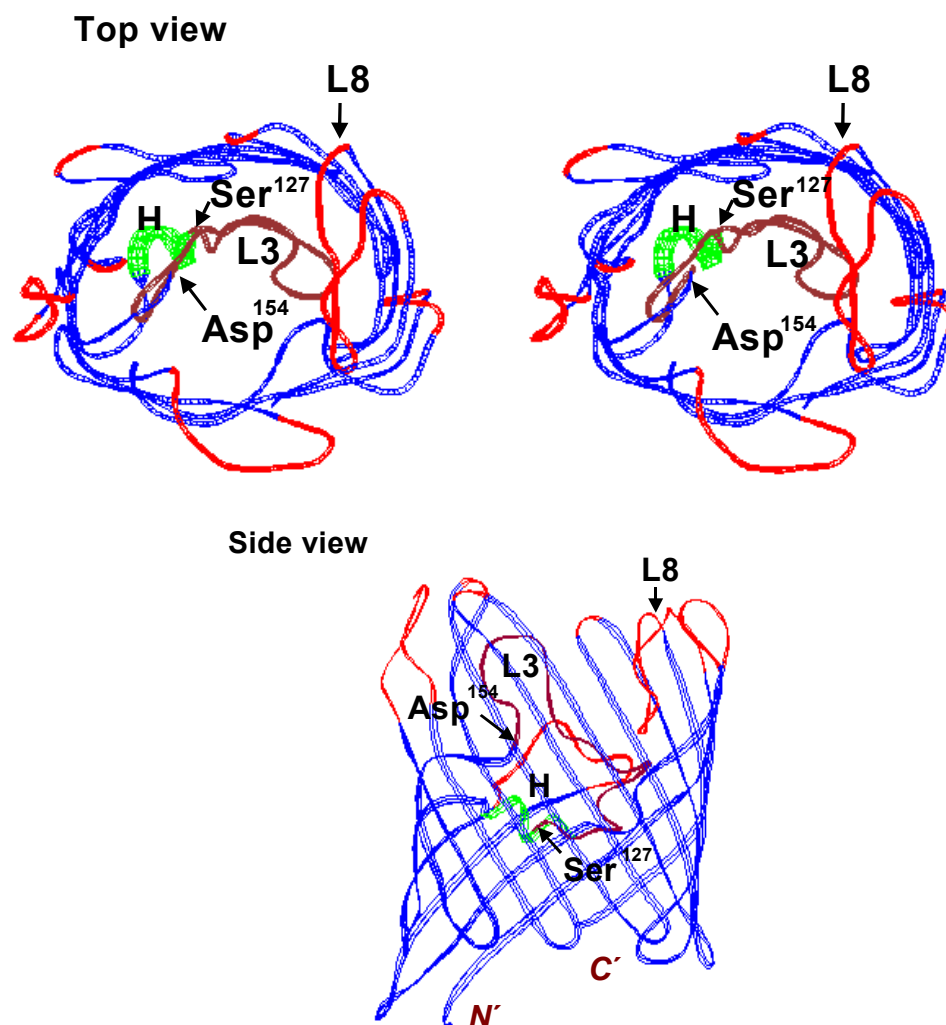


Figure 3.39 Predicted 3D structure of *BpsOmp38* and *BthOmp38* using Swiss-Model.

The representative diagram was drawn using Swiss-pdb Viewer version 3.7b2 based on the 3D-structure of Omp32 porin from *Comamonas acidovorans*. This figure shows 16 β -strands and 8 loops. The longest loop (L3), residues Ser¹²⁷ to Asp¹⁵⁴ folds inside the barrel. H is an α -helix. N' and C' represent N-terminal end and C-terminal ends, respectively.

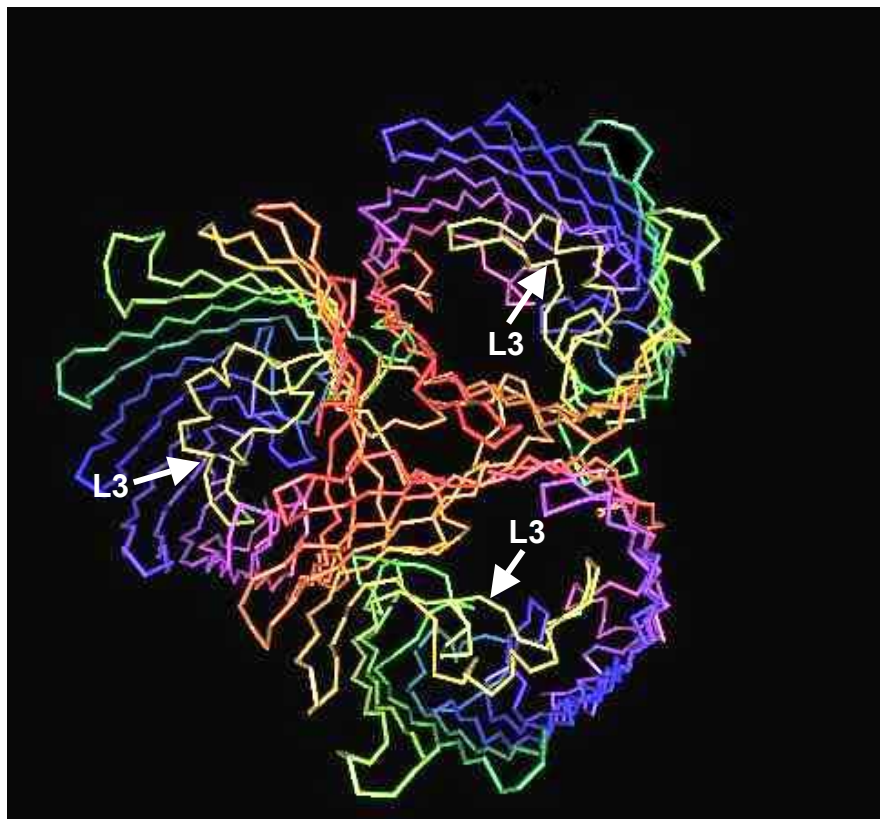


Figure 3.40 The predicted structure of trimeric Omp₃₈ as displayed by Cn3D version 4.1 from RPS-BLAST.

Each domain is shown using a ROYGBIV define color cycle along each chain from *N* to *C* terminus. The longest loop 3 (L3), which restricts the size of solutes to pass through, is shown in yellow and pointed out by white arrows.

3.15 Preliminary crystallization of the Omp38 porins

The purified refolded *Bps*Omp38 and *Bth*Omp38 (approx. 3 mg/ml) were used in preliminary crystallization set up using the sitting drop method as described in Method 2.2.24. After 2 days of incubation at 25 °C, microcrystals were observed when 0.2 M lithium sulfate in 0.1 M Tris-HCl, pH 8.5 or 0.5 M ammonium sulfate in 0.1 M Tris-HCl, pH 8.5 were precipitants. The irregular shapes of the obtained crystals observed under stereo light microscope had an average size of ~20 µm x ~20 µm x ~20 µm (Figures 3.41 and 3.42). Crystals of salts were also seen when 1 M di-Na/K phosphate in 0.1 M Tris-HCl, pH 8.5 or 0.1 M di-ammonium phosphate were used as precipitants (Figure 3.43). To confirm that the crystals obtained were protein crystals, a single crystal from each well was fished out and mixed with 5x SDS sample buffer, then heated at 95 °C for 5 min and the sample mixture was analyzed on 12% SDS-PAGE. Figure 3.44 shows SDS-PAGE of the Omp38 crystals grown in 0.2 M lithium sulfate in 0.1 M Tris-HCl, pH 8.5, (lanes 1 and 4) or 0.5 M ammonium sulfate in 0.1 M Tris-HCl, pH 8.5, as precipitants (lanes 2 and 5)

A**B**

Figure 3.41 Preliminary crystallization of *BpsOmp38*.

(A) Crystals of *BpsOmp38* grown in 0.2 M lithium sulfate in 0.1 M Tris-HCl, pH 8.5.

(B) Crystals of *BpsOmp38* grown in 0.5 M ammonium sulfate in 0.1 M Tris-HCl, pH 8.5.

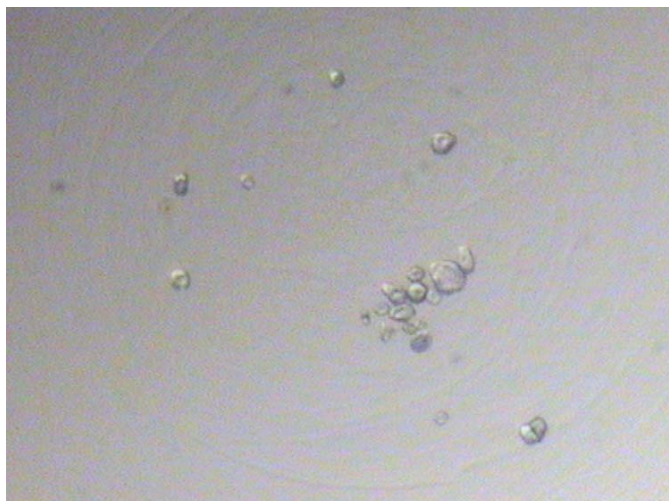
A**B**

Figure 3.42 Preliminary crystallization of *BthOmp38*.

(A) Crystals of *BthOmp38* grown in 0.2 M lithium sulfate in 0.1 M Tris-HCl, pH 8.5.

(B) Crystals of *BthOmp38* grown in 0.5 M ammonium sulfate in 0.1 M Tris-HCl, pH 8.5.

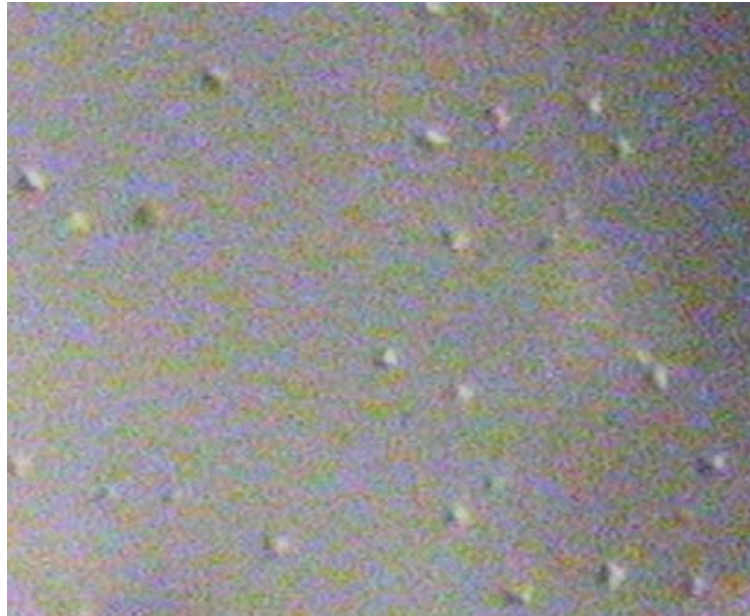


Figure 3.43 Salt crystals obtained in preliminary crystallization experiments.

The salt crystals were observed when 1M di-Na/K phosphate in 0.1 M Tris-HCl, pH 8.5 or 0.1 M di-ammonium phosphate were precipitants.

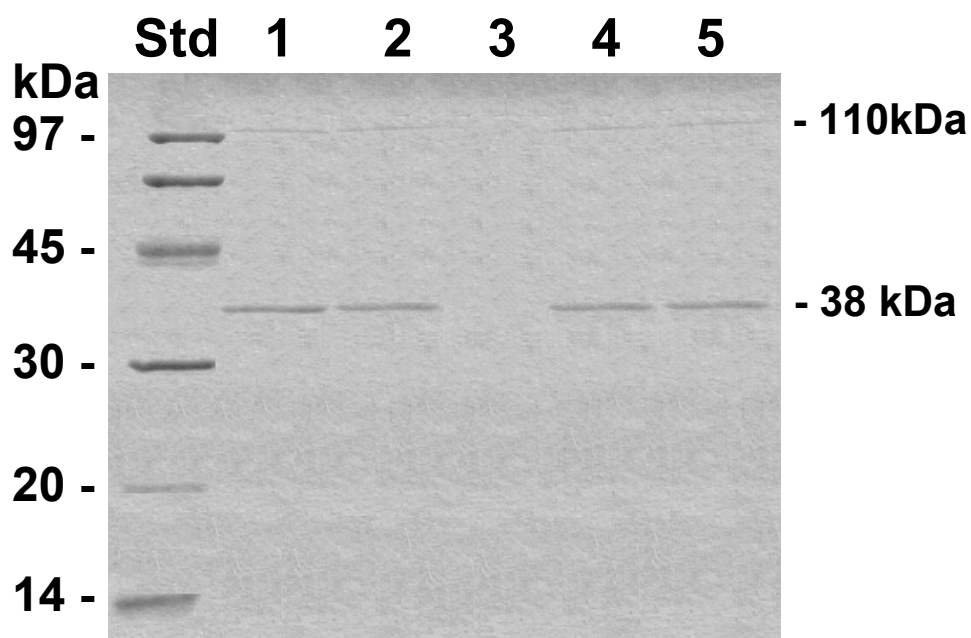


Figure 3.44 SDS-PAGE of *BpsOmp38* and *BthOmp38* crystals.

Lanes: Std., standard protein markers; 1, a crystal of *BpsOmp38* grown in 0.2 M lithium sulfate in 0.1 M Tris-HCl, pH 8.5; 2, a crystal of *BpsOmp38* grown in 0.5 M ammonium sulfate in 0.1 M Tris-HCl, pH 8.5; 3, a crystal of salt grown in 1M di-Na/K phosphate in 0.1 M Tris-HCl, pH 8.5 and 0.1 M di-ammonium phosphate; 4, a crystal of *BthOmp38* grown in 0.2 M lithium sulfate, 0.1 M Tris-HCl, pH 8.5; 5, a crystal of *BthOmp38* grown in 0.5 M ammonium sulfate in 0.1 M Tris-HCl, pH 8.5.

Chapter IV

Discussion

4.1 Isolation and purification of the native Omp38 protein

The cell envelope of Gram-negative bacteria consists of two membranes, an outer membrane and an underlying inner or cytoplasmic membrane (Hancock, 1991). Small hydrophilic molecules, such as most nutrients, penetrate the cell wall of these bacteria through unique pore-forming proteins called porins (Nikaido, 1992; Nikaido, 1994; Nikaido and Vaara, 1985). Since many porins usually form detergent-stable homotrimer and contain heat-modifiable property, several previous reports success in isolation and purification of porins using SDS extract in technique (Mizuno and Kageyama, 1979; Nikaido, 1994; Jap and Walian, 1996). Originally, Rosenbusch (1974) reported that major outer membrane proteins of various *E. coli* strains were tightly associated with peptidoglycan. This complex appeared to be stable in 2% SDS solution at 60 °C, but was dissociated when it was subjected to boiling at 100 °C for 5 min (Rosenbusch, 1974). However, Hazumi *et al.* (1978) isolated a peptidoglycan-associated protein (O-14) of an *E. coli* strain. The complex was found to be stable in SDS solution at 30 °C but not at 60 °C.

Recently, Gotoh *et al.* (1994) isolated the trimer of the 38-kDa peptidoglycan-associated protein, namely OM-1, from various strains of *B. pseudomallei* using 2% SDS at 37°C for 15 min. The protein was further purified by Sephacryl S-200 HR gel filtration chromatography. It has been postulated that the OM-1 protein may

function as a general diffusion pore, which allows transportation of nutrients and small hydrophilic antibiotics into the cells. Differences in antibiotic permeability may give rise to antibiotic resistance of *Burkholderia pseudomallei* and pathogenicity of the bacterium to melioidosis. To address this idea, the OM-1 of *B. pseudomallei* has been isolated and purified in this study. The first part of this thesis has aimed to isolate a trimeric porin (M_r 110,000) from an outer membrane of *Burkholderia pseudomallei* ATCC23343 and *B. thailandensis* ATCC700388. The *B. pseudomallei* OM-1 and the protein homologue from the closely related non-pathogenic bacterium *B. thailandensis* were isolated. Their functions as a porin channels was verified and their secondary structure was investigated experimentally. The proteins have been referred in this study as Omp38 as they have been isolated as outer membrane proteins with the monomeric M_r subunit of 38,000, as revealed by SDS-PAGE.

Initially, the method for isolation of *Bps*Omp38 (from *B. pseudomallei*) and *Bth*Omp38 (from *B. thailandensis*) was carried out according to Gotoh *et al.* (1994). However, the peptidoglycan-associated protein could not be isolated following Gotoh's protocol because the protein complex appeared to be not stable during cytoplasmic and inner membrane extraction steps using 2% SDS at 37 °C. The method for the Omp38 isolation was then modified by reducing the concentration of SDS from 2 % as described by Gotoh *et al.* (1994) to 0.5%. The trimeric protein (M_r 110,000) dissociated into three identical monomers (M_r 38,000) when it was heated at 95 °C for 5 min. The monomeric protein has similar M_r with the monomeric M_r of other bacterial porins, such as Omp32 of *Comamonas acidovorans* (M_r 32,000) (Gerbl-Riger *et al.*, 1991), protein F of *Pseudomonas aeruginosa* (M_r 35,250) (Nikaido *et al.*, 1991) and PorB of *Chlamydia trachomatis* (M_r 37,000) (Kubo and

Stephens, 2000). Moreover, the patterns of trimeric and monomeric *BpsOmp38* and *BthOmp38* migration on SDS-PAGE were observed to be identical in this study (see Figure 3.3). These results were similar to the results obtained for OM-1 of *B. pseudomallei* ATCC23343 isolated and purified by Gotoh *et al.* (1994).

4.2 Cloning and expression of *Omp38*

Based on tryptic peptide mass analysis obtained from MALDI-TOF MS and capillary HPLC/MS and the incomplete *B. pseudomallei* genome database information, the genes encoding *BpsOmp38* and *BthOmp38* were identified, isolated and sequenced. Nucleotide sequences of the full-length *BpsOmp38* and *BthOmp38* were 98% identical. The putative amino acid sequences of *BpsOmp38* and *BthOmp38* were 99.7% identical, and the deduced amino acid sequences of both mature proteins were 100% identical. According to the conserved domain prediction information, the translated *BpsOmp38* and *BthOmp38* were likely to be porins as their conserved sequences aligned well with the conserved sequences of several Gram-negative bacterial porins in protein databases available from the NCBI homepage.

Previous reports demonstrated that expression of porins using several plasmid systems were difficult since high expression of intact heterologous gene products were usually lethal to *E. coli* host cells (Carbonetti and Sparling, 1987; Gotschlich *et al.*, 1987; Barlow *et al.*, 1987; Carbenetti, *et al.*, 1988, Bolstad and Jensen, 1993). However, a few reports have expressed porins lacking signal peptide sequences as inclusion bodies (aggregated form). For example, expression of *Haemophilus influenzae* type b Hib in *Bacillus subtilis* using pKTH288 (Dahan *et al.*, 1996) and

Neisseria species class 3 porin in *E. coli* BL21(DE3) $\Delta ompA$ using pET17b (Qi, *et al.*, 1994), *Rhodopseudomonas blastica* porin in *E. coli* BL21(DE3)pLysS using pET3a (Schmid *et al.*, 1996), *Burkholderia cepacia* OpcP in *E. coli* JM109 using pTrc99A (Tsujiimoto *et al.*, 1997), *Orientia tsutsugamushi* r56 in *E. coli* BL21 using pET11a (Ching, *et al.*, 1998), and *Mycobacterium smegmatis* MspA in *E. coli* BL21(DE3) using pET24(+) (Heinz *et al.*, 2003).

In this study, *BpsOmp38* and *BthOmp38* lacking their signal peptides were successfully expressed as inclusion bodies in *E. coli* Origami(DE3) using the pET23d(+) vector system. Generally, *E. coli* Origami(DE3) host strain is properly employed to express highly soluble proteins (Manufacturer's instruction, Novagen). However, this host strain was chosen in this work to express Omp38 because anti-*BpsOmp38* antibodies did not recognize the whole cell protein bands of *E. coli* Origami(DE3) on Western blotting. In contrast, other *E. coli* host strains including HMS174(DE3), NovaBlue(DE3) and BL21(DE3)pLysS, appeared to express endogenous outer membrane proteins with $M_r \sim 35,000-40,000$, which overlapped with the M_r of monomeric Omp38. Therefore, these *E. coli* strains were not appropriate for expression of Omp38.

Since anti-*BpsOmp38* could recognize the expressed proteins and their peptide fragments were found to be identical with those of the native proteins, it provided a strong evidence that the expressed proteins were Omp38. To our best knowledge, this is the first time that successful expression of functional *BpsOmp38* and *BthOmp38* in an *E. coli* system has been reported.

4.3 Refolding of the expressed Omp38

Amphiphilic molecules, for instant phospholipids and detergents, were used to facilitate proper refolding of bacterial porins (Pebay-Peyroula *et al.*, 1995). In this study, strategies using different amphiphilic molecules have been tried following previously published reports to functionally refold the expressed Omp38. For example, the precipitated form of the expressed Omp38 obtained from inclusion bodies was initially solubilized using two different solutions: i) using 1% (w/v) SDS system and, ii) using 6 M guanidinium hydrochloride. To preliminarily test for effects of different detergents and phospholipids in the Omp38 refolding, a combination of such reagents including CHAPS, LDAO, MEGA-9, β -Octyl glucoside (β -OG), Decly-maltoside, Octyl-POE, phosphatidylcholine (or lecithin), Tween 20, Triton X-100 and a short chain phospholipid of diheptanoyl phosphatidylcholine (C_7) (modified from Eisele and Rosenbusch (1990) and Schmid *et al.* (1996)) was added to the solubilized expressed proteins. It has been found that lecithin helped the protein to refold, which was applicable for functional assays. However, the protein prepared from lecithin appeared to be inappropriate for X-ray crystallization, as lecithin is a relatively large amphiphilic molecule, thus generating poor X-ray diffraction patterns as reported previously (Eisele and Rosenbusch, 1990). A mixture of LDAO and phospholipid (C_7) and a mixture of β -OG and phospholipid (C_7) also helped the Omp38 to refold, but the refolding process seemed to take place incompletely. Some of the protein monomer (approx. 30%) and dimer (approx. 5%) were still found in the reaction mixture. SDS, an anionic detergent, at conc. 1% (w/v) could also be used but it tended to disrupt protein crystallization (Eiselé *et al.*, 1991). Moreover, a previous report has shown that SDS binds to macromolecules in such a way that it is difficult to

remove or exchange (McPherson, 1999). Guanidinium hydrochloride was useful for solubilizing inclusion bodies but interrupted the purification using ion-exchange chromatography by which the protein could not be trapped on the column. The Omp38 protein was aggregated and precipitated when other detergents were tried. No re-solubilization or refolding was observed using a detergent or phospholipid alone. Because the use of solubilized reagents in both SDS and 6 M guanidinium hydrochloride systems resulted in relatively low yields of the refolded proteins, therefore these methods were not used for Omp38 refolding. A different strategy was also tried following the protocol used for refolding of the recombinant major outer membrane protein antigen (r56) of *Orientia tsutsugamushi* (Ching *et al.*, 1998). This method employed serial steps of dialysis to remove 8 M urea from the solubilised expressed protein solution, leading to slow refolding of the protein while the concentration of urea was gradually reduced. However, it has been found in this study that refolding of Omp38, employing the same method, still could not be achieved, as the protein tended to aggregate in the buffer prior to complete removal of urea. Therefore, the method for refolding still needed to be optimized.

There have been several studies stating that Zwittergent® 3-14 promoted refolding of porins in the absence of membrane components, while remaining the native properties of membrane-extracted proteins (Qi *et al.*, 1994; Pullen *et al.*, 1995; Ulmer *et al.*, 1992). Therefore, various concentrations of Zwittergent® 3-14 (0.5, 2, 5, 10 and 15% (w/v)) in a refolding solution containing 200 mM NaCl, 10 mM EDTA and 0.02% NaN₃ in 20 mM Tris-HCl, pH 7.0, were tested for refolding of the expressed Omp38 (See Method 2.2.18). The result showed that addition of 20 mM

CaCl₂ to the renaturing solution containing 10% Zwittergent® 3-14 helped the monomeric Omp38 to re-associate into a trimeric conformation. Using such a system, the protein could be almost completely refolded with residual amounts of monomeric (<3%) and dimeric (~5%) Omp38 (see Figure 3.23) remained to be observed. Interestingly, completely folding was observed when the protein mixture was heated at 95 °C for 5 min, and the solution was left standing overnight at room temperature. This can be explained that heating followed by cooling may help the misfolded protein to undergo conformational rearrangements by shifting the solution equilibrium towards trimeric conformation, eventually leading to properly refolding of the protein. In addition, it has been noticed that after the protein mixture was passed through gel filtration chromatography to reduce the concentration of the detergent, the protein solution still remained clear. This indicated a relatively stable conformation of the obtained trimeric protein. This finding has been confirmed by the identical secondary structure of the refolded and native proteins, as determined by CD spectroscopy (see Figures 3.24 and 3.36). However, it is important to note that when protein concentrations in the 8 M urea were in excess of 10 mg/ml prior to dilution with the Zwittergent® 3-14, the amounts of trimers seemed to decrease and the protein appeared to re-aggregate. This observation was also found in expression and refolding of Neisserial porins in *E. coli* (Qi *et al.*, 1994). Moreover, using only Zwittergent® 3-14 detergent prior to solubilizing the protein with 8 M urea, refolding of the expressed Omp38 was not accomplished.

4. 4 Biological activities of the native and refolded Omp38

Proteoliposome-swelling assays were employed to study the pore-forming activities of *Bps*Omp38 and *Bth*Omp38. The reconstitution of the trimeric Omp38 into proteoliposomes allowing permeation of small hydrophilic sugars with $M_r < 650$ indicated that the Omp38 acted as a porin-like channel. The protein was likely to form a general diffusion pore because permeation of solutes through the channel seemed to depend solely on the molecular weight of the solutes (Nikaido, 1994; Tokunaga *et al.*, 1979).

Although highest diffusion rate corresponded to the smallest sugar, L-arabinose (150 Da), D-glucose (180 Da) permeated measurably faster than other sugars with the same molecular weight (D-mannose and D-galactose). *B. pseudomallei* and *B. thailandensis*, like other Gram-negative bacteria, utilize glucose as a primary source of carbon for cell growth, and enhanced glucose permeation may be functionally significant (Nitzan *et al.*, 1999). *B. thailandensis* can utilize L-arabinose, while *B. pseudomallei* cannot (Brett *et al.*, 1998). However, the two porins displayed a similar relative diffusion rate for L-arabinose, suggesting that the Omp38 was not a sugar-specific channel for L-arabinose. On the basis of very similar sugar permeability via the unusually large channels of *E. coli* OmpG and the 42-kDa outer membrane porin of *Serratia liquefaciens* (Nitzan *et al.*, 1999 and Fajaro *et al.*, 1998), the diameter of the Omp38 porins could be estimated to be in the range of 1.2-2.0 nm. This range was nearly the same to PorB class 2 protein from *Neisseria meningitidis* (diameter ~1.6 nm) (Minetti *et al.*, 1997), but it was slightly larger than OmpF from *E. coli* (diameter ~1.1 nm)

(Nikaido *et al.*, 1991). Hence, Omp38 porin represents a large channel, which allows a greater variety of nutrients to be taken up.

Melioidosis is a severe disease and successful treatment of melioidosis patients is difficult because *B. pseudomallei* is inherently resistant to a variety of antibiotics (Moor *et al.*, 1999). Resistance to antibiotics may occur due to (i) alteration of the drug targets (Spratt, 1994), (ii) degradation of the drugs by enzymes such as beta-lactamases (Livermore, 1995), (iii) extrusion of the drugs by efflux pumps of broad specificity (Nikaido, 1996), and (iv) decrease in permeability of the cell envelope (Lee *et al.*, 1991; Lee *et al.*, 1992; Masuda *et al.*, 1995; Nikaido, 1994; Parr *et al.*, 1987; Rice *et al.*, 1993). In this study, liposome swelling assays were used to monitor whether or not *BpsOmp38* and *BthOmp38* involved in permeability of various groups of antibiotics e.g. aminoglycosides, carbapenems, cepheims, fluoroquinolones and lincosamides. Results (see Table 3.4 A and B) showed that the relative permeability of various antibiotics through refolded and native *BpsOmp38* and *BthOmp38* were similar. The tested antibiotics passed through the Omp38 pores depending solely on size exclusion limit ($M_r < 650$), but not on the physicochemical properties of the Omp38 pores. Therefore, Omp38 was unlikely to involve in the resistant property of *B. pseudomallei*. The antibiotic resistance may occur by other mechanisms of bacterium.

Moreover, effects of anti-*BpsOmp38* polyclonal antibodies on pore activity of *BpsOmp38* and *BthOmp38* were also tested using liposome-swelling assays. The results in Figures 3.29, 3.30, 3.31 and 3.32 showed that the antibodies inhibited the permeability of sugar solutes through Omp38. Wyllie *et al.* (1998) reported that the MOMP of *Chlamydia psittaci*-specific monoclonal antibody could modify the

opening and closing states of MOMP channel on planar lipid bilayer study. After addition of anti-MOMP monoclonal antibody, the opening states of MOMP was reduced to a much lower amplitude. Kubo and Stephens (2000) used anti-PorB polyclonal antibodies to neutralize infectivity of *C. trachomatis* to hamster kidney cells (HaK) and the results showed that up to 88% of HaK cells were not infected in an *in vitro* neutralization. These results suggested the idea that porins have little or no variability between serotypes as well as being conserved between species (Kubo and Stephens, 2000). The vaccine can be used for the prevention of bacterial infections or killing bacteria by protection of nutrient sources for bacterial growing to pass through porin channels (Kubo and Stephens, 2000). Since *BpsOmp38* and *BthOmp38* were homologous and conserved among various strains of *B. pseudomallei* (Gotoh *et al.*, 1994), *BthOmp38* may be used as a potential candidate for development of a recombinant DNA or synthetic subunit vaccine against *B. pseudomallei* infection. Moreover, *B. thailandensis* is a non-pathogenic bacterium (Brett *et al.*, 1997), therefore it is convenient and safe to be used in laboratory.

4.5 Structural analysis

To evaluate the secondary structure of the Omp38 porin, FTIR and CD spectroscopy were performed. FTIR analysis showed that native Omp38 was consisted almost entirely of β -pleated sheets and was likely to form an anti-parallel β -barrel structure, as similarly reported for other bacterial porins (Forst *et al.*, 1998; Schirmer *et al.*, 1995; Cowan, *et al.*, 1992). The IR patterns of both proteins were almost identical with slight differences found in the turns & loops and lipopolysaccharide

regions. It is not known whether this may be reflected in real differences in the final conformations of the otherwise identical proteins.

The analysis also showed that the Omp₃₈ preparations always contained varying amounts of lipopolysaccharide (LPS). Although both proteins were isolated and purified by the same procedure, the native *Bps*Omp₃₈ contained higher amount of LPS than native *Bth*Omp₃₈. The presence of LPS in the purified proteins could be observed on SDS-PAGE with discrete bands in the unheated samples (Eisele and Rosenbusch, 1990; Arockiasamy and Krishnaswamy, 2000). The idea of a strong porin-LPS interaction is supported by the fact that solubilisation of the Omp₃₈ by a strong detergent (SDS) and gel-filtration failed to remove the LPS completely. However, small amounts of LPS remaining in the *Bps*Omp₃₈ sample helped to improve solubility of the protein, and did not show much effect on the immunoblots, MS analysis and liposome swelling assays carried out in this study.

CD spectra of native *Bps*Omp₃₈ and *Bth*Omp₃₈ showed that the protein conformation was high in β -sheet content, which is also a typical characteristic of other porins such as protein F of *Pseudomonas aeruginosa* strain PAO (Mizuno and Kageyama, 1979), PorB of *Neisseria meningitidis* (Conceição *et al.*, 1997), OprF of *P. aeruginosa* (Brinkman *et al.*, 2000), and MspA of *E. coli* (Heinz *et al.*, 2003). Since α -helical structural content was so low that it could not be observed by either FTIR or CD spectroscopy. CD spectroscopy was also used to monitor refolding stages of the Omp₃₈ expressed in *E. coli*. The CD spectra that gave almost superimposable between

the refolded and native proteins indicated that folding experiments using the renaturing buffer containing Zwittergent® 3-14 were carried out successfully (see Figures 3.34 and 3.45).

Like native Omp₃₈, refolded Omp₃₈ exhibited the heat-modifiable property and was resistant to SDS since the trimer of Omp₃₈ could not be dissociated when the protein sample was mixed with SDS sample buffer alone but dissociated upon heating at 95 °C for 5 min. This has been observed to be general properties of Gram-negative porins (Gotoh *et al.*, 1994; Arockiasamy and Krishnaswamy, 2000). Gel filtration chromatography also proved that the functional Omp₃₈ was composed of homotrimeric subunits.

4.6 Topology and 3D structural model prediction

Omp₃₈ has been predicted to be one of several porins that usually form trimers and have an individual subunit that folds into 16 or 20-stranded barrels (Koebnik *et al.*, 2000). Pfam search for conserved domains from protein databases using RPS-BLAST indicated that the Omp₃₈ proteins belong to a family of Gram-negative bacterial porins. As shown in Figure 3.17, the relatively low sequence homology observed between the porin family seems to be a general observation among porins (Minetti *et al.*, 1997). Amino acid sequence alignments within β -subdivision of proteobacteria showed that *Bps*Omp₃₈ shared 99.7% identity with *Bth*Omp₃₈, 68% identity with *B. cepacia* OpcP₁, and 35.8% identity with the mature protein of *Comamonas acidovorans* Omp₃₂. It has also been observed that Omp₃₈ and *E. coli* OmpF did not

align very well. Prediction of membrane topology strongly suggested that Omp₃₈ was located on the outer membrane of the bacterial cells and folded into a 16-stranded barrel with 8 loops and 8 short periplasmic turns. These findings corresponded with the 3D structure also predicted in this study (see Figure 3.39). Based on the 3D structure prediction, Omp₃₈ was closest similarity to an anion-selective porin, Omp₃₂, from *C. acidovorans* (Zeth *et al.*, 2000). The *N*-terminal amino acids of Omp₃₈ were apparently exposed to the periplasm (see Figure 3.39) and not folded back towards the *C*-terminal phenylalanine as found with OmpF and PhoE from *E. coli* (Cowan *et al.*, 1992). This free space was filled with the bound peptide in *C. acidovorans* Omp₃₂, indicating that corresponding porin-peptide interactions that was stable during preparation and crystallization (Zeth *et al.*, 2000). The longest loop (L₃) that folds into the β-barrel has been suggested to constrict the size of the pore (Breden *et al.*, 2002; Cowan *et al.*, 1992). Loop 8 (L₈), the second longest loop, also folds into the barrel interior and contributes to the formation of the particularly narrow external channel opening. Interestingly, residues Glu⁶⁸ → Ala⁷⁶ and Ser³²⁶ → Thr³²⁹ of Omp₃₈, which contain turn2 (T8) and turn8 (T8) contributed to polar and nonpolar interactions between the interfaces of adjacent monomers (Zeth *et al.*, 2000). These amino acid clusters were almost invariable (Figure 3.17) and might therefore play an essential role in monomer-monomer contact in porins of β-proteobacteria including *C. acidovorans*, *B. cepacia*, *B. pseudomallei* and *B. thailandensis*.

4.7 Preliminary crystallization

Crystallization of Omp₃₈ was carried out using the sitting drop method. The conditions used in crystallization experiments were similar to the conditions employed in crystallization of the Omp₃₂ porin from *Comamonas acidovorans*. The Omp₃₂ crystals were grown in precipitants containing 1.7 to 1.8 M lithium sulfate, 0.1 M Hepes, pH 7.5 and 1.3 to 1.4 M ammonium sulfate, 0.1 M Tris-HCl, pH 8.6 by a hanging drop method (Zeth *et al.*, 1998). In this study, small crystals were obtained (Figure 3.41 and 3.42) when the refolded Omp₃₈ was grown in 0.2 M lithium sulfate or 0.5 M ammonium sulfate in 0.1 M Tris-HCl, pH 8.5 for 2 days. Typically, the size of irregular crystals was about 20 μm x 20 μm x 20 μm . However, conditions for growing Omp₃₈ crystals still need to be optimized to obtain crystals that are suitable for X-ray diffraction analysis. For example, different refolding conditions should be tried by using other detergents or phospholipids. When Zwittergent® 3-14 was used, reproducible renaturation was observed but the yield was consistently low ($\leq 10\text{-}20\%$).

Given the fact that appropriate concentrations for protein crystallization are about 10-20 mg/ml, the concentration of Omp₃₈ (3 mg/ml) used in this study seemed to be relatively low and only small crystals could only be observed. This study failed to concentrate the protein to obtain higher concentration using either Centricon membrane concentrator or PEG 20,000 powder (McRee 1993) as the proteins appeared to absorb on the concentrator membrane or dialysis bag during the preparation. On the other hand, when the volume of the protein mixture was reduced, the protein solution

became turbid or precipitated. In such a case, dialysis against low ionic strength buffer was then required to recover a homogeneous mixture. As a result, the yield obtained after dialysis dramatically reduced. In order to obtain the good quality crystals, conditions for protein preparation and crystallization must be optimized further.

Recently, genetic manipulation has been developed to express several bacterial porins in which proteins can be processed and translocated to the outer membrane of bacterial cells. For example, *Brucella melitensis* Omp31 was expressed using pGEM-7Zf (Vizcaíno *et al.*, 1996), *Fusobacterium nucleatum* T18 FOMA expressed using the pMMB67 system (Haake and Wang, 1997) and *Chlamydia trachomatis* MOMP was expressed using the pET3a system (Jones *et al.*, 2000). Along with condition optimization to obtain highly purified and properly folded Omp38, these expression systems may also be tried in the future to obtain higher yield of Omp38 for crystallization purpose.

Chapter V

Conclusion

In this study, *BpsOmp38* and *BthOmp38* porins were isolated from the outer membrane of *B. pseudomallei* ATCC23343 and *B. thailandensis* ATCC700388 respectively using SDS extractions technique following a chromatographic purification using Sephacryl S-200 HR filtration. SDS-PAGE patterns of the purified *BpsOmp38* and *BthOmp38* were almost identical. The trimeric proteins migrated on SDS-PAGE as M_r 110,000 and were dissociated into three identical monomers of M_r 38,000 when the proteins were heated at 95 °C for 5 min in SDS sample buffer. Liposome-swelling assays revealed that both proteins exhibited porin-like activity, allowing small sugars with M_r <650 to pass through. Structural analysis using Fourier Transform Infrared spectroscopy showed that *Omp38* contained predominant β -sheet structure, which is also a typical characteristic of all Gram-negative porins. Anti-*BpsOmp38* polyclonal antibodies were raised in a white rabbit using protein gel bands of the purified native *BpsOmp38*. Western blot analysis revealed that anti-*BpsOmp38* antibodies recognized both 110-kDa protein (presumably trimeric) and a 38-kDa protein (presumably monomeric). These results showed that *BpsOmp38* and *BthOmp38* are homologues. Tryptic peptide fragments of *BpsOmp38* and *BthOmp38* obtained by MALDI-TOF MS and capillary HPLC ESI-MS/MS gave an unambiguous match with an outer membrane protein, *OpcP1*, of *B. cepacia* in the protein database. This allowed an open reading frame corresponding to the *Omp38*

sequence to be located in the incomplete *B. pseudomallei* genome database. Conserved domain prediction indicated that Omp38 is a member of the porin superfamily. The genes that encode *BpsOmp38* and *BthOmp38* were subsequently isolated and sequenced. Nucleotide sequences of *BpsOmp38* and *BthOmp38* were found to be 98% identical. The putative amino acid sequences of *BpsOmp38* and *BthOmp38* precursors were 99.7% identical, although the amino acid sequences of the processed proteins were 100% identical. The nucleotide sequences of *BpsOmp38* and *BthOmp38* have been deposited in the GenBank database under GenBank accession numbers AY312416 and AY312417, respectively.

The pET23d(+) system was used for expressing the mature *BpsOmp38* and *BthOmp38* in *E. coli* Origami(DE3) as inclusion bodies. Western blot analysis using anti-Omp38 antibodies showed that an expressed protein of 38 kDa was Omp38. Moreover, MALDI-MS fingerprint data gave at least four peptide masses of the expressed *BpsOmp38* and *BthOmp38* matching with four peptide sequences of the native *BpsOmp38*.

The expressed Omp38 was purified by SP Fast Flow HiTrap[™] column following with DEAE Fast Flow HiTrap[™] column. The purified protein (conc. <10 mg/ml) was refolded using a refolding solution (20 mM Tris-HCl, pH 7.0 containing 10% (w/v) Zwittergent® 3-14, 200 mM NaCl, 20 mM CaCl₂, 10 mM EDTA and 0.02% NaN₃), then heated at 95 °C for 5 min and subsequently allowed to stand at room temperature overnight. Successful refolding of Omp38 was confirmed by SDS-PAGE analysis and Circular Dichroism spectroscopy. Liposome-swelling assays showed that the purified refolded Omp38 had non-specific channel activities.

The refolded protein also had the heat-modifiable property like native Omp38 and other Gram-negative porins.

Various groups of antibiotics that have been reported to be potential candidates for melioidosis treatments were used for antibiotic susceptibility tests of *B. pseudomallei* ATCC23343 and *B. thailandensis* ATCC700388 using the disc diffusion technique. These antibiotics included aminoglycosides (amikacin and gentamicin), carbapenems (imipenem and meropenem), cepheims (cefepime, ceftazidime, and cefotaxime), β -lactam/ β -lactamase inhibitor combinations (amoxicillin/clavulanic acid), lincosamides (clindamycin), macrolides (erythromycin), phenicols (chloramphenicol), tetracyclines (tetracycline), fluoroquinolones (ciprofloxacin), ansamycin (rifampin), and folate pathway inhibitors (trimethoprim/sulfamethoxazole). Both bacteria were susceptible to most of the antibiotics tested, while being resistant to gentamicin, clindamycin and erythromycin. On the other hand, *B. thailandensis* seemed to resist to amikacin and rifampin while *B. pseudomallei* did not.

Liposome-swelling assays showed that the Omp38 proteins were not the specific channels for any antibiotics. Moreover, the antibodies against *BpsOmp38* could inhibit the pore activity of Omp38.

Circular Dichroism spectra and molecular weight determination by Sephacryl S-200 filtration chromatography of native and refolded Omp38 revealed that Omp38 was composed of β -sheet structure and stable in trimeric form.

Membrane topology prediction by the method of Diederichs *et al.* (1998) showed that Omp38 was located at the outer membrane of *B. pseudomallei* and *B. thailandensis*. The protein was consisted of 16 transmembrane domains, 8 external

loops and 8 periplasmic turns. The 3D structure of Omp38 protein was predicted using I23D+, Swiss-Model and 3D PSSM and showed that Omp38 had most similarity to the anion selective porin Omp32 of *C. acidovorans*. In agreement with membrane topology prediction, Omp38 was predicted to have a β -barrel structure with 16 transmembrane strands, 8 short periplasmic turns and 8 external loops. The longest loop L3 acted as a pore-confined loop responsible for the size selectivity of the channel. Based on amino acid alignment, Turn 2 and Turn 8 (T2 and T8) situated in the trimer contact region within β -Proteobacteria.

In preliminary crystallization experiments, small crystals of Omp38 (~20 μm x ~20 μm x ~20 μm) were grown under the buffer condition containing 0.2 M lithium sulfate in 0.1 M Tris-HCl, pH 8.5 and 0.5 M ammonium sulfate in 0.1 M Tris-HCl, pH 8.5 as precipitant. For future work, crystallization of Omp38 still need to be improved and 3 dimensional structure may be solved using X-ray crystallography.

References

References

- Abrecht, H., Goormaghtigh, E., Ruyschaert, J. M., and Homble, F. (2000) Structure and orientation of two voltage-dependent anion-selective channel isoforms. An attenuated total reflection fourier-transform infrared spectroscopy study. **J. Biol. Chem.** 75: 40992-40999.
- Amero, S. A., James, T. C., and Elgin, S. C. R. (1994). Production of antibodies using proteins in gel bands. In: J. M. Walker (ed.) **Basic protein and peptide protocols** (pp 401-406). New Jersey: Human Press.
- Andersen, C., Jordy, M., and Benz, R. (1995) Evaluation of the rate constants of sugar transport through maltoporin (LamB) of *E. coli* from the sugar-induced current noise. **J. Gen. Physiol.** 105: 385-401.
- Arakawa, M. (1990) Infection with *Pseudomonas pseudomallei*. **Rinsho Byori** 38: 1226-1231.
- Arockiasamy, A., and Krishnaswamy, S. (2000) Purification of integral outer-membrane protein OmpC, a surface antigen from *Salmonella typhi* for structure-function studies: a method applicable to Enterobacterial major outer-membrane protein. **Anal. Biochem.** 283: 64-70.
- Ashdown, L. R., Johnson, R. W., Koehler, J. M., and Cooney, C. A. (1989) Enzyme linked immunosorbent assay for the diagnosis of clinical and subclinical melioidosis. **J. Infect. Dis.** 160:253-260.

- Ausubel, F. M., Brent, R., Kingston, R. E., Moore, D. D., Seidman, J. G., and Struhl, K. (1999). **Short protocols in molecular biology**. (4th ed.). New York: John Wiley & Sons.
- Barlow, A., K., Heckels, J. E., and Clarke, I. N. (1987) Molecular cloning and expression of *Neisseria meningitidis* Class 1 outer membrane protein in *Escherichia coli* K12. **Infect. Immun.** 55: 2734-2740.
- Behlau, M., Mills, D. J., and Quader, H. (2001) Projection structure of the monomeric porin OmpG at 6 Å resolution. **J. Mol. Biol.** 305: 71-77.
- Benz, R., Woitzik, D., flammann, H. T., and Vos-Scheperkeuter, H. (1987) Pore forming activity of the major outer membrane protien of *Rhodobacter capsulatus* in lipid bilayer membrane. **Arch. Microbiol.** 148: 226-230.
- Bianco, N., Neshat, S., and Poole, K. (1997) Conservation of the multidrug resistance efflux gene oprM in *Pseudomonas aeruginosa*. **Antimicrob. Agents. Chemother.** 41: 853-856.
- Bolstad, A., and Jensen, H. B. (1993) Complete sequence of *Omp1*, the structural gene encoding the 40-kDa outer membrane proteins of *Fusobacterium nucleatum* strain Fev1. **Gene** 132: 107-112.
- Breden, J., Saint, N., Mallea, M. D. E., Molle, G., Pages, J. M. and Simonet, V. (2002) Alteration of pore properties of *Escherichia coli* OmpF induced by mutation of key residues in anti-loop 3 region. **Biochem. J.** 363: 521-528

- Brett, P. J., Deshazer, D., and Woods, D. E. (1997) Characterisation of *Burkholderia pseudomallei* and *Burkholderia pseudomallei*-like strains. **Epidemiol. Infect.** 118: 137-148.
- Brett, P. J., DeShazer, D., and Woods, D. E. (1998) *Burkholderia thailandensis* sp. Nov., description of a *Burkholderia pseudomallei*-like species. **In. J. Syst. Bacteriol.** 48: 317-320.
- Brinkman, F. S. L., Bains, M., and Hancock, R. E. W. (2000) The amino terminus of *Pseudomonas aeruginosa* outer membrane protein OprF forms channels in lipid bilayer membranes: correlation with a three-dimensional model. **J. Biol.** 182: 5251-5255.
- Bryan, L. E., Wong, S., Woods, D. E., Dance, D. A. B., and Chaowagul, W. (1994) Passive protection of diabetic rats with antisera specific for the polysaccharide portion of the lipopolysaccharide isolated from *Pseudomonas pseudomallei*. **Can. J. Infect. Dis.** 5: 170-178.
- Bulieris, P. V., Behrens, S., Holst, O., and Kleinschmidt, J. H. (2003) Folding and insertion of the outer membrane protein OmpA is assisted by the chaperone Skp and by lipopolysaccharide. **J. Biol. Chem.** 278: 9092-9099.
- Carbonetti, N. H., Simnad, V. I., Seifert, H. S., So, M., and Sparling, P. F. (1988) Genetics of protein I of *Neisseria gonorrhoeae*, construction of hybrid porins. **Proc. Natl. Acad. Sci. USA** 85: 6841-6845.
- Carbonetti, N. H., and Sparling, P. F. (1987) Molecular cloning and characterization of the structural gene for protein I, the major outer membrane protein of *Neisseria gonorrhoeae*. **Proc. Natl. Acad. Sci. USA** 86: 2172-2175.

- Chaowagul, W., Suputtamongkol, Y., Dance, D. A. B., Rajchanuvong, A., Pattara-arechachai, J., and White, N. J. (1993) Relapse in Melioidosis: Incidence and risk factors. **J. Infect. Dis.** 168: 1181-1185.
- Ching, W. M., Wang, H., Eamsila, C., Kelly, D. J., and Dasch, G. A. (1998) Expression and refolding of truncated recombinant major outer membrane protein antigen (r56) of *Orientia tsutsugamushi* and its use in enzyme-linked immunosorbent assays. **Clin. Diagn. Lab. Immunol.** 5: 519-526.
- Conceição, A. S. A., Joseph, M., Tai, J. Y., Blake, M. S., Pullen, J. K., Liang, S. M., and Remeta, D. P. (1997) Structural and functional characterization of a recombinant PorB class 2 protein from *Neisseria meningitidis*. **J. Biol. Chem.** 272: 10710-10720.
- Conlan, S., Zhang, Y., Cheley, S., and Bayley, H. (2000) Biochemical and biophysical characterization of OmpG: a monomeric porin. **Biochemistry** 39: 11845-11854.
- Cowan, S. W., Garavito, R. M., Jansonius, J. N., Jenkins, J. A., Karisson, R., König, N., Pai, E. F., Pauptit, R. A., Rizkallah, P. J., Rosenbusch, J. P., Rummel, G., and Schirmer, T. (1995) The structure of OmpF porin in a tetragonal crystal form. **Structure** 3: 1041-1050.
- Cowan, S. W., Schirmer, T., Rummel, G., Steiert, M., Ghosh, R., Pauptit, R. A., Jansonius, J. N., and Rosenbusch, J. P. (1992) Crystal structure explain functional properties of two *E. coli* porins. **Nature** 358: 727-733.
- Currie, B., Smith-Vaughan, H., Golledge, C., Buller, N., Sriprakash, K. S., and Kemp, D. J. (1994) *Pseudomonas pseudomallei* isolates collected over 25 years from

- a non-tropical endemic focus show clonality on the basis of ribotyping. **Epidemiol. Infect.** 113: 307-312.
- Dahan, D., Srikumar, R., Laprade, R., and Coulton, J. W. (1996) Purification and refolding or recombinant *Haemophilus influenzae* type b porin produced in *Bacillus subtilis*. **FEBS Lett.** 392: 304-308.
- Dance, D. A. B. (1991) Melioidosis: the tip of the iceberg. **Clin. Microbiol. Rev.** 4: 52-60.
- Dance, D. A. B. (2000) Ecology of *Burkholderia pseudomallei* and the interactions between environmental *Burkholderia* spp. And human-animal hosts. **Acta Tropica** 74: 159-168.
- Dance, D. A., Wuthiekanun, V., Naigowit, P., and White, N. J. (1989) Identification of *Pseudomonas pseudomallei* in clinical practice: use of simple screening tests and API 20NE. **J. Clin. Pathol.** 42: 645-648.
- Dannenber, A. M., Lu, Z., and He, W. (1996) Laboratory investigation of ecological factors influencing the environmental presence of *Burkholderia pseudomallei*. **Microbiol. Immun.** 40: 451-453.
- Dannenber, A. M., and Scott, E. M. (1958) Melioidosis: pathogenesis and immunity in mice and hamsters. II. Studies with avirulent strains of *Malleomyces pseudomallei*. **Am. J. Pathol.** 34: 1099-1121.
- Dargent, B., Hofmann, W., Pattus, F., and Rosenbusch, J. P. (1986) The selectivity filter of voltage-dependent channels formed by phosphorin (PhoE protein) from *E. coli*. **EMBO J.** 5: 773-778.
- Dharakul, T., Tassaneetrithep, B., Trakulsomboon, S., and Songsivilai, S. (1999) Phylogenetic analysis of Ara⁺ and Ara⁻ *Burkholderia pseudomallei* isolates and

- development of a multiplex PCR procedure for rapid discrimination between the two biotypes. **J. Clin. Microbiol.** 37: 1906-1912.
- Dhiansiri, T., and Puapairoj, T. (1988) Pulmonary melioidosis: clinical-radiologic correlation in 183 cases in northeastern Thailand. **Radiology** 166: 711-715.
- Diederichs, K., Freigang, J., Umhau, S., Zeth, K., and Breed, J. (1998) Prediction by a neural network of outer membrane beta-strand protein topology. **Protein Sci.** 7: 2413-2420.
- Dutzler, R., Rummel, G., Albertí, S., Allés, S. H., Phale, P. S., Rosenbusch, J. P., Benedí, V. J., and Schirmer, T. (1999) Crystal structure and functional characterization of OmpK36, the osmoporin of *Klebsiella pneumoniae*. **Structure** 7: 425-434.
- Eisele, J. L., and Rosencusch, J. P. (1990) In vitro folding and oligomerization of a membrane protein. Transition of bacterial porin from random coil to native conformation. **J. Biol. Chem.** 265: 10217-10220.
- Ellis J. F., and Titball R. W. (1999) *Burkholderia pseudomallei*: medical, veterinary and environmental aspects. **Infect. Dis. Rev.** 1: 174-181.
- Engel, A., Massalski, A., Schindler, M., Dorset, D. L., and Rosenbusch, J. P. (1985) Porin channels merge into single outlets in *Escherichia coli* outer membranes. **Nature** 371: 643-645.
- Evans, W. H., and Graham, J. M. (1991). Protein organization. In: D. Rickwood (ed.). **Membrane structure and function.** (pp 18-20). New York: Oxford University Press .
- Everett, E. D., and Nelson, R. A. (1975) Pulmonary melioidosis: observation in thirty nine cases. **Am. Rev, Respir. Dis.** 112:331-340.

- Forst, D, Welte, W., Wacker, T., and Diederichs, K. (1998) Structure of the sucrose-specific porin ScrY from *Salmonella typhimurium* and its complex with sucrose. **Nat. Struct. Biol.** 5: 37-46.
- Garavito, R. M., and Rosenbusch, J. P. (1986) Isolation and crystallization of bacterial porin. **Methods Enzymol.** 125: 309-328.
- Gerbl-Rieger, S., Peters, J., Kellermann, J., Lottspeich, F., and Baumeister, W. (1991) Nucleotide and derived amino acid sequences of the major porin of *Comamonas acidovorans* and comparison of porin primary structures. **J. Bacteriol.** 173: 2196-2205.
- Goh, S. H., Potter, S., Wood, J. O., Hemmingsen, S. M., Reynolds, R. P., and Chow, A. W. (1996) HSP60 gene sequences as universal targets for microbial species identification: studies with coagulase-negative staphylococci. **J. Clin. Microb.** 34: 818-823.
- Gotoh, N., White, N. J., Chaowagul, W., and Woods, D. (1994). Isolation and characterization of the outer-membrane proteins of *Burkholderia (Pseudomonas) pseudomallei*. **Microbiology** 140: 797-805.
- Gotschlich, E. C., Seiff, M. E., Blake, M. S., Koomey, M. (1987) Porin protein of *Neisseria gonorrhoeae*: cloning and gene structure. **Proc. Nalt. Acad. Sci. USA** 84: 8135-8139.
- Haake, S. K., and Wang, X. (1997) Cloning and expression of FOMA, the major outer-membrane protein gene from *Fusobacterium nucleatum* T18. **Archs. Oral Biol.** 1: 19-24.
- Hancock, R. E. W. (1987) Role of porins in outer membrane permeability. **J. Bacteriol.** 169: 929-933.

- Hancock R. E. W. (1991) Bacterial outer membranes: evolving concepts. **Features** 57: 175-182.
- Hancock, R. E., W., and Benz, R. (1986) Demonstration and chemical modification of a specific phosphate binding site in the phosphate-starvation inducible outer membrane porin protein P of *Pseudomonas aeruginosa*. **Biochem. Biophys. Acta** 860: 699-707.
- Hazumi, N., Yamada, H., and Mizushima, S. (1978) Two new peptidoglycan-associated proteins in the outer membrane of *Escherichia coli* K-12. **FEMS. Micro. Lett.** 4, 275-277.
- Heinz, C., Karosi, S., and Niederweis, M. (2003) High-level expression of the mycobacterial porin MspA in *Escherichia coli* and purification of the recombinant protein. **J. Chromatogr.** 790: 337-348.
- Hirsch, A., Breed, J., Saxena, K., Richter, O. M., Ludwig, B., Diederichs, K., and Welte, W. (1997) The structure of porin from *Paracoccus denitrificans* at 3.1 Å resolution. **FEBS Lett.** 404: 208-210.
- Howe, C., Sampath, A., and Spotnitz, M. (1971) The *Pseudomallei* group. **J. Infect. Dis.** 124: 598-606.
- Ip, M., Osterberg, L. G., Chau, P. Y., and Raffin, T. A. (1995) Pulmonary melioidosis. **Chest** 108: 1420-1424.
- Jap, B. K., and Walian, P. J. (1996) Structure and functional mechanism of porins. **Physiol. Rev.** 76: 1073-1088.
- Jawetz, E., Melnick, J. L., and Adelberg, E. A. (1995). **Medical microbiology**. USA: Appleton and Lange.

- Jones H. M., Kubo, A., and Stephens, R. S. (2000) Design, expression and functional characterization of a synthetic gene encoding the *Chlamydia trachomatis* major outer membrane protein. **Gene** 258: 173-181.
- Jordy, M., Andersen, C., Schulein, K., Ferenci, T., and Benz, R. (1996) Rate constants of sugar transport through two LamB mutants of *Escheichia coli*: comparison with wild-type maltoporin and LamB *Salmonella typhimurium*. **J. Mol. Biol.** 259: 666-678.
- Karshikoff, A., Spassov, V., Cowan, S. A., Ladenstein, R., and Schirmer, T. (1994) Electrostatic properties of two porin channels from *E. coli*. **J. Mol. Biol.** 240: 372-384.
- Koebnik, R., Locher, K. P., and Van Gelder, P. (2000) Structure and function of bacterial outer membrane proteins: barrels in a nutshell. **Mol. Microbiol.** 37: 239-253
- Korteland, J., Tommassen, J., and Lugtenberg, B. (1982) PhoE protein pore of the outer membrane of *Escherichia coli* K12 is a particularly efficient channel for organic and inorganic phosphate. **Biochem. Biophys. Acta** 690: 282-289.
- Kreusch, A., and Schulz, G. E. (1994) Refined structure of the porin from *Rhodopseudomonas blastica*. Comparison with the porin from *Rhodobacter capsulatus*. **J. Mol. Biol.** 243: 891-905.
- Kubo, A., and Stephens, R. S. (2000) Characterization and functional analysis of PorB, a *Chlamydia* porin and neutralizing target. **J. Mol. Biol.** 38: 772-780.
- Laemmli, U. K. (1970). Cleavage of structural proteins during assembly of head of bacteriophage-T₄. **Nature** 227: 680-685.

- Lee, E. H., Nicolas, M. H., Kitzis, M. D., Plaloux, G., Collatz, E., and Gutmann, I. (1991) Association of two resistance mechanisms in a clinical isolate of *Enterobacter cloacae* with high-level resistance to imipenem. **Antimicrob. Agents Chemother.** 35: 1093-1098.
- Lee, E. H., collatz, E., Trias, J., and Gutmann, I. (1992) Diffusion of beta-lactam antibiotics into proteoliposomes reconstituted with outer membranes of isogenic imipenem-susceptible and resistant strains of *Enterobacter cloacae*. **J. Gen. Microbiol.** 138: 2347-2351.
- Levine, H. B., and Maurer, R. L. (1958) Immunization with an induced avirulent auxotrophic mutant of *Pseudomonas pseudomallei*. **J. Immunol.** 81: 433-438.
- Livermore, D. M. (1995) β -lactamases in laboratory and clinical resistance. **Clin. Microbiol. Rev.** 8: 557-584.
- Luckey, M., and Nikaido, H. (1980) Specificity of diffusion channels produced by lamda phage receptor protein of *Escherichia coli*. **Proc. Natl. Acad. Sci. USA** 77: 167-171.
- Mäntele, W., and Fabian, H. (2002). Infrared spectroscopy of proteins. In: J. M., Chalmers and P. R., Griffiths (eds.). **Handbook of vibrational spectroscopy.** (pp 1-27). Chichester: John Wiley and Sons.
- Masuda, N., Sakagawa, E., and Ohya, S. (1995) Outer membrane proteins responsible for multiple drug resistance in *Pseudomonas aeruginosa*. **Antimicrob. Agents. Chemother.** 39: 645-649.
- McCormick, J. B., Sexton, D. J., McMurray, J. G., Carey, E., Hayes, P. F., and Feldman, R. A. (1975) Human-to-human transmission of *Pseudomonas pseudomallei*. **Ann. Intern. Med.** 83: 512-513.

- McPherson, A. (1999) **Crystallization of biological macromolecules**. New York: Cold spring harbor laboratory press.
- McRee, D. E. (1993) **Practical protein crystallography**. USA: Academic press.
- Meyer, J. E. W., Hofnung, M., and Schulz, G. E. (1997) Structure of maltoporin from *Salmonella typhimurium* ligated with a nitro-phenyl-maltotrioxide. **J. Mol. Biol.** 119: 149-157.
- Minetti, C. A. S. A., Tai, J. Y., Blake, M. S., Pullen, J. K., Liang, S. M., and Remeta, D. P. (1997) Structural and functional characterization of a recombinant PorB class 2 protein from *Neisseria meningitidis*. **J. Biol. Chem.** 272: 10710-10720.
- Mizuno, T., and Kageyama, M. (1979) Isolation and characterization of major outer membrane proteins of *Pseudomonas aeruginosa* strain PAO with special reference to peptidoglycan-associated protein. **J. Biochem. (Tokyo)** 86: 979-989.
- Moat A. G., and Foster, J. W. (1995). **Microbial physiology**. New York: Wiley-Liss.
- Moore, R. A., Deshzer, D., Reckseidler, S., Weissman, A., and Woods, D. E. (1999) Efflux-mediated aminoglycoside and macrolide resistance in *Burkholderia pseudomallei*. **Antimicrob. Agents. Chemother.** 43: 465-470.
- Nikaido, H. (1992) Porins and specific channels of bacterial outer membranes. **Mol. Microbiol.** 6: 435-442.
- Nikaido, H. (1994) Porins and specific diffusion channels in bacterial outer membrane permeability. **Microbiol. Rev.** 49: 1-32.
- Nikaido, H. (1994) Prevention of drug access to bacterial targets: permeability barriers and active efflux. **Science** 264: 382-388.

- Nikaido, H. (1996) Multidrug efflux pumps of Gram-negative bacteria. **J. Bacteriol.** 178: 5853-5859.
- Nikaido, H, Nikaido, K., and Harayama, S. (1991) Identification and characterization of porins in *Pseudomonas aeruginosa*. **J. Biol. Chem.** 266: 770- 779.
- Nikaido, H. and Rosenberg, E. Y. (1983) Porin channels in *Escherichia coli*: studies with liposomes reconstituted from purified proteins. **J. Bacteriol.** 153: 241-252.
- Nikaido, H and Vaara, M. (1985) Molecular basis of bacterial outer membrane permeability. **Microbiol. Rev.** 49: 1-32.
- Nitzan, Y., Orlovsky, K. and Pechatnikov, I. (1999) Characterization of porins isolated from the outer membrane of *Serratia liquefaciens*. **Curr. Microbiol.** 8: 71-79.
- Olsen, G. J., and Woese, C. R. (1993) Ribosomal RMA: a key to phylogeny. **FASEB J.** 7: 113-123.
- Odou, M. F., Singer, E., and Dubreuil, L. (2001) Description of complex forms of a porin in *Bacteroides fragilis* and possible implication of this protein in antibiotic resistance. **Anaerobe** 7:219-225.
- Parr, T. R., Moore, R. A., Moore, L. V., and Hancock, R. E. W. (1987) Role of porins in intrinsic antibiotic resistance of *Pseudomonas cepacia*. **Antimicrob. Agents. Chemother.** 31: 121-123.
- Pebay-Peyroula, E., Garavito, R. M., Rosenbusch, J. P., Zulauf, M., and Timmins, P. A. (1995) Detergent structure in tetragonal crystals of OmpF porin. **Structure** 3: 1051-1059.
- Prescott, L., Harley, J. P., and Klein, D. A. (1999) **Microbiology**. USA: McGraw-Hill.

- Prevatt, A. L., and Hunt, J. S. (1957) Chronic systemic melioidosis. **Am. J. Med.** 23: 810-823.
- Pullen, J. K., Liang, S. M., Blake, M. S., Mates, S., and Tai, J. Y. (1995) Production of *Haemophilus influenzae* type-b porin in *Escherichia coli* and its folding into the trimeric form. **Gene** 152: 85-88.
- Qi, H. L., Tai, J. Y., and Blake, M. S. (1994) Expression of large amounts of *Neisseria* porin proteins in *Escheichia coli* and Refolding of the proteins into native trimers. **Infect. Immun.** 62: 2432-2439.
- Raetz, C. R. H. (1993) Bacterial endotoxins: Extraordinary lipids that activate eucaryotic signal transduction. **J. Bacteriol.** 175: 5745-5753.
- Ramsay, S. C., Labrooy, J., Norton, R., and Webb, B. (2001) Demonstration of different patterns of musculoskeletal, soft tissue and visceral involvement in melioidosis using 99m Tc stannous colloid white cell scanning. **Nucl. Med. Commun.** 22: 1193-1199.
- Randall-Hazelbauer, L., and Schwartz, M. (1973) Isolation of the bacteriophage lambda receptor from *E. coli*. **J. Bacteriol.** 116: 1436-1446.
- Reckseidler, S., Deshzer, D., Sokol, P. A., and Woods, D. E. (2001) Detection of bacterial virulence genes by subtractive hybridization: identification of capsular polysaccharide of *Burkholderia pseudomallei* as a major virulence determinant. **Infect. Immun.** 69: 34-44.
- Rice L. B., Carias, L. L., Etter, L., and Shlase, D. M. (1993) Resistance to cefoprazone-sulbactam in *Klebsiella pneumoniae*: evidence for enhanced resistance resulting from the coexistence of two different resistance mechanisms. **Antimicrob. Agents Chemother.** 37: 1061-1064.

- Ringuet, H., Akoua-Koffi, C., Honore, S., Varnerot, A., Vincent, V., Berche, P., Gaillard, J. L., and Pierre-Audigier, C. (1999) Hsp65 sequencing for identification of rapidly growing mycobacteria. **J. Clin. Microbiol.** 37: 852-857.
- Rosenbusch, J. R. (1974) Characterization of the major envelope protein from *Escherichia coli*. Regular arrangement on the peptidoglycan and unusual dodecyl sulfate binding. **J. Biol. Chem.** 249, 8019-8029.
- Saint, N., Lou, K. L., Widmer, C., Luckey, M., Schirmer, T., and Rosenbusch, J. P. (1996) Structural and functional characterization of OmpF porin mutants selected for larger pore size. II. Functional characterization. **J. Biol. Chem.** 271: 20676-20680.
- Sambrook, J., Fritsch, E. F., and Maniatis, T. (1989). **Molecular cloning: a laboratory manual** (2nd ed.). New York: Cold Spring Harbor Laboratory Press.
- Schirmer, T. (1998) General and specific porins from bacterial outer membranes. **J. Struct. Biol.** 121: 101-109.
- Schirmer, T., Keller, T. A., Wang, Y. F., and Rosenbusch, J. P. (1995) Structural basis for sugar translocation through maltoporin channels at 3.1 Å resolution. **Science** 267: 512-514.
- Schlech, W. F., Turchik, J. B., Westlake, R. E., Klein, G. C., Band, J. D., and Weaver, R. E. (1981) Laboratory-acquired infection with *Pseudomonas pseudomallei* (melioidosis). **N. Engl. J. Med.** 305: 1133-1135.

- Schmid, B., KrÖmer, M., and Schulz, G. E. (1996) Express of porin from *Rhodopseudomonas blastica* in *Escherichia coli* inclusion bodies and folding into exact native structure. **FEBS Lett.** 381: 111-114.
- Schülein, k., Schmid, K., and Benz, R. (1991) The sugar-specific outer membrane channel ScrY contains functional characteristics of general diffusion pores and substrate specific porins. **Mol. Microbiol.** 5: 2233-2241.
- Shevchenko, A., Wilm, M., Vorm, O., and Mann, M. (1996) Mass spectrometric sequencing of proteins from silver-stained polyacrylamide gels. **Anal. Chem.** 68: 850-858.
- Simpson, A. J. H., Howe, P. A., Wuthiekanun, V., and White, N. J. (1999) A comparison of lysis-centrifugation, pour plate and conventional blood culture methods in the diagnosis of septicemic melioidosis. **J. Clin. Pathol.** 52: 616-619.
- Siritapetawee J., Prinz, H., Samosornsuk, W., Ashley, R. H., and Suginta, W. (2004) Functional reconstitution, gene isolation and topology modelling of porins from *Burkholderia pseudomallei* and *Burkholderia thailandensis*. **Biochem. J.** 377: 579-87.
- Smith, M. D., Angus, B., Wuthiekanun, V., and White, N. J. (1997) Arabinose assimilation defines a non-virulent biotype of *Burkholderia pseudomallei*. **Infect. Immun.** 65: 4319-4321.
- Smith, M. D., Wuthiekanun, V., Walsh, A. L., and Pitt, T. L. (1993) Latex agglutination test for identification of *Pseudomonas pseudomallei*. **J. Clin. Pathol.** 46: 374-375.

- Songsivilai, S., and Dharakul T. (2000) Multiple replicons constitute the 6.5-megabase genome of *Burkholderia pseudomallei*. **Acta. Trop.** 74: 169-179.
- Sonthayanon, P., Krasao, P., Wuthiekanun, V., Panyim, S., and Tungpradabkul, S. (2002) A simple method to detect and differentiate *Burkholderia pseudomallei* and *Burkholderia thailandensis* using specific flagellin gene primers. **Mol. Cell. Prob.** 16: 217-222.
- Spratt, B. G. (1994) Resistance to antibiotics mediated by target alterations. **Science** 264: 368-393.
- Steinmetz, I., Reganzerowski, A., Brenneke, B., Häußler, S., Simpson, A., and White, N. J. (1999) Rapid identification of *Burkholderia pseudomallei* by latex agglutination based on an exopolysaccharide-specific monoclonal antibody. **J. Clin. Microbiol.** 37: 225-228.
- Suputtamongkol, Y., Hall, A. J., Dance, D. A. B., Chaowagul, W., Rajchanuvong, A., Smith, M. D., and White, N. J. (1994) The epidemiology of melioidosis in Ubon Ratchatani, Northeast Thailand. **Int. J. Epidemiol.** 23: 1082-1090.
- Tiangpitayakorn, C., Songsivilai, S., Piyasangthong, N., and Dharakul, T. (1997) Speed of detection of *Burkholderia pseudomallei* in blood cultures and its correlation with the clinical outcome. **Am. J. Trop. Med. Hyg.** 57: 96-99.
- Tokunaga, M., Tokunaga, H., Okajima, Y., and Nakae, T. (1979) Characterization of porins from the outer membrane of *Salmonella typhimurium* 2. Physical properties of the functional oligomeric aggregates. **Eur. J. Biochem.** 95: 441-448.

- Tsujimoto, H., Gotoh, N., Yamagishi, J. Oyamada, Y., and Nishino, T. (1997) Cloning and expression of the major porin protein gene *opcP* of *Burkholderia* (formerly *Pseudomonas*) *cepacia* in *Escherichia coli*. **Gene** 186: 113-118.
- Ulmer, J.B., Burke, C. J., Shi, C.,Friedman, A., Donnelly, J. J., and Liu, M. A. (1992) Pore formation and mitogenicity in blood cells by the class 2 protein of *Nesseria meningitidis*. **J. Biol. Chem.** 267: 19266-19271.
- Veen, H. W. V., Putman, M., Klompenburg, W. V., Heijne, R., Margolles, A., and Konings, W. N. (1998) Basic mechanisms of antibiotic resistance: molecular properties of multidrug transporters. **MJM** 4: 56-66.
- Vendrous, N. A., Chow, D., and Liong, E. (1988) Experimental vaccine against *Pseudomonas pseudomallei* infections in captive cetaceans. **Dis. Aquat. Organ.** 5: 157-161.
- Vizcaíno, N., Cloeckart, A. Zygmunt, M. S., and Dubray, G. (1996) Cloning, nucleotide sequence, and expression of the *Brucella melitensis omp31* gene coding for an immunogenic major outer membrane protein. **Infect. Immun.** 64: 3744-3751.
- Walsh, A. L., Smith, M. D., Wuthiekanun, V., Suputtamongkol, Y., Desakorn, V., Chaowagul, W., and White, N. J. (1994) Immunofluorescence microscopy for the rapid diagnosis of melioidosis. **J. Clin. Pathol.** 47: 377-379.
- Walsh, A. L., and Wuthiekanun, V. (1996) The laboratory diagnosis of melioidosis. **Br. J. Biomed. Sci.** 53: 549-253.
- Wang, Y. F,m Dutzler, R., Rizkallah, P. J., Rosenbusch, J. P., and Schirmer, T. (1997) Channel specificity: Structural basis for sugar discrimination and differential flux rates in maltoporin. **J. Mol. Biol.** 272: 56-63.

- Warawa, J. and Woods, D.E. (2002) Melioidosis vaccines. **Expert Rev. Vaccines**. 1: 477-82.
- Weiss, M. S., Abele, U., Weckesser, J., Welte, W., Schiltz, E., and Schulz, G. E. (1991) Molecular architecture and electrostatic properties of a bacterial porin. **Science** 254: 1627-1630.
- Weiss, M. S., and Schulz, G. E. (1992) Structure of porin refined at 1.8 Å resolution. **J. Mol. Biol.** 277: 493-509.
- White, N. J. (2003) Melioidosis. **The Lancet** 361: 1715-1722.
- Woo, P. C. Y., Woo, G. K. S., Lau, S. K. P., Wong, S. S. Y., and Yuen, K. Y. (2002) Single gene target bacterial identification: *groEL* gene sequencing for discriminating clinical isolates of *Burkholderia pseudomallei* and *Burkholderia thailandensis*. **Diag. Microb. Infect. Dis.** 44: 143-149.
- Woods, G. L., and Washington, J. A. (1995). Antibacterial susceptibility test: dilution and disk diffusion methods. In: P. R. Murray *et al.* (ed.). **Manual of clinical microbiology**. (pp 1327-1341). Washington DC: American Chemical Society.
- Wyllie, S., Ashley, R. H., Longbottom, D., and Herring, A. J. (1998) The major outer membrane protein of *Chlamydia psittaci* functions as a porin-like ion channel. **Infect. Immun.** 66: 5202-5207.
- Yoshimura, F., Zalman, L. S. and Nikaido, H. (1983) Purification and properties *Pseudomonas aeruginosa* porin. **J. Biol. Chem.** 258: 2308-2314.
- Zeth, K., Diederichs, K., Welte, W. and Engelhardt, H. (2000) Crystal structure of Omp₃₂, the anion-selective porin from *Comamonas acidovorans*, in complex with a periplasmic peptide at 2.1 Å resolution. **Structure** 8: 981-992.

Zeth, K., Schnaible, V., Przybylski, M., Welte, W., Diederichs, K., and Engelhardt, H.

(1998) Crystallization and preliminary X-ray crystallographic studies of the native and chemically modified anion-selective porin from *Comamonas acidovorans*. **Acta Cryst. D**54: 650-653.

Appendices

Appendix A

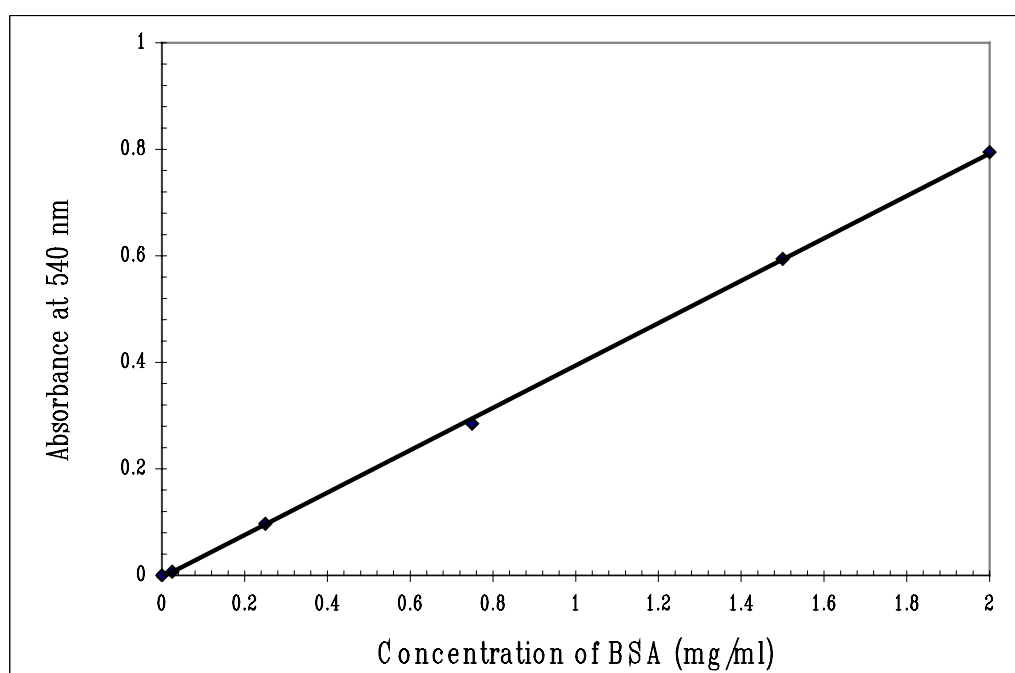
0.5 McFarland turbidity standard preparation

Add 0.5 ml of 0.048 M BaCl₂ (1.175% (w/v) BaCl₂·H₂O) to 99.5 ml of 0.36 N H₂SO₄ (1% (v/v)). Distribute ~5 ml into screw cap tubes of the same size used to prepare the inoculum. Tightly seal and store in the dark at room temperature.

Agitate vigorously before use.

Appendix B

Stand curve of BSA by BCA Protein Assay



Appendix C

Plasmid maps

1. pGEM®-T Vector circle map

The pGEM®-T Vector Systems are convenient systems for the cloning of PCR products. The pGEM®-T Vector is prepared by cutting Promega's pGEM®-5Zf(+) Vector with *EcoR* V and adding a 3' terminal thymidine to both ends. These single 3'-T overhangs at the insertion site greatly improve the efficiency of ligation of a PCR product into the plasmid by preventing recircularization of the vector and providing a compatible overhang for ligation of PCR products generated by certain thermostable polymerases. These polymerases often add a single deoxyadenosine, in a template-independent fashion, to the 3'-ends of amplified fragments.

The multiple cloning site is flanked by recognition sites for the restriction enzyme *Bst*Z I, allowing release of the insert by a single-enzyme digestion. Alternatively, a double digestion may be used to release the insert from the vector. The pGEM®-T Vector System II contains JM109 Competent Cells in addition to all of the pGEM®-T Vector System I components.

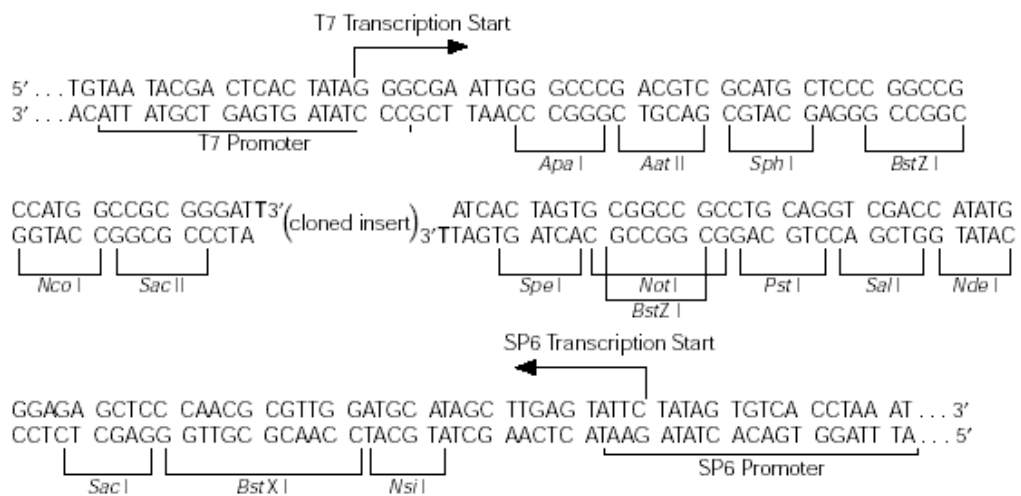
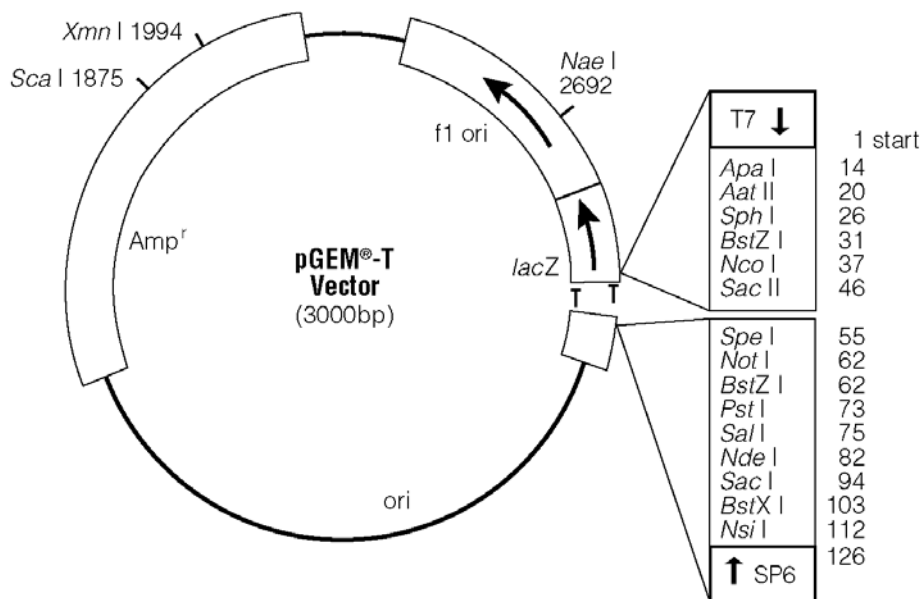
The feature of pGEM®-T Vector System II

-Rapid Ligation: The 2X Rapid Ligation Buffer provided allows reactions to be completed in 1 hour at room temperature.

-Blue/White Screening: T7 and SP6 RNA polymerase promoters flank a multiple cloning region within the α -peptide coding region for β -galactosidase.

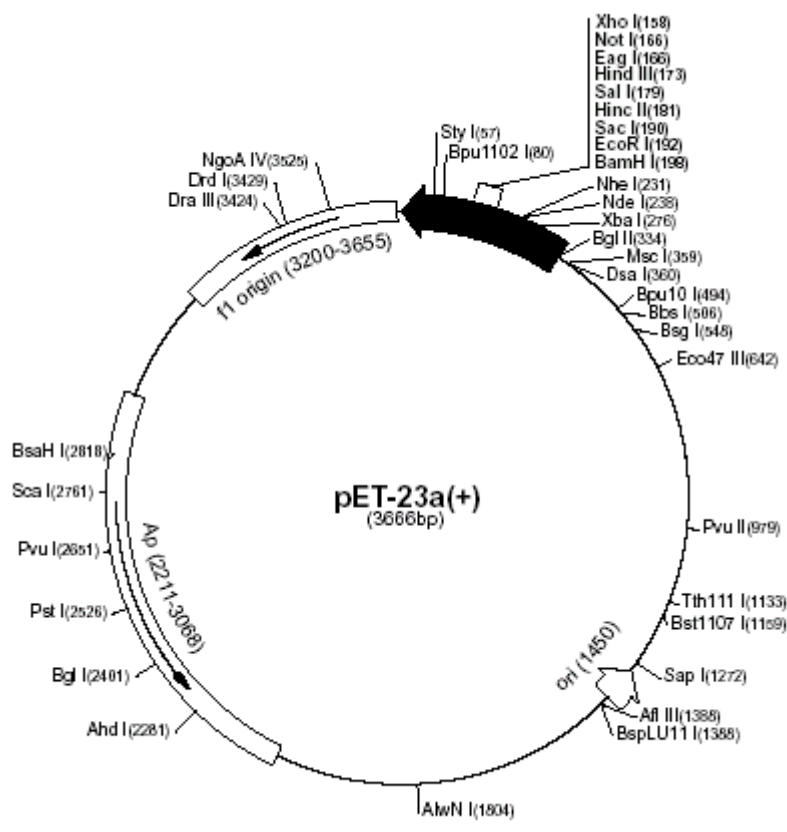
Insertional inactivation of the α -peptide allows recombinant clones to be directly identified by color screening on indicator plates.

-f1 Origin of Replication: Allows the preparation of single-stranded DNA



2. pET-23d(+) Vector

The pET-23d(+) vector carry an N-terminal T7•Tag sequence plus an optional C-terminal His•Tag sequence. The cloning/expression region of the coding strand transcribed by T7 RNA polymerase is shown below. The fl origin is oriented so that infection with helper phage will produce virions containing single-stranded DNA that corresponds to the coding strand. Therefore, single-stranded sequencing should be performed using the T7 terminator primer. The pET-23d(+) plasmids contain the gene for ampicillin resistance (β -lactamase) in the same orientation as the target gene. If the T7 transcription terminator is removed during cloning, IPTG-dependent accumulation of β -lactamase (M_r 31.5 kDa) is usually observed along with the target protein, due to efficient read-through transcription by T7 RNA polymerase.



T7 promoter primer #69348-3

Bgl II
T7 promoter
Xba I
rbs

AGATCTCGATCCCGGAAATTAATACGACTCACTATAGGGAGACCACAACGGTTTCCCTCTAGAAATAATTTTGTTTAACTTTAAGAAGGAGA

Nde I Nhe I
T7-Tag
pET-23a
BamH I EcoR I Sac I
Hinc II Sal I Hind III
Eag I Not I
Xho I
His-Tag

TATACATATGGCTAGCATGACTGGTGGACAGCAAATGGGTCGGGATCCGAATTCGAGCTCCGTCGACAAGCTTGCGGCCGCACTCGAGCACCACCACCACCACCCTGA
 MetAlaSerMetThrGlyGlyGlnGlnMetGlyArgGlySerGluPheGluLeuArgArgGlnAlaCysGlyArgThrArgAlaProProProProProLeu

pET-23d <u>Nco I</u> ...TACCATGGCTAGC... MetAlaSer...	pET-23b ...GGTCGGGATCCGAATTCGAGCTCCGTCGACAAGCTTGCGGCCGCACTCGAGCACCACCACCACCACCCTGA ...GlyArgAspProAsnSerSerSerValAspLysLeuAlaAlaAlaLeuGluHisHisHisHisHisEnd pET-23c,d ...GGTCGGATCCGAATTCGAGCTCCGTCGACAAGCTTGCGGCCGCACTCGAGCACCACCACCACCACCCTGA ...GlyArgIleArgIleArgAlaProSerThrSerLeuArgProHisSerSerThrThrThrThrThrGlu
--	---

Bpu1102 I
T7 terminator

GATCCGGCTGCTAACAAAGCCCGAAAGGAAGCTGAGTTGGCTGCTGCCACCGCTGAGCAATAACTAGCATAACCCCTTGGGGCTCTAAACGGGTCTTGAGGGGTTTTTGTG

T7 terminator primer #69337-3

pET-23a-d(+) cloning/expression region

Appendix D

Competent cell preparation

1. The *E. coli* DH5 α host strain

E. coli DH5 α strain, a cloning host strain, was used to prepare competent cells by using CaCl₂ methods as described by Sambrook *et al.* (1989). A single colony of *E. coli* DH5 α was inoculated into 5 ml of LB broth (Appendix E) and grown at 37°C overnight (12-14 h) with 150 rpm shaking. The overnight culture was used as inoculum for preparation of competent cells. One milliliter of the inoculum culture (1%) was added into a 500-ml flask containing 100 ml of LB broth and grown at 37°C with 240 rpm shaking until the optical density (OD) at 600 nm was about 0.3-0.4 (about 3 h). The cell culture was transferred into a pre-chilled polypropylene tube, chilled on ice for 10 min, and pelleted by centrifugation at 3,000 x g at 4°C, 10 min. The cell pellets were resuspended completely and gently with 20 ml of ice-cold CaCl₂ solution (60 mM CaCl₂, 10 mM PIPES, pH 7.0, 15% glycerol) (Appendix E). The resuspended cells were pelleted by centrifugation as described above. The cell pellets were resuspended completely and gently again with 20 ml of ice-cold CaCl₂ solution and chilled on ice for 30 min. The pellets were centrifuged as above, resuspended in 2 ml ice-cold CaCl₂ solution containing 7% dimethyl sulfoxide (DMSO), and aliquoted into microtubes (100 μ l/tube). These competent cells were immediately kept at -70°C in a freezer until transformation.

2. The *E. coli* Origami(DE3) host strain

Preparation *E. coli* Origami(DE3) competent cells were carried out using the same protocol as *E. coli* DH5 α host strain as described in Appendix D1. The difference was antibiotics; tetracycline (12.5 $\mu\text{g/ml}$), and kanamycin (15 $\mu\text{g/ml}$) were added in the LB broth and LB agar (Appendix E) for selection of host strain.

Appendix E

Solution preparation

1. Reagents for bacterial culture and competent cell transformation

1.1 LB broth containing antibiotics (1 L)

Dissolve 10 g Bacto Tryptone, 5 g Bacto Yeast Extract and 5 g NaCl in 800 ml distilled water. Adjust pH to 7.2 with NaOH and the volume to 1 L with distilled water. Autoclave the solution at 121°C for 15 min. Allow the medium to cool to 50°C before adding antibiotics with concentration recommended for each cloning system and store at 4°C.

1.2 LB plate with 100 µg/ml of ampicillin (1 L)

Dissolve 10 g Bacto Tryptone, 5 g Bacto Yeast Extract, 5 g NaCl and 15 g Bacto agar in 800 ml distilled water. Adjust pH to 7.2 with NaOH and the volume to 1 L with distilled water. Sterilize by autoclaving at 121°C for 20 min. Allow the medium to cool to 50°C, then add ampicillin to a final concentration 100 µg/ml. Pour medium into Petri-dishes. Allow the agar to harden, and keep at 4°C.

1.3 LB agar plate with 100 µg/ml of ampicillin, 15 µg/ml kanamycin, 12.5 µg/ml tetracyclin (1 L)

Dissolve 10 g Bacto Tryptone, 5 g Bacto Yeast Extract, 5 g NaCl and 15 g Bacto agar in 800 ml distilled water. Adjust pH to 7.2 with NaOH and the volume to 1 L with distilled water. Sterilize by autoclaving at 121°C for 20 min. Allow the medium to cool to 50°C, then add ampicillin to a final concentration 100 µg/ml, kanamycin 15 µg/ml, 12.5 µg/ml tetracyclin. Pour medium into Petri-dishes, allow the agar to harden, and keep at 4°C.

1.4 LB plate with 100 µg/ml of ampicillin/IPTG/X-Gal

Make the LB plates with ampicillin as above. Then spread 50 µl of 100 mM IPTG and 25 µl of 50 mg/ml X-Gal over the surface of the plates and allow to absorb for 10 min before use.

1.5 Antibiotics solution stock

Ampicillin (100 mg/ml): dissolve 100 mg ampicillin in 1 ml sterile distilled water.

Kanamycin (30 mg/ml): dissolve 30 mg kanamycin in 1 ml sterile distilled water.

Tetracyclin (12.5 mg/ml): dissolve 12.5 mg tetracyclin in 1 ml absolute alcohol.

Filter sterile all antibiotics solution and keep at -20°C.

1.6 IPTG stock solution (100 mM)

Dissolve 0.12 g IPTG (isopropyl thio-β-D-galactoside) in distilled water and make up as final volume of 5 ml. Sterilize by filter sterilize and store at -20°C.

1.7 X-gal stock solution

Dissolve 50 mg X-gal in dimethylformamide (DMF) and store in a dark bottle at -20°C.

2. Reagent for competent cell preparation

2.1 CaCl₂ Solution (60 mM CaCl₂, 10 mM PIPES pH 7.0, 15% glycerol)

To prepare 100 ml solution, mix the stock solution as follow:

- 6 ml of 1 M CaCl₂ (14.7 g/100 ml, filter sterile)
- 10 ml of 100 mM PIPES (piperazine-1,4-bis(2-ethanesulfonic acid)), pH 7.0 (3.02 g/100 ml adjust pH with KOH, filter sterile)
- 15 ml of 100% glycerol (autoclave at 121°C, 15 min)

Add sterile distilled water to bring a volume up to 100 ml. Store the solution at 4°C.

2.2 SOC media (1 L)

Dissolve 20 g Bacto Tryptone, 5 g Bacto Yeast Extract, 10 ml 1M of NaCl (5.85 g/100 ml), 2.5 ml 1 M KCl (7.44 g/100 ml) in distilled water and make to 980 ml final volume. Sterilize by autoclaving at 121°C for 20 min. Allow the medium cool to room temperature, then add 5 ml of 1 M MgCl₂·6H₂O (20.33 g/100 ml), 5 ml of 1 M MgSO₄·7 H₂O (12.30 g/100 ml), 10 ml of 2 M of glucose (36 g/100 ml) which were filter sterilized. Store the solution at 4°C.

3. Reagents for isolation plasmid DNA (boiling prep)

3.1 STET (100 mM NaCl, 10 mM Tris, pH 8.0, 1 mM EDTA, 5% Triton X-100) (100 ml)

Mix 20 ml of 1 M NaCl (sterile), 2 ml of 1 M Tris-HCl, pH 8.0 (sterile), 0.4 ml of 0.5 M EDTA, pH 8.0 (sterile), 5 ml Triton X-100 and adjust the volume to 100 ml with sterile distilled water. Store at room temperature.

3.2 3 M Sodium acetate buffer, pH 4.8 (100 ml)

Dissolve 24.6 g sodium acetate in 80 ml distilled water. Adjust pH to 4.8 with glacial acetic acid and the volume to 100 ml with distilled water. Sterilize by autoclaving at 121°C for 20 min. Store at room temperature.

3.3 RNase A (10 mg/ml)

Dissolve 10 mg RNase A in 10 mM Tris-HCl, pH 7.4, 15 mM NaCl (sterile). Store at -20°C.

3.4 1 M Tris-HCl, pH 7.4 and pH 8.0 (100 ml)

Dissolve 12.11 g of Tris Base in 80 ml distilled water. Adjust pH with HCl to pH 7.4 or 8.0 and a volume to 100 ml with distilled water and autoclave at 121°C for 20 min. Store at room temperature.

3.5 0.5 M EDTA (pH 8.0) (100 ml)

Dissolve 18.61 g EDTA (disodium ethylene diamine tetraacetate $\cdot 2\text{H}_2\text{O}$) in 70 ml distilled water. Adjust pH to 8.0 with NaOH (about 20 g) and the volume to 100 ml with distilled water. Sterilize by autoclaving at 121°C for 20 min. Store at room temperature.

4. Reagent for agarose gel electrophoresis

4.1 50 X TAE for agarose gel electrophoresis (1 L)

Mix 242 g Tris base, 57.1 ml glacial acetic acid, 100 ml 0.5 M EDTA (pH 8.0) and adjust the volume to 1 L with distilled water. Store at room temperature.

4.2 6 X DNA loading dye (10 ml)

Mix 0.025 g Bromophenol blue, 0.025 g xylene cyanol and 3 ml of 100% glycerol in distilled water to a 10 ml final volume and store at 4 °C.

5. Reagents for bacterial Genomic DNA isolation by using Miniprep protocol

5.1 CTAB/NaCl solution

Dissolved 4.1 g NaCl in 80 ml distilled water and slowly add 10 g CTAB (hexadecyltrimethyl ammonium brodmide) while heating and stirring. If necessary, heat to 65 °C to dissolve. Adjust final volume to 100 ml.

5.2 TE saturated phenol (pH 9.0)

Mix 300 ml TE (pH 8.0), 300 ml melted phenol at 50°C, and 4.5 g 8-hydroxyquinoline. Incubate at 4°C overnight. Remove supernatant. Store at 4°C

5.3 Chloroform solution (Chloroform: Isoamylalcohol = 24:1)

Mix 960 ml chloroform with 40 ml isoamylalcohol. Store at room temperature.

6. Solutions for protein

6.1 SDS-gel loading buffer (5 X stock) (2.5 M Tris, 10% SDS, 0.5% Bromophenol blue, 50% glycerol)

Dissolve 0.30 g Tris Base, 1 g SDS, 0.05 g Bromophenol blue, 5 ml glycerol and adjust pH to 6.8 with HCl and the volume to 8 ml with distilled water. Before use add 20 μ l of 2-mercapthoethanol to 80 μ l of solution mixture. Store at room temperature.

6.2 1.5 M Tris-HCl, pH 8.8 (100 ml)

Dissolve 18.17 g Tris Base in 80 ml distilled water. Adjust pH to 8.8 with HCl and the volume to 100 ml with distilled water. Store at 4°C.

6.3 0.5 M Tris-HCl, pH 6.8 (100 ml)

Dissolve 6.06 g Tris Base in 80 ml distilled water. Adjust pH to 6.8 with HCl and the volume to 100 ml with distilled water. Store at 4°C.

6.4 30% Acrylamide solution (100 ml)

Dissolve 29 g acrylamide and 1 g *N, N'*-methylene-bis-acrylamide in distilled water to a volume 100 ml. Mix the solution by stirring for 1 h to be homogenous and filter through Whatman membrane No. 1. Store in the dark bottle at 4°C.

6.5 Tris-Glycine electrode buffer (5 X stock) (1 L)

Dissolve 30.29 g Tris Base, 144 g glycine, 5 g SDS in distilled water. Adjust pH to 8.3 with HCl and the volume to 1 L with distilled water.

6.6 Staining solution with Coomassie brilliant blue for protein

Mix 1 g Coomassie brilliant blue R-250, 400 ml methanol, 500 ml distilled water and 100 ml glacial acetic acid and filter through a Whatman No. 1.

6.7 Destaining solution for Coomassie Stain

Mix 400 ml methanol, 100 ml glacial acetic acid, and add distilled water to a final volume of 1000 ml.

6.8 10% (w/v) Ammonium persulfate (1 ml)

Dissolve 100 mg ammonium persulfate in 1 ml distilled water. Store at -20°C.

6.9 12% Separating gel SDS-PAGE (10 ml)

Mix the solution as follow:

1.5 M Tris (pH 8.8)	2.5 ml
Distilled water	3.3 ml
10% (w/v) SDS	0.1 ml
30% acrylamide solution	4.0 ml
10% (w/v) ammonium persulfate	0.1 ml
TEMED	0.004 ml

6.10 5% Stacking gel SDS-PAGE (5 ml)

Mix the solution as follow:

0.5 M Tris (pH 6.8)	1.26 ml
Distilled water	2.77 ml
10% (w/v) SDS	0.05 ml
30% acrylamide solution	0.83 ml
10% (w/v) ammonium persulfate	0.05 ml
TEMED	0.005 ml

7. Solution for western blotting

7.1 1 X Phosphate buffer saline (PBS) (1.59 mM KH_2PO_4 , 8.4 mM Na_2HPO_4 , 2.68 mM KCl, 137 mM NaCl)

Dissolve 0.216 g KH_2PO_4 , 1.192 g Na_2HPO_4 , 0.199 g KCl, 8 g NaCl in distilled water and make to 1 L final volume.

7.2 1 X PBST (1.59 mM KH_2PO_4 , 8.4 mM Na_2HPO_4 , 2.68 mM KCl, 137 mM NaCl, 0.02% Tween 20)

Dissolve 0.216 g KH_2PO_4 , 1.192 g Na_2HPO_4 , 0.199 g KCl, 8 g NaCl, 0.2 ml Tween 20 in distilled water and make to 1 L final volume.

8. Amido Black stain for membrane

8.1 Amido Black stain

Dissolve 0.1 g Amido Black 10-B powder in the mixture of 45 ml of methanol, 10 ml of acetic acid and 45 ml of distilled water.

8.2 Destain solution for Amido Black stain

Mix 40 ml methanol, 10 ml glacial acetic acid, and add distilled water to a final volume of 100 ml.

9. Stock buffer and diluents for preparation of stock solutions of antimicrobial agents

Antimicrobial agents	Stock buffer	Diluent
Amikacin	Distilled water	Distilled water
Cefepime	100 mM Phosphate buffer, pH 6.0	100 mM Phosphate buffer, pH 6.0
Cefotaxime	Distilled water	Distilled water
Ceftazidime	Distilled water	Distilled water
Ciprofloxacin	Distilled water	Distilled water
Clindamycin	Distilled water	Distilled water
Gentamicin	Distilled water	Distilled water
Meropenem	Distilled water	Distilled water

Appendix F

Crystal screening kit for membrane protein and scoring sheet

MembFac (HR2-114) - Scoring Sheet				
Sample:		1 Clear Drop	6 Needles 1D	
Buffer:		2 Phase Separation	7 Plates 2D	
Reservoir Volume:		3 Regular Granular Precipitate	8 Xtal <0.2 mm	
Drop:		4 Birefringent Precipitate	9 Xtal >0.2 mm	
Temperature:		5 Spherulites		
Drop:				
Temperature:		Date	Date	Date
1. 12% MPD, 0.1 M Na Acetate pH 4.6, 0.1 M Sodium Chloride				
2. 12% PEG 4000, 0.1 M Na Acetate pH 4.6, 0.1 M Zinc Acetate				
3. 10% PEG 4000, 0.1 M Na Acetate pH 4.6, 0.2 M Ammonium Sulfate				
4. 12% iso-Propanol, 0.1 M Na Acetate pH 4.6, 0.1 M Sodium Chloride				
5. 12% PEG 4000, 0.1 M Na Acetate pH 4.6				
6. 1.0 M Ammonium Sulfate, 0.1 M Na Acetate pH 4.6				
7. 1.0 M Magnesium Sulfate, 0.1 M Na Acetate pH 4.6				
8. 18% PEG 400, 0.1 M Na Acetate pH 4.6, 0.1 M Magnesium Chloride				
9. 1.0 M Ammonium Phosphate, 0.1 M Na Acetate pH 4.6, 0.1 M Lithium Sulfate				
10. 12% PEG 6000, 0.1 M Na Acetate pH 4.6, 0.1 M Sodium Chloride				
11. 12% PEG 6000, 0.1 M Na Acetate pH 4.6, 0.1 M Magnesium Chloride				
12. 18% PEG 400, 0.1 M Na Citrate pH 5.6, 0.1 M Sodium Chloride				
13. 12% PEG 4000, 0.1 M Na Citrate pH 5.6, 0.1 M Lithium Sulfate				
14. 10% iso-Propanol, 0.1 M Na Citrate pH 5.6, 0.1 M Sodium Citrate				
15. 12% MPD, 0.1 M Na Citrate pH 5.6, 0.1 M Sodium Chloride				
16. 1.0 M Magnesium Sulfate, 0.1 M Na Citrate pH 5.6				
17. 12% PEG 4000, 0.1 M Na Citrate pH 5.6, 0.1 M Sodium Chloride				
18. 12% PEG 6000, 0.1 M Na Citrate pH 5.6, 0.1 M Lithium Sulfate				
19. 4% MPD, 0.1 M Na Citrate pH 5.6, 0.1 M Magnesium Chloride				
20. 0.1 M Sodium Chloride, 0.1 M Na Citrate pH 5.6				
21. 4% PEG 400, 0.1 M Na Citrate pH 5.6, 0.1 M Lithium Sulfate				
22. 1.0 M Ammonium Sulfate, 0.1 M ADA pH 6.5				
23. 12% PEG 4000, 2% iso-Propanol, 0.1 M ADA pH 6.5, 0.1 M Lithium Sulfate				
24. 1.0 M di-Ammonium Phosphate, 0.1 M ADA pH 6.5				
25. 12% PEG 6000, 0.1 M ADA pH 6.5, 0.1 M Magnesium Chloride				
26. 12% MPD, 0.1 M ADA pH 6.5				
27. 1.0 M Magnesium Sulfate, 0.1 M ADA pH 6.5, 0.1 M Lithium Sulfate				

Crystal screening kit for membrane protein and scoring sheet (continued)

MembFac (HR2-114) - Scoring Sheet				
Sample:		1 Clear Drop	6 Needles 1D	
Buffer:		2 Phase Separation	7 Plates 2D	
Reservoir Volume:		3 Regular Granular Precipitate	8 Xtal <0.2 mm	
Drop:		4 Birefringent Precipitate	9 Xtal >0.2 mm	
Temperature:		5 Spherulites		
Drop:				
Temperature:		Date	Date	Date
28. 4% PEG 400, 0.1 M ADA pH 6.5, 0.3 M Lithium Sulfate				
29. 1.0 M di-Na/K Phosphate, 0.1 M Na HEPES pH 7.5, 0.1 M Ammonium Sulfate				
30. 10% PEG 4000, 0.1 M Na HEPES pH 7.5, 0.1 M Sodium Chloride				
31. 18% PEG 400, 0.1 M Na HEPES pH 7.5, 0.1 M Magnesium Chloride				
32. 1.0 M K/Na Tartrate, 0.1 M Na HEPES pH 7.5				
33. 18% PEG 400, 0.1 M Na HEPES pH 7.5, 0.1 M Ammonium Sulfate				
34. 10% PEG 4000, 0.1 M Na HEPES pH 7.5, 0.1 M Ammonium Sulfate				
35. 12% MPD, 0.1 M Na HEPES pH 7.5, 0.1 M Sodium Citrate				
36. 1.0 M Sodium Citrate, 0.1 M Na HEPES pH 7.5				
37. 4% PEG 400, 0.1 M Na HEPES pH 7.5, 0.6 M Magnesium Sulfate				
38. 4% MPD, 0.1 M Na HEPES pH 7.5, 0.6 M Magnesium Sulfate				
39. 0.1 M K/Na Tartrate, 0.1 M Na HEPES pH 7.5, 0.1 M Lithium Sulfate				
40. 12% MPD, 0.1 M Tris HCl pH 8.5, 0.1 M Lithium Sulfate				
41. 1.0 M di-Na/K Phosphate, 0.1 M Tris HCl pH 8.5, 0.1 M di-Ammonium Phosphate				
42. 0.1 M Sodium Acetate, 0.1 M Tris HCl pH 8.5				
43. 0.1 M Sodium Chloride, 0.1 M Tris HCl pH 8.5				
44. 12% PEG 6000, 0.1 M Tris HCl pH 8.5, 0.1 M di-Ammonium Phosphate				
45. 0.4 M Magnesium Sulfate, 0.1 M Tris HCl pH 8.5, 0.1 M K/Na Tartrate				
46. 0.2 M Lithium Sulfate, 0.1 M Tris HCl pH 8.5				
47. 0.5 M Ammonium Sulfate, 0.1 M Tris HCl pH 8.5				
48. 5% PEG 400, 0.1 M Tris HCl pH 8.5, 0.1 M Sodium Citrate				

Appendix G

Typical observation in a crystallization experiment



Clear Drop



Skin/Precipitate



Precipitate



Precipitate/Phase



Quasi Crystals



Microcrystals



Needle Cluster



Plates



Rod Cluster



Single Crystal

Appendix H
Journal publication

Functional reconstitution, gene isolation and topology modelling of porins from *Burkholderia pseudomallei* and *Burkholderia thailandensis*

Jaruwan SIRITAPETAWE^{*}, Heino PRINZ[†], Worada SAMOSORN[‡], Richard H. ASHLEY[§] and Wipa SUGINTA^{*1}

^{*}School of Biochemistry, Suranaree University of Technology, Nakhon Ratchasima 30000, Thailand, [†]Max-Planck-Institut für Molekulare Physiologie, Otto-Hahn-Strasse 11, 44227 Dortmund, Germany, [‡]Department of Medical Technology, Faculty of Allied Health Science, Thammasat University, Pathumthani 12120, Thailand, and [§]Department of Biomedical Sciences, University of Edinburgh, George Square, Edinburgh EH8 9XD, U.K.

The intracellular pathogen *Burkholderia pseudomallei* is the causative agent of tropical melioidosis, and *Burkholderia thailandensis* is a closely-related Gram-negative bacterium that does not cause serious disease. Like other bacteria, the major outer membrane (OM) porins of *Burkholderia* strains, *BpsOmp38* and *BthOmp38* may have roles in antibiotic resistance and immunity. We purified both proteins and found them to be immunologically related, SDS-resistant, heat-sensitive trimers with M_r of approx. 110 000. In functional liposome-swelling assays, both proteins showed similar permeabilities for small sugar molecules, compatible with a pore diameter of between 1.2 and 1.6 nm. Secondary structure analysis by FTIR (Fourier-transform infrared) spectroscopy revealed almost identical spectra with predominantly β -sheet structures, typical of bacterial porins. MALDI-TOF (matrix-assisted laser-desorption ionization-time

of flight) MS and ESI/MS (electrospray ionization MS) analysis of each protein showed extensive sequence similarities to the OpcP1 porin from *Burkholderia cepacia* (later found to be 76.5% identical). Based on information from the incomplete *B. pseudomallei* genome-sequencing project, the genes encoding *Omp38* were identified and amplified by PCR from *B. pseudomallei* and *B. thailandensis* genomic DNA. The nucleotide sequences are 99.7% identical, and the predicted processed proteins are 100% identical. Topology prediction and molecular modelling suggest that this newly-isolated and cloned porin is a 16-stranded β -barrel and the external loops of the protein could be important determinants of the immune response to infection.

Key words: *Burkholderia*, cloning, diffusion pore, *Omp38*, topology.

INTRODUCTION

Burkholderia pseudomallei (formerly *Pseudomonas pseudomallei*), the causative agent of tropical melioidosis, is a motile Gram-negative bacterium mainly endemic to South-East Asia [1]. In addition to occurring in people who come into contact with contaminated soil or water in endemic areas, the infection is more common in immunosuppressed patients and must be recognized early and treated with appropriate antibiotics to ensure survival. Although the bacterium can cause acute or sub-acute symptoms, most cases are asymptomatic and it can activate many years after the initial exposure, causing chronic illness [2]. However, little is known about the climatic, physical, chemical and biological factors, which control the proliferation and survival of *Burkholderia* spp.

Burkholderia thailandensis is a closely related non-pathogenic soil organism originally isolated in Central and North-East Thailand [3]. Although the two organisms are very similar ([4,5], but see [5a]), they are different in their genetic and biochemical properties. The rRNA sequence of *B. thailandensis* differs from that of *B. pseudomallei* by 15 nucleotides, and there are significant differences in genomic macrorestriction patterns between the organisms [6]. The biochemical profiles of these two species differ in that *B. thailandensis* utilizes L-arabinose, whereas *B. pseudomallei* does not [7]. *B. thailandensis* is also substantially less virulent in Syrian golden hamster models of infection [4]. It has been reported that more than 99% of cases of melioidosis

are caused by *B. pseudomallei*, whereas *B. thailandensis* is only responsible for less than 1% [8]. Therefore efficient identification of *B. pseudomallei* and *B. thailandensis* is crucial in guiding clinical management of patients with suspected melioidosis.

Treatment of tropical melioidosis has proven to be extremely difficult. *B. pseudomallei* secretes potent bacteriocins that block protein synthesis in macrophages, as well as in phagocytes. These bacteriocins may be responsible for the extensive abscess formation associated with the disease [9]. There is no published evidence to relate non-pathogenicity of *B. thailandensis* with high susceptibility to antibiotics. However, it has been well established that *B. pseudomallei* is resistant to many antibiotics including β -lactams, aminoglycosides, macrolides and polymyxins [1,10]. In some cases, this is because of low permeability of these compounds through the outer membrane of the bacteria [11]. Given that these hydrophilic molecules often diffuse through water-filled porins [12], the characteristics of specific porin channels may be significant determinants of antibiotic sensitivity. In conjunction with peptidoglycan and LPS (lipopolysaccharide), porins are receptors for bacteriophages and bacteriocidins, and they also have a significant structural role in maintaining the integrity of the cells [13]. In addition, porins may play an important role in the immune response to infection. For example, an unrelated porin in another intracellular pathogen, the major outer membrane (OM) protein (MOMP) of *Chlamydia trachomatis*, is an immunodominant surface antigen that elicits both antibody production and T-cell response [14].

Abbreviations used: ESI/MS, electrospray ionization MS; FTIR, Fourier-transform infrared; L1 (etc.), Loop 1 (etc.); LPS, lipopolysaccharide; MALDI-TOF, matrix-assisted laser-desorption ionization-time-of-flight; MS/MS, tandem MS; OM, outer membrane.

¹ To whom correspondence should be addressed (e-mail wipa@ccs.sut.ac.th).

The sequences for *Omp38* from *Burkholderia pseudomallei* and *Burkholderia thailandensis* have been deposited in the DDBJ, EMBL, GenBank[®] and GSDN Nucleotide Sequence Databases under the accession numbers AY312416 and AY312417 respectively.

Porins have been identified in many Gram-negative bacteria, and several porins from *Escherichia coli* (e.g. OmpF, OmpC, OmpG and PhoE) have been well-characterized in terms of their biochemical, functional, genetic, immunochemical and structural properties [15]. In particular, all porins appear to contain abundant β -sheet structures [16]. The OM of the related organism *Burkholderia cepacia* (responsible for fatal lung infections in cystic fibrosis) contains an 81 kDa porin designated OpcP0, which also shows low permeability to β -lactams [17]. This protein contains two subunits: a major 36 kDa protein designated OpcP1, and a minor 27 kDa protein, designated OpcP2. OpcP1 has been cloned and expressed in *E. coli* [18]. The predicted OpcP1 protein precursor contains 361 residues, including a 20-residue signal sequence. The calculated M_r of 35 696 for the mature protein is in agreement with the OpcP1 protein band of 36 kDa by SDS/PAGE. Similarity of the amino acid sequences between OpcP1 and several other Gram-negative bacterial porins strongly suggests that OpcP1 is the pore-forming component of OpcP0. This notion is also supported by the similarity of the hydropathy plots of OpcP1 and the major *E. coli* porin, OmpF [17].

In the present study, we describe the isolation of *BpsOmp38* from *B. pseudomallei* and *BthOmp38* from *B. thailandensis*, and characterize them using FTIR (Fourier-transform infrared) spectroscopy, MALDI-TOF (matrix-assisted laser-desorption ionization-time-of-flight) MS and nanoESI/MS. Peptide mass fingerprinting showed the amino acid sequences of the proteins to be identical, and enabled us to identify and isolate the gene encoding *BpsOmp38* from the partially sequenced *B. pseudomallei* genome. We have also cloned its homologue from *B. thailandensis* genomic DNA, and the predicted proteins have been subjected to topology prediction and structural modelling.

EXPERIMENTAL

Materials

Bacterial culture medium and bacteriological agar were purchased from Scharlau Chemie (Barcelona, Spain). Cetyltrimethylammonium bromide, dithiothreitol, iodoacetamide, ammonium hydrogen carbonate, D-stachyose, D-melezitose, D-sucrose, L-arabinose, D-glucose and D-mannose were from Acros Organics (Morris Plains, NJ, U.S.A.). Proteinase K and trypsin (sequencing grade) were from Promega. Sephacryl S-200[®] HR resin and Dextran T-40 were from Amersham Biosciences. Detergents used for protein preparation were purchased from Carlo Erba Reagenti (Milan, Italy). All other reagents for general laboratory use were from Sigma-Aldrich and Carlo Erba Reagenti. *Taq* DNA polymerase was purchased from Promega. Primers for PCR amplification were synthesized by Profligo Singapore (Singapore Science Park II, Singapore).

Preparation of OM proteins

B. pseudomallei (ATCC 23 343) and *B. thailandensis* (ATCC 700 388) were grown in LB (Luria-Bertani) broth at 37 °C with vigorous shaking. Cells were harvested at late exponential phase by centrifugation at 10 000 g at 4 °C for 20 min. Crude peptidoglycan was isolated using a modification of the method of Gotoh et al. [19]. Briefly, cells from 2 litres of late-exponential culture were washed once and resuspended in 10 ml of 10 mM Tris/HCl, pH 8.0, containing 1 mM PMSF and 2 mg of hen's-egg lysozyme. The suspension was sonicated using a Sonoplus Ultrasonic homogenizer with a 6 mm diameter probe (50 % duty cycle; amplitude setting, 20%; total time, 5 min), and large cellular debris and unbroken cells were removed by centrifuga-

tion at 10 000 g for 30 min. Cell membranes were recovered from the lysates by microcentrifugation at 12 000 g for 1 h, suspended in 10 mM Tris/HCl, pH 8.0, containing 0.5% (w/v) SDS, and heated at 30 °C for 1 h to solubilize most of the remaining cytoplasmic and membrane proteins. A complex of non-solubilized peptidoglycan sheets (crude peptidoglycan) was then pelleted by microcentrifugation at 12 000 g for 1 h and heated in 4 ml of 10 mM Tris/HCl, pH 8.0, containing 2% (w/v) SDS and 0.5 M NaCl at 37 °C for 1 h. Solubilized peptidoglycan-associated proteins were then separated from insoluble peptidoglycan by microcentrifugation at 12 000 g for 1 h.

Proteoliposome-swelling assay

The preparation of proteoliposomes and the determination of diffusion rates were based on the detailed methods described previously [19–21]. Briefly, mixtures of 2.4 μ mol of phosphatidylcholine and 0.2 μ mol of diacetyl phosphate in chloroform were dried by vacuum-centrifugation and the phospholipid films were resuspended in 0.2 ml of distilled water and mixed with 50 μ g of purified Omp (outer membrane protein). The mixtures were sonicated for 7 min in a water bath at 20 °C, dried overnight by vacuum-centrifugation, and resuspended in 0.2 ml of 10 mM Tris/HCl, pH 8.0, containing 15% (w/v) Dextran T-40, to form proteoliposomes. The proteoliposomes were diluted into 0.6 ml of an iso-osmotic sugar solution (prepared as described in the Results section), and changes in absorbance were measured at 400 nm for 60 s. The relative permeabilities of the pore-forming proteins were assumed to be proportional to the initial swelling rates [22], and each experiment was repeated at least three times using liposomes without any protein, or liposomes containing BSA, as negative controls.

SDS/PAGE and immunological analysis

Purified *B. pseudomallei* Omp38 (2 μ g) was separated by SDS/PAGE as a monomer using 12% (v/v) acrylamide and 8 M urea in a Laemmli buffer system [23]. Following electrophoresis, the protein was stained with Coomassie Blue. After destaining, the protein band was excised from the gel, emulsified with 50 μ l of Freund's complete adjuvant (Pierce), and used to raise rabbit polyclonal antiserum [24]. Antisera titres and cross-reactivity between *B. pseudomallei* and *B. thailandensis* proteins (5 μ g each) were analysed by Western blotting with enhanced chemiluminescence (ECL[®]; Amersham Biosciences) detection, using 1:10 000 dilutions of the anti-Omp38 antiserum in PBS, pH 7.4, in the presence of 0.2% (v/v) Tween 20 and 5% (w/v) non-fat dried milk. Protein concentrations were determined using a BCA (bicinchoninic acid) kit (Pierce).

Protein identification and peptide mass analysis by MALDI-TOF MS and ESI/MS

Protein identification was performed in two steps: for the initial analysis, the protein bands from SDS gels (see above) were excised, destained, reduced, alkylated with iodoacetamide and digested with sequencing-grade trypsin (Promega) following a standard protocol [25]. After overnight digestion at 37 °C, the peptides were extracted and dried in a SpeedVac vacuum centrifuge. A small fraction of these tryptic peptides was analysed by MALDI-TOF MS (Voyager-DE Pro in reflective mode) in an α -cyano-4-hydroxycinnamic acid matrix for the peptide 'mass fingerprinting'. The remaining peptides were separated by capillary HPLC using a 0–40% linear gradient of acetonitrile containing 0.1% acetic acid, then detected directly by ESI/MS

(Thermo Finnigan LCQ Deca) using the proprietary 'triple play' mode for obtaining MS/MS (tandem MS) sequence information for the relevant peptides. Databank searching was performed with the MS-Fit program (<http://prospector.ucsf.edu/>) for MALDI mass fingerprint data, and with the Sequest search program (<http://fields.scripps.edu/sequest/index.html>) for MS/MS data from the HPLC-MS run. In some experiments, the proteins (not gel pieces) were completely digested with sequencing-grade Trypsin in a buffer containing 5 mM CaCl₂ and 100 mM NH₄HCO₃, and the resulting peptides were applied to an Agilent 1100 HPLC connected to the LCQ ESI/MS. Mass spectra of whole proteins were obtained with linear MALDI-TOF (Voyager-DE Pro) using sinapinic acid (3,5-dimethoxy-4-hydroxycinnamic acid) as the matrix.

FTIR spectroscopy measurements

FTIR spectroscopy measurements were carried out using a Bruker IFS-66 FTIR spectrometer equipped with a DTGS (deuterated triglycine sulphate) detector. The porins were measured in home-made demountable equipped cells with CaF₂ windows. Aliquots of the protein solutions (5 μ l, 10 mg/ml) were first dried under vacuum for 5 min with ²H₂O (5 μ l). To compensate for ²H₂O absorption, buffer solutions were subtracted using the same cells. The path length was about 50 μ m. FTIR spectra of the protein solutions were recorded using identical scanning parameters. Typically, the nominal physical resolution was 4 cm⁻¹ using a Happ-Genzel apodization function for Fourier-transformation and a zero-filling factor of 4 to yield a data encoding interval of one data point per wavenumber and 32 scans were accumulated before performing the Fourier-transform analysis to optimize the signal-to-noise ratio. The protein spectrum was obtained after subtracting the buffer spectrum from the spectrum of the protein solution measured under the same conditions. To eliminate spectral contributions due to atmospheric water vapour, the instrument was continuously purged with dry air. Spectral contributions from residual water vapour were eliminated using water vapour spectra measured under identical conditions. The absorption region 1000–4000 cm⁻¹ was primarily monitored. However, to obtain secondary structure information on the proteins, the amide I and II absorption regions between 1500 and 1800 cm⁻¹ were specifically acquired for second derivative plots.

Preparation of genomic DNA and cDNA cloning and sequencing

Genomic DNA was prepared using the protocol of Ausubel et al. [26]. PCR primers were synthesized by Proligo. Amplification reactions were carried out using *Taq* polymerase and the products were cloned into pGEM[®]-T vector and sequenced in both directions using an automated sequencer [Biotechnology Sequencing Unit (BSU), Thailand].

Structural prediction and molecular modelling

Protein sequences were aligned using ClustalW (<http://www.ebi.ac.uk/clustalw/>) and displayed using GeneDoc (<http://www.psc.edu/biomed/genedoc/>). Signal peptide cleavage sites were predicted using SignalP V1.1 (<http://www.cbs.dtu.dk/services/SignalP/>) and transmembrane domains obtained using prediction of the protein localization sites (<http://www.psorth.org/psorth/index.html>). RPS-BLAST (<http://www.ncbi.nih.gov/BLAST>) was used to identify conserved domains, and protein structures were modelled and displayed using 3D-PSSM (<http://www.sbg.bio.ic.ac.uk/~3dpssm>), 123D+ search (<http://123d.ncifcrf.gov>), and Swiss-Model (<http://www.expasy.org/swissmod>).

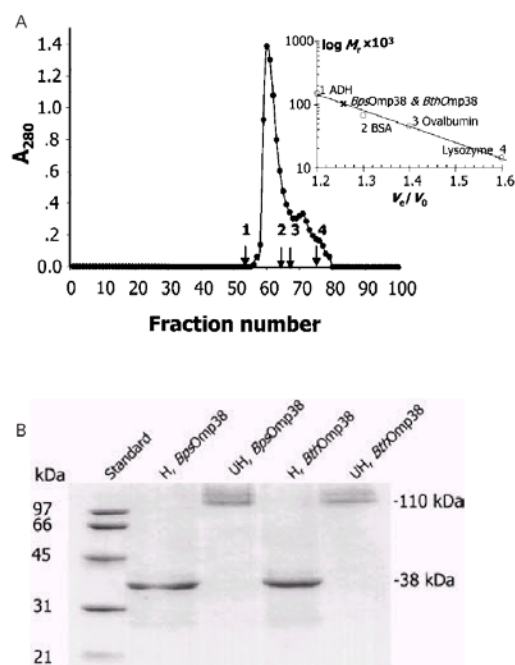


Figure 1 Elution profile and urea SDS/PAGE of *BpsOmp38* and *BthOmp38*

(A) Gel-filtration chromatography (Sephacryl S-200[®] HR, Amersham Biosciences). Proteins released from *B. pseudomallei* crude peptidoglycan in 10 mM Tris/HCl, pH 8.0, containing 2% (w/v) SDS and 0.5 M NaCl, were applied to a column (1.5 cm \times 95 cm) equilibrated in 10 mM Tris/HCl, pH 8.0, containing 1% (w/v) SDS and 0.5 M NaCl. Fractionation was carried out at a flow rate of 1 ml \cdot min⁻¹, and 2 ml fractions were collected. The A_{280} of the eluted protein was measured. The profile for *B. thailandensis* protein was identical. The inset displays the obtained calibration curve determining the M_r of *BpsOmp38* and *BthOmp38*. (B) SDS/PAGE analysis of *BpsOmp38* and *BthOmp38* proteins purified from *B. pseudomallei* under heated (H) or unheated (UH) conditions. Samples were prepared in the sample buffer containing 8 M urea at 25 $^{\circ}$ C for UH *BpsOmp38* and UH *BthOmp38* or at 95 $^{\circ}$ C, 5 min for H *BpsOmp38* and H *BthOmp38*.

RESULTS

Purification of *BpsOmp38* and *BthOmp38*

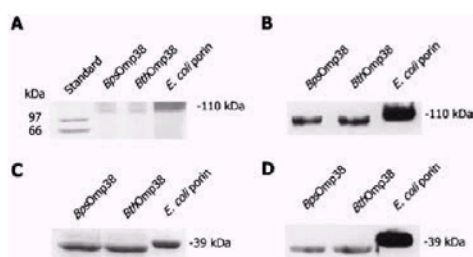
Crude peptidoglycan isolated from *B. pseudomallei* and *B. thailandensis* (see the Experimental section) was used as the starting material to purify trimeric OM porins. Following SDS-extraction, the peptidoglycan fraction was purified further by size-exclusion chromatography (200 ml Sephacryl S-200[®] HR column) in the presence of 1% (w/v) SDS and 0.5 M NaCl. Eluted protein was detected by measuring the absorbance of the eluate at 280 nm, and peak fractions were analysed by SDS/PAGE (12.5%) in the presence of urea [23].

For each organism, the major protein peak obtained after size-exclusion chromatography (Figure 1A) corresponded to an M_r of approx. 100000. As shown in Figure 1(B), this relatively high molecular mass band shifted to an M_r of approx. 38000 after heating at 95 $^{\circ}$ C for 5 min. Taken together, the results from size-exclusion chromatography and SDS/PAGE suggested that the isolated proteins were SDS-resistant homotrimers comprising monomers of an M_r of approx. 38000, consistent with trimeric

Table 1 Omp38 purification from both *B. pseudomallei* and *B. thailandensis*

The results are the means of two separate experiments for each protein.

Purification step	<i>B. pseudomallei</i> (mg)	Yield (%)	<i>B. thailandensis</i> (mg)	Yield (%)
1. Crude peptidoglycan	492.0	100	296.0	100
2. OM fraction	175.4	36	107.4	36
3. Peptidoglycan-associated fraction				
0.5% (w/v) SDS extraction	5.4	1.1	3.4	1.1
2% (w/v) SDS and 0.5 M NaCl extraction	5.0	1.0	3.0	1.0
4. Sephacryl S200 filtration and dialysis	0.8	0.2	0.6	0.2

**Figure 2** Immunoblots of *BpsOmp38*, *BthOmp38* and *E. coli* BL21 (DE3) porin

(A) Non-denatured (unheated) SDS/PAGE analysis and (B) corresponding immunoblot using anti-*BpsOmp38* polyclonal antibodies. (C) Denatured (heated at 95 °C for 5 min) SDS/PAGE analysis and (D) corresponding immunoblot. Note that because of differences in exposure times, it was not possible to carry out immunoblots of both heated and unheated samples on the same gel.

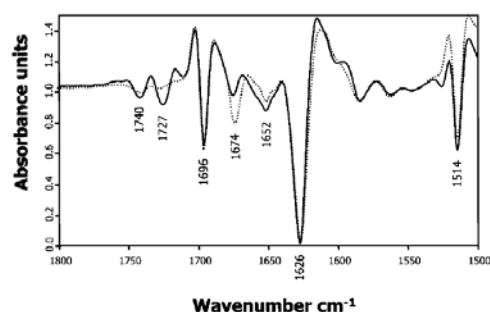
OM porins. Similar results were seen in ten independent preparations. The proteins isolated from *B. pseudomallei* and *B. thailandensis* were therefore designated *BpsOmp38* and *BthOmp38* respectively. The final yield of each protein obtained from a 2 litre culture was approx. 0.2% (800 µg and 600 µg for *B. pseudomallei* and *B. thailandensis* respectively) (Table 1).

Antibody production and immunoblotting analysis

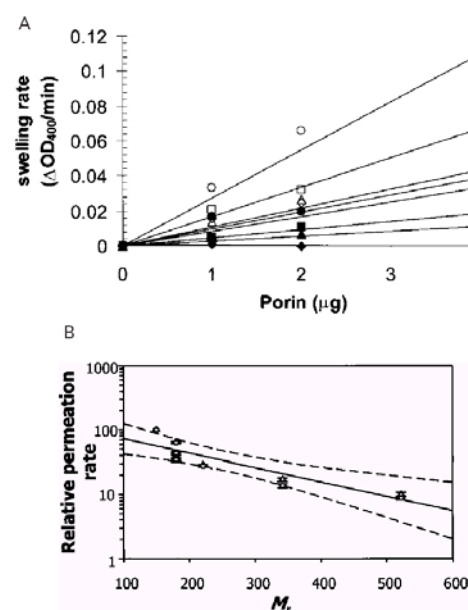
The protein band corresponding to the *B. pseudomallei* Omp38 monomer was excised from a gel and used to raise a rabbit polyclonal antiserum as described in the Experimental section. The antibodies cross-reacted with both proteins on immunoblots, and recognized both the high molecular mass, presumed trimeric, protein band in non-denatured samples (Figures 2A and 2B) and a 39 kDa protein from *E. coli* BL21(DE3) OM fraction (Figures 2C and 2D). In addition, the antibodies also strongly recognized the protein band corresponding to OpcP0 (81 kDa), the monomeric protein bands corresponding to OpcP1 (36 kDa) and OpcP2 (27 kDa), as well as a non-identified 18 kDa of *B. cepacia* OM crude fraction (results not shown) [17]. None of these proteins was recognized by rabbit pre-immune serum, suggesting that the *Burkholderia* proteins may be structurally related to at least one porin from *E. coli* and *B. cepacia*.

Secondary-structure analysis using FTIR

The second derivative spectra obtained from FTIR measurements revealed extensive secondary structure similarity between

**Figure 3** FTIR analysis of *BpsOmp38* and *BthOmp38*

Secondary derivative spectra of *BpsOmp38* (—) and *BthOmp38* (---) between 1500 and 1800 cm⁻¹ were normalized using the IR band of Tyr (1514 cm⁻¹) and superimposed. Signals at amide I region: 1626 cm⁻¹ represents β -sheets; 1652 cm⁻¹ and 1674 cm⁻¹ represent turns and loops; 1696 cm⁻¹ represents antiparallel β -pleated sheets; 1727 cm⁻¹ and 1740 cm⁻¹ represent LPS [27].

**Figure 4** Liposome-swelling assay

(A) Relative diffusion rates for neutral saccharides were determined by liposome-swelling assays using proteoliposomes containing various amounts of *BpsOmp38* and *BthOmp38*, together with 2.4 µmol of phosphatidylcholine and 0.2 µmol of diacetyl phosphate (final volume, 600 µl). The following symbols represent, in order, L-arabinose (○); D-glucose (□); D-mannose (△); D-galactose (◇); N-acetylglucosamine (●); D-sucrose (■); D-melezitose (▲); stachyose (◆). (B) Relative permeabilities. Initial relative swelling rates for liposomes containing purified *B. pseudomallei* (△) and *B. thailandensis* (○) porins plotted on a logarithmic scale against the M_r of the permeating solute (abscissa). Results are means \pm S.E.M. ($n=3$ experiments for each protein; rate for arabinose = 100%). The size-dependent swelling rates for the two porins are indistinguishable, and the straight line is a regression fit to all the data. The broken lines indicate the 95% confidence limits of the fit. The near-limiting M_r defined as 5% relative permeability through both *Burkholderia* porins is 650 (cf. 450 for *E. coli* porin reconstituted under the same conditions; results not shown).

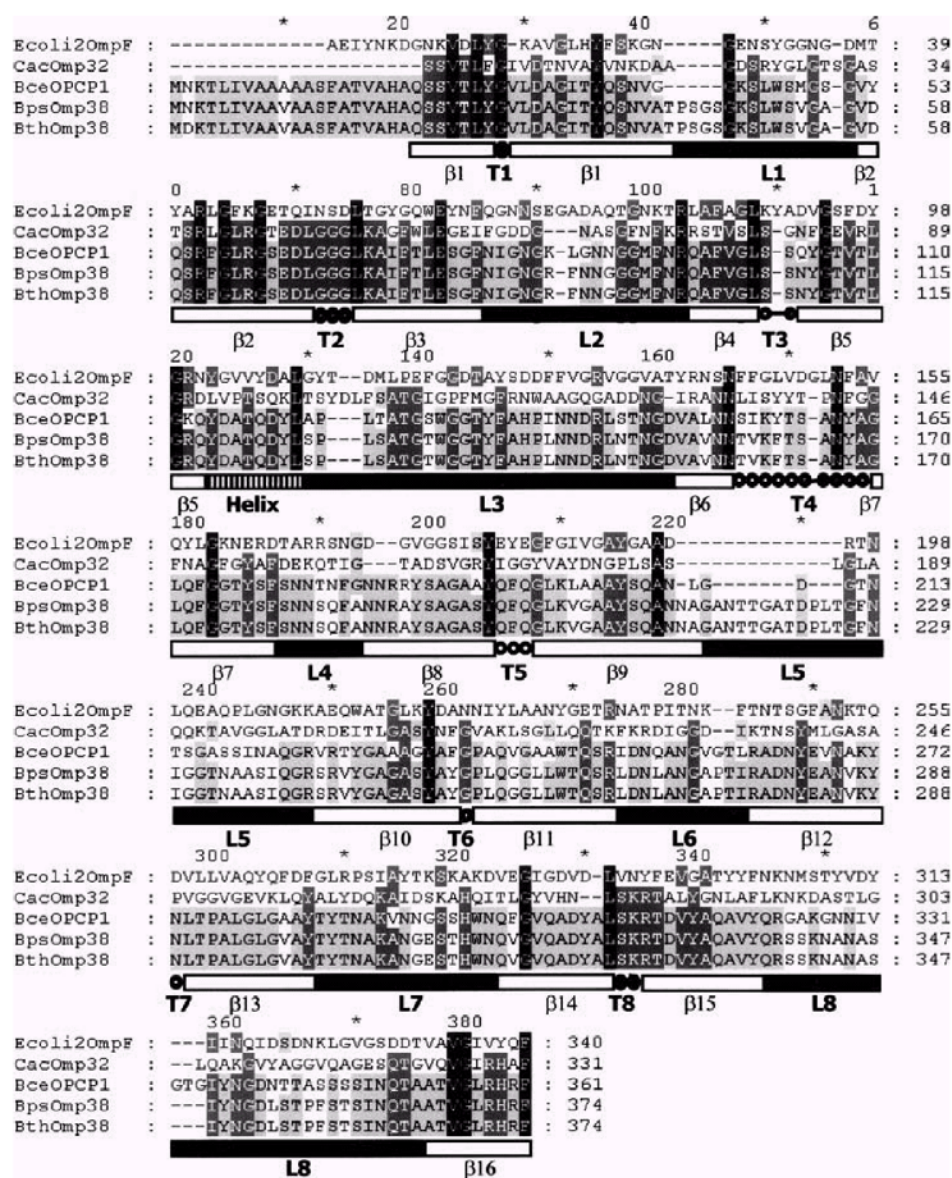


Figure 5 Alignment of *BpsOmp38* and *BthOmp38* with other OM porins

Porins were selected on the basis of a high degree of amino acid identity with Omp38. The secondary structures of *BpsOmp38* and *BthOmp38* were predicted by comparison with porins of known structure (OmpF and Omp32). Ecoli2OmpF, OmpF porin from *E. coli*; CacOmp32, anion-selective porin from *C. acidovorans*; BceOPCP1, OpcP1 porin from *B. cepacia*; BpsOmp38, Omp38 porin from *B. pseudomallei* A. T. C. C. 23343; BthOmp38, Omp38 porin from *B. thailandensis* A. T. C. C. 700388. Open box, β strand; closed box, loop; hatched box, α helix; circle, turn.

BpsOmp38 and *BthOmp38*, and their spectra could almost be directly superimposed, apart from differences in the ester carbonyl stretching regions (signals at 1727 cm^{-1} and 1740 cm^{-1}) (Figure 3) [27], which most probably originate from residual LPS tightly bound to the porin. It was noticeable that *BpsOmp38*

contained more associated LPS than *BthOmp38*. The secondary derivative plots in the amide I ($1600\text{--}1700\text{ cm}^{-1}$) region demonstrated that both proteins contained predominantly β -sheet, as indicated by the two distinct peaks at 1626 cm^{-1} and 1696 cm^{-1} , typical for the antiparallel β -pleated sheets of porins [27,28].

Minor contributions at 1652 cm^{-1} and 1674 cm^{-1} were tentatively assigned to be loop and turn structures.

Liposome swelling assay

Our data strongly suggested that *BpsOmp38* and *BthOmp38* were likely to be porins, and that they had been isolated in a non-denatured, possibly native, conformation. In particular, both membrane proteins retained significant secondary and quaternary structures (comprising mainly β -sheet, and SDS-resistant, heat-sensitive trimers respectively). The apparent retention of normal folding suggested that they might form functional channels, and we tested this idea by assaying solute transport in liposome-swelling assays.

Following reconstitution, the relative diffusion rates of L-arabinose, D-glucose, D-mannose, D-galactose, *N*-acetylglucosamine, D-sucrose and D-melezitose into multilamellar liposomes were determined, as described in the Experimental section, after establishing iso-osmotic buffer conditions in the presence of the large impermeable sugar, stachyose (667 Da). Absorbance changes for each sample were positive, and increased linearly with time from the outset of each recording (results not shown), confirming that the starting conditions were iso-osmotic and the proteoliposomes were properly equilibrated. The diffusion rates of all the sugars that were tested increased linearly with protein concentration (Figure 4A), and the rates clearly depended on the M_r of the solute.

As shown in Figure 4(B), the relative diffusion rates through *BpsOmp38* and *BthOmp38* porins were indistinguishable, with a 'limiting' M_r of approx. 650 (defined as the value corresponding to 5% relative permeability). The rates were clearly different from the rates through *E. coli* OM porin (mainly OmpF, under the growth conditions used), which, when reconstituted under exactly the same conditions, had a limiting M_r of approx. 450 (results not shown).

Gene isolation, cloning and sequencing

We analysed the primary structures of *BpsOmp38* and *BthOmp38* in order to identify the corresponding genes from genome sequences. As identified by MALDI-TOF MS, the masses of *BpsOmp38* and *BthOmp38* were 37 159 and 37 108 respectively. This is identical within the mass-dependent peak broadening of MALDI-TOF protein measurements. MALDI mass fingerprints of tryptic fragments obtained from in-gel digests revealed almost identical peptide ensembles. When these peptides were separated on a capillary HPLC and subjected to partial fragmentation (ESI/MS and MS/MS sequence analysis), eight *BpsOmp38* peptides (TDVYAQAVYQR, GSEDLGGGLK, SLWSVGAGVDQSR, LNTNGDVAVNNTVK, AYSAGASYQFQGLK, QAFVGLSSNYGTVTLGR, AIFTLESFNGNIGR and NANASIYNGDLS-TPFSTINQTAATVGLR) and four identical *BthOmp38* peptides (GSEDLGGGLK, SLWSVGAGVDQSR, QAFVGLSSNYGTVTLGR and AIFTLESFNGNIGR) gave an unambiguous match to the OM porin OpcP1 of *B. cepacia*. Each of these peptides could also be aligned with a single predicted open reading frame in contig 836 of the *B. pseudomallei* genome (<http://www.ncbi.nlm.nih.gov/sutils/genomtable.cgi>).

Accordingly, we amplified full-length *BpsOmp38* and *BthOmp38* cDNAs, each containing 1112 nucleotides, from appropriate genomic DNA using the following sense primer: 3'-ATGAACAAGACTCTGATTGTTGCA-5', and antisense primer: 3'-GAAGCGGTGACGCAGACCAA-5' using *Taq* DNA polymerase. The cDNAs were cloned into pGEM[®]-T vector and were

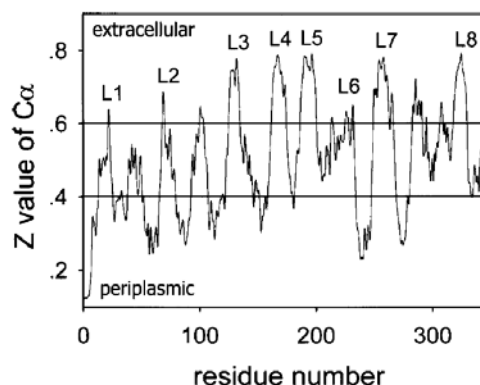


Figure 6 Predicted transmembrane topologies of *BpsOmp38* and *BthOmp38*

Trajectories of successive C_{α} carbons plotted against residue number for the identical predicted *B. pseudomallei* and *B. thailandensis* porins (see the Experimental section). The Z value (scaled from 0–1) corresponds to the predicted position of each C_{α} carbon relative to the plane of the membrane. Values < 0.4 represent positions in periplasmic turns, values between 0.4 and 0.6 are predicted to be in transmembrane crossings, and values > 0.6 represent extracellular loops. Putative membrane crossings are defined as trajectories bounded by periplasmic and extracellular domains. Sixteen such membrane crossings (often with lengths compatible with a tilted β -strand) can be identified, and the corresponding external loops are labelled L1–L8.

transformed into *E. coli* host strain DH5 α . The sequences of both inserts were determined [29] and have been deposited in the GenBank[®] database under the accession numbers AY312416 and AY312417 for *BpsOmp38* and *BthOmp38* respectively. The DNA sequences were >98% identical, giving almost 100% identity of the putative amino acid sequences translated from the corresponding nucleotide sequences with the exception that the second *N*-terminal residue, asparagine, in the *BpsOmp38* sequence was replaced by aspartic acid in the *BthOmp38* sequence.

When these sequences were used to calculate the masses of our tryptic peptides, we could identify almost every peptide from the prior HPLC–MS analysis. As expected, the exceptions were peptides containing fewer than four amino acid residues. The first amino acid detected by HPLC–MS was Ala⁴¹ and the last was (as expected) Arg³⁷¹. The peptide composition as analysed by HPLC–MS was identical for both proteins.

Protein structure prediction

SignalP was used to predict Omp38 signal sequences, and when these were removed, the calculated M_r of the identical, processed, leaderless proteins was 37 163.5. This value agrees well with the estimate from MALDI-TOF analysis of the purified proteins.

The predicted amino acid sequences of the pre-proteins were next analysed for similarity with *Burkholderia* and other Gram-negative bacterial porins (Figure 5). The membrane topology of Omp38 was predicted by the method of Diederichs et al. [30], and the three-dimensional structure of the protein was analysed using 123D+ and Swiss-Model. Omp38 had most similarity to the anion-selective porin Omp32 [Protein DataBank (PDB) code 1e54a], (35.8% identity when using Swiss-Model). The predicted topology of 16 transmembrane domains, eight loops and eight periplasmic turns is compatible with a 16-stranded porin

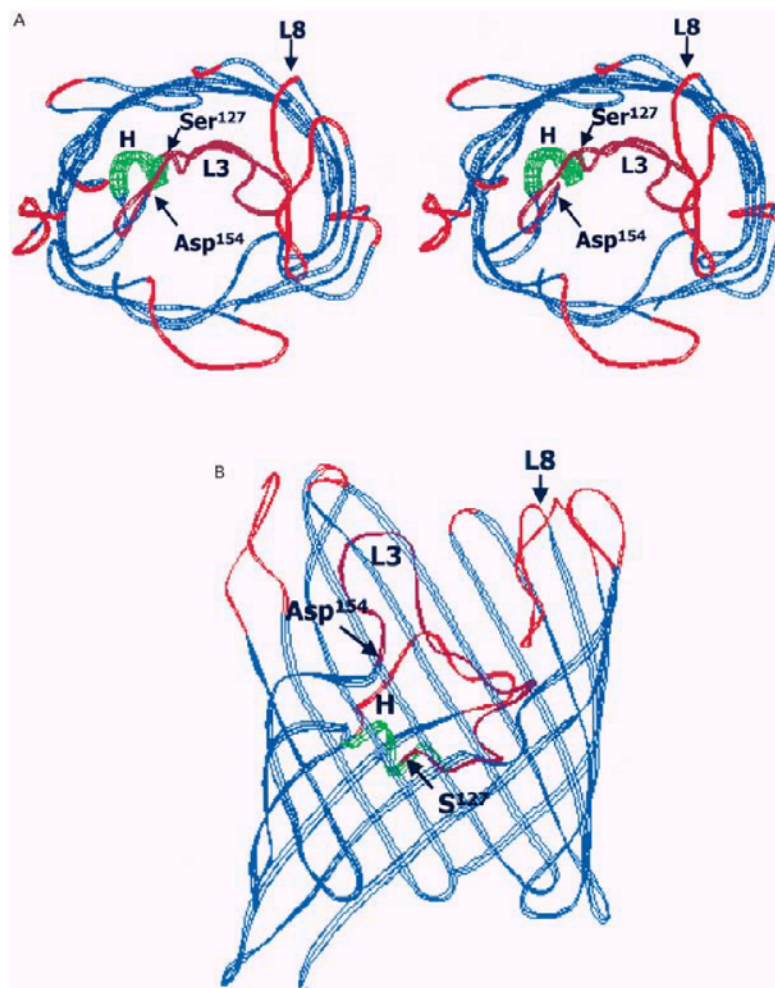


Figure 7 Predicted three-dimensional structures of *BpsOmp38* and *BthOmp38* using Swiss-Model

The representation was drawn using Swiss-pdb Viewer version 3.7b2 and was built by alignment with the closest homologue (Omp32 porin from *C. acidovorans*). This figure shows 16 strands and eight loops. The longest loop (L3) (Ser¹²⁷–Asp¹⁵⁴) folds inside the barrel. (A) Stereo image (top view) of Omp38. (B) Side view of Omp38.

β -barrel in which the N-terminus forms a salt bridge with the C-terminus immediately after a periplasmic turn, and based on both transmembrane topology prediction and three-dimensional structure modelling, Omp38 has a β -barrel structure with 16 transmembrane strands, eight short periplasmic turns and eight external loops (Figures 6 and 7).

The longest loop, Loop 3 (L3: Ser¹²⁷ \rightarrow Asp¹⁵⁴), contains two short, antiparallel β -strands at the very beginning and the end of the loop, and a short right-handed α -helix (Tyr¹¹⁹ \rightarrow Leu¹²⁶) was found to precede the long L3. This loop is characteristic of many porins as a pore-confined loop responsible for the size-selectivity of the channel [31,32].

DISCUSSION

Porins play crucial roles in the interactions between Gram-negative bacteria and their environment. In the present study, we purified and characterized the major OM porin of the pathogenic bacterium, *B. pseudomallei*, and the equivalent porin from the closely-related non-pathogenic bacterium, *B. thailandensis*. When the oligomeric proteins (M_r 110000) were heated to 95 °C, they disassociated into M_r 38000 monomers. This process was irreversible, and it has been suggested that upon heating, porin β -sheets are converted into α -helices, preventing reassembling into trimers [33,34].

When reconstituted in liposomes for functional analysis, the results were consistent with those expected for 'general diffusion porins' [15,35]. Although the highest diffusion rate corresponded to the smallest sugar, L-arabinose (150 Da), D-glucose (180 Da) permeated measurably faster than other sugars with the same molecular mass (D-mannose and D-galactose). *B. pseudomallei* and *B. thailandensis*, like other Gram-negative bacteria, utilize glucose as a primary source of carbon for cell growth, and enhanced glucose permeation may be functionally significant. *B. thailandensis* can utilize L-arabinose, whereas *B. pseudomallei* cannot [4]. However, the two porins displayed a similar relative diffusion rate for L-arabinose (Figure 4), suggesting that Omp38 is not a sugar-specific channel for L-arabinose. On the basis of very similar sugar permeability through the unusually large channels of *E. coli* OmpG and the 42 kDa *Serratia liquefaciens* porin [22,36], the diameter of the 38 kDa porin protein can be estimated to be in the range 1.2–2.0 nm. The size-exclusion limit of Omp38 was larger than that of the *E. coli* porin when various sugars were subjected to permeability measurements under the same conditions (results not shown). Hence, *Bps*Omp38 and *Bth*Omp38 porins represent large channels, which allow a greater variety of nutrients to be taken up.

FTIR analysis showed that Omp38 contained predominantly β -strands and was likely to form the antiparallel β -barrel characteristic of bacterial OM porins [37–39]. The IR patterns of both proteins were almost identical with slight differences found in the turns and loops, and LPS regions. It is not known whether this may be reflected in genuine differences in the final conformations of the otherwise identical proteins. The analysis also showed that Omp38 preparations always contained varying amounts of LPS. Although both were isolated and purified by the same procedure, *Bps*Omp38 contained a greater amount of LPS than *Bth*Omp38 (Figure 3). The data in Figure 1(B) also suggest the presence of LPS in the purified proteins, with a 'ladder' of several bands in the unheated samples (cf. Eisele and Rosenbusch [40]). The idea of a strong porin–LPS interaction is supported by the fact that solubilization of Omp38 by a strong detergent (SDS) and gel-filtration failed to remove the LPS completely. However, small amounts of LPS remaining in the *Bps*Omp38 sample helped to improve solubility of the protein, and did not show much effect on the immunoblots, MS analysis and liposome-swelling assays carried out in this study.

We isolated the gene encoding Omp38 from *B. pseudomallei* and *B. thailandensis* genomic DNA after identifying the genes following protein MS analysis. We found that almost all the back-translated amino acid sequences of both organisms could be matched to peptide fragment data from capillary HPLC–ESI/MS of the native porins. Some amino acid sequences in the mature proteins could not be identified using HPLC–ESI/MS. At high concentrations, membrane proteins tend to aggregate, and this might hinder analysis by HPLC–ESI/MS and MALDI–MS [41].

Omp38 is one of a large number of porins that usually form trimers and have individual subunits that fold into 16- or 20-stranded barrels [16]. Topology and three-dimensional prediction programs strongly suggest that Omp38 folds as a 16-stranded barrel with eight loops and eight turns, with the closest similarity to the anion-selective porin from *Comamonas acidovorans* [31]. The longest loop (L3) folds into the barrel. This loop, which contains a short α -helix, has been suggested to constrict the size of the pore [32,39]. L8, which is the second longest loop, also folds into the barrel interior and contributes to the formation of the particularly narrow external channel opening.

Based on the three-dimensional structure of *E. coli* OmpF and PhoE [39], L3 was found to fold into the channel and to define a constriction zone, which governs pore activity. The

cluster of acid residues in L3, located in front of a positively charged cluster of basic amino acid residues (anti-L3), creates an intense electrostatic field in the pore. The resulting charge distribution regulates diffusion of solutes through the pore [32,39,42]. Several residues of L3 have been suggested to be involved in channel activity [32,43], especially Asp¹¹³ and Glu¹¹⁷. These residues participate in the architecture of the negative cluster. In addition, site-directed mutagenesis data revealed that Gly¹¹⁹ was associated with colicin resistance, drastic alterations in diffusion and antibiotic susceptibility, and local structural alterations focused inside the lumen [44,45].

In the present study, we have cloned and sequenced the genes encoding Omp38 porins from both *B. thailandensis* and *B. pseudomallei*, and have shown the proteins to be identical. Further work is underway to determine the importance of Omp38 in antibiotic resistance and immunity, and to determine its three-dimensional structure by protein crystallization and X-ray diffraction.

This work was supported by a Suranaree University of Technology Grant (grant number: SUT-106-46-36-02), by a Shell Studentship (to J. S.), by a grant from the German Academic Exchange Service 'DAAD' (to W. S.), and by the Wellcome Trust (to R. H. A.). We thank Professor Dieter Naumann at the Robert-Koch Institute, Berlin, Germany, for help with FTIR measurements and Dr Albert Schulte at Ruhr University of Bochum, Germany, for his advice on the manuscript.

REFERENCES

- Moor, R. A., DeShazer, D., Reckseidler, S., Weissman, A. and Woods, D. E. (1999) Efflux-mediated aminoglycoside and macrolide resistance in *Burkholderia pseudomallei*. *Antimicrob. Agents Chemother.* **43**, 465–470.
- Badsha, H., Edwards, C. J. and Chng, H. H. (2001) Melioidosis in systemic lupus erythematosus: the importance of early diagnosis and treatment in patients from endemic areas. *Lupus* **10**, 821–823.
- Brett, P. J., DeShazer, D. and Woods, D. E. (1997) Characterization of *Burkholderia pseudomallei* and *Burkholderia pseudomallei*-like strains. *Epidemiol. Infect.* **118**, 137–148.
- Brett, P. J., DeShazer, D. and Woods, D. E. (1998) *Burkholderia thailandensis* sp. nov., description of a *Burkholderia pseudomallei*-like species. *Int. J. Syst. Bacteriol.* **48**, 317–320.
- Yabuuchi, E., Kosako, Y., Oyaizu, H., Yano, I., Hotta, H., Hashimoto, Y., Ezaki, T. and Arakawa, M. (1992) Proposal of *Burkholderia* gen. nov. and transfer of seven species of the genus *Pseudomonas* homology group 11 to the new genus, with the type species *Burkholderia cepacia* (Palleroni and Holmes 1981) comb. nov. *Microbiol. Immunol.* **36**, 1251–1275.
- Erratum (1993) *Microbiol. Immunol.* **37**, 335.
- Chaiyaroj, S. C., Kolmori, K., Koonpaew, S., Anantagool, N., White, N. J. and Sirisinha, S. (1999) Differences in genomic macrorestriction patterns of arabinose-positive (*Burkholderia thailandensis*) and arabinose-negative *Burkholderia pseudomallei*. *Microbiol. Immunol.* **43**, 625–630.
- Wuthiekanun, V., Smith, M. D., Dance, D. A., Walsh, A. L., Pitt, T. L. and White, N. J. (1996) Biochemical characteristics of clinical and environmental isolates of *Burkholderia pseudomallei*. *J. Med. Microbiol.* **45**, 408–412.
- Woo, P. C. Y., Woo, G. K. S., Lau, S. K. P., Wong, S. S. Y. and Yuen, K. Y. (2002) Single gene target bacterial identification. *groEL* gene sequencing for discriminating clinical isolates of *Burkholderia pseudomallei* and *Burkholderia thailandensis*. *Diagn. Microbiol. Infect. Dis.* **44**, 143–149.
- Gridley, D. S. (1999) Non-fermenting aerobic Gram-negative bacilli. In *Essentials of Diagnostic Microbiology* (Shimeld, L. A., ed.), pp. 206–221. Delmar Publishers, New York.
- Simpson, A. J. H., Opal, S. M., Angus, J. M., Palarly, J. E., Parejo, N. A., Chaowagul, W. and White, N. J. (2000) Differential antibiotic-induced endotoxin release in severe melioidosis. *J. Infect. Dis.* **181**, 1014–1019.
- Bianco, N., Neshat, S. and Poole, K. (1997) Conservation of the multidrug resistance efflux gene *oprM* in *Pseudomonas aeruginosa*. *Antimicrob. Agents Chemother.* **41**, 853–856.
- Goodman, B. E. (2002) Transport of small molecules across cell membranes: water channels and urea transporters. *Adv. Physiol. Educ.* **26**, 146–157.

- 13 Albertí, S., Rodríguez-Quiñones, F., Schirmer, T., Rummel, G., Tomas, J. M., Rosenbusch, J. P. and Benedí, V. J. (1995) A porin from *Klebsiella pneumoniae*: sequence homology, three-dimensional model, and complement binding. *Infect. Immun.* **63**, 903–910
- 14 Wolf, K., Fischer, E., Mead, D., Zhong, G., Peeling, R., Whitmore, B. and Caldwell, H. D. (2001) *Chlamydia pneumoniae* major outer membrane protein is a surface-exposed antigen that elicits antibodies primarily directed against conformation-dependent determinants. *Infect. Immun.* **69**, 3082–3091
- 15 Nikaido, H. (1994) Porins and specific diffusion channels in bacterial outer membrane permeability. *Microbiol. Rev.* **49**, 1–32
- 16 Koebnik, R., Locher, K. P. and Van Gelder, P. (2000) Structure and function of bacterial outer membrane proteins: barrels in a nutshell. *Mol. Microbiol.* **37**, 239–253
- 17 Gotoh, N., Nagino, K., Wada, D., Tsujimoto, H. and Nishino, T. (1994) *Burkholderia* (formerly *Pseudomonas*) *cepacia* porin is an oligomer composed of two component proteins. *Microbiology* **140**, 3285–3291
- 18 Tsujimoto, H., Gotoh, N., Yamagishi, J., Oyama, Y. and Nishino, T. (1997) Cloning and expression of the major porin protein gene *opcP* of *Burkholderia* (formerly *Pseudomonas cepacia*) in *Escherichia coli*. *Gene* **186**, 113–118
- 19 Gotoh, N., White, N. J., Chaowagul, W. and Woods, D. (1994) Isolation and characterization of the outer-membrane proteins of *Burkholderia* (*Pseudomonas pseudomallei*). *Microbiology* **140**, 797–805
- 20 Nikaido, H. and Rosenberg, E. Y. (1983) Porin channels in *Escherichia coli*: studies with liposomes reconstituted from purified proteins. *J. Bacteriol.* **153**, 241–252
- 21 Yoshimura, F., Zalman, L. S. and Nikaido, H. (1983) Purification and properties *Pseudomonas aeruginosa* porin. *J. Biol. Chem.* **258**, 2308–2314
- 22 Nitzan, Y., Orlovsky, K. and Pechatnikov, I. (1999) Characterization of porins isolated from the outer membrane of *Serratia liquefaciens*. *Curr. Microbiol.* **8**, 71–79
- 23 Arcklasamy, A. and Krishnaswamy, S. (2000) Purification of integral outer-membrane protein OmpC, a surface antigen from *Salmonella typhi* for structure–function studies: a method applicable to enterobacterial major outer-membrane protein. *Anal. Biochem.* **283**, 64–70
- 24 Amero, S. A., James, T. C. and Elgin, S. C. R. (1994) Production of antibodies using proteins in gel bands. In *Basic Protein and Peptide Protocols*. (Walker, J. M., ed.), pp. 401–406. Humana Press, Totowa
- 25 Shevchenko, A., Wilm, M., Vorm, O. and Mann, M. (1996) Mass spectrometric sequencing of proteins silver-stained polyacrylamide gels. *Anal. Chem.* **68**, 850–858
- 26 Ausubel, F. M., Brent, R., Kingston, R. E., Moore, D. D., Smith, J. A. and Struh, K. (1999) *Short Protocols in Molecular Biology*, 4th edn, pp. 2–12. Wiley & Sons, New York
- 27 Mantele, W. and Fabian, H. (2002) Infrared spectroscopy of proteins. In *Handbook of Vibrational Spectroscopy* (Chalmers, J. M. and Griffiths, P. R., ed.), pp. 1–27. John Wiley & Sons, Chichester
- 28 Abrecht, H., Goormaghtigh, E., Ruyschaert, J. M. and Homble, F. (2000) Structure and orientation of two voltage-dependent anion-selective channel isoforms: an attenuated total reflection Fourier-transform infrared spectroscopy study. *J. Biol. Chem.* **275**, 40992–40999
- 29 Sanger, F., Nicklen, S. and Coulson, A. R. (1977) DNA sequencing with chain-terminating inhibitors. *Proc. Natl. Acad. Sci. U.S.A.* **74**, 5463–5467
- 30 Diederichs, K., Freigang, J., Umhau, S., Zeth, K. and Breed, J. (1998) Prediction by aneural network of outer membrane β -strand protein topology. *Protein Sci.* **7**, 2413–2420
- 31 Zeth, K., Diederichs, K., Welte, W. and Engelhardt, H. (2000) Crystal structure of Omp32, the anion-selective porin from *Comamonas acidovorans*, in complex with a periplasmic peptide at 2.1 Å resolution. *Structure* **8**, 981–992
- 32 Breden, J., Saint, N., Mallea, M. D. E., Molle, G., Pagès, J. M. and Simonet, V. (2002) Alteration of pore properties of *Escherichia coli* OmpF induced by mutation of key residues in anti-loop 3 region. *Biochem. J.* **363**, 521–528
- 33 Labesse, G., Garnotel, E., Bonnel, S., Dumas, C., Pagès, J. M. and Bolla, J. M. (2001) MOMP, a divergent porin from *Campylobacter*: cloning and primary structural characterization. *Biochem. Biophys. Res. Commun.* **280**, 380–387
- 34 Tokunaga, M., Tokunaga, H., Okajima, Y. and Nakae, T. (1979) Characterization of porins from the outer membrane of *Salmonella typhimurium*: 2. Physical properties of the functional oligomeric aggregates. *Eur. J. Biochem.* **95**, 441–448
- 35 Cowan, S. W. (1993) Bacterial porins: lessons from three high-resolution structures. *Curr. Opin. Struct. Biol.* **3**, 501–507
- 36 Fajardo, D. A., Cheung, J., Ito, C., Sugawara, E., Nikaido, H. and Misra, R. (1998) Biochemistry and regulation of a novel *Escherichia coli* K-12 porin protein, OmpG, which produces unusually large channels. *J. Bacteriol.* **180**, 4452–4459
- 37 Forst, D., Welte, W., Wacker, T. and Diederichs, K. (1998) Structure of the sucrose-specific porin ScrY from *Salmonella typhimurium* and its complex with sucrose. *Nat. Struct. Biol.* **5**, 37–46
- 38 Schirmer, T., Keller, T. A., Wang, Y. F. and Rosenbusch, J. P. (1995) Structural basis for sugar translocation through maltoporin channels at 3.1 Å resolution. *Science* **267**, 512–514
- 39 Cowan, S. W., Schirmer, T., Rummel, G., Steiert, M., Ghosh, R., Pauptit, R. A., Jansonius, J. N. and Rosenbusch, J. P. (1992) Crystal structures explain functional properties of two *Escherichia coli* porins. *Nature (London)* **358**, 727–733
- 40 Eisele, J. L. and Rosenbusch, J. P. (1990) *In vitro* folding and oligomerization of a membrane protein. Transition of bacterial porin from random coil to native conformation. *J. Biol. Chem.* **265**, 10217–10220
- 41 Ho, Y. P. and Hsu, P. H. (2002) Investigating the effects of protein patterns on microorganism identification by high-performance liquid chromatography–mass spectrometry and protein database searches. *J. Chromatogr. A* **976**, 103–111
- 42 Karshikoff, A., Spassov, V., Cowan, S. W., Ladenstein, R. and Schirmer, T. (1994) Electrostatic properties of two porin channels from *Escherichia coli*. *J. Mol. Biol.* **240**, 372–384
- 43 Phale, P. S., Schirmer, T., Prilipov, A., Lou, K. L., Hardmeyer, A. and Rosenbusch, J. P. (1997) Voltage gating of *Escherichia coli* porin channels: role of the constriction loop. *Proc. Natl. Acad. Sci. U.S.A.* **94**, 6741–6745
- 44 Jeanteur, D., Schirmer, T., Fourel, D., Simonet, V., Rummel, G., Widmer, C., Rosenbusch, J. P., Pattus, F. and Pagès, J. M. (1994) Structural and functional alterations of a colicin-resistant mutant of OmpF porin from *Escherichia coli*. *Proc. Natl. Acad. Sci. U.S.A.* **91**, 10675–10679
- 45 Simonet, V., Mallaé, M. and Pagès, J. M. (2000) Substitutions in the eyelet region disrupt cefepime diffusion through the *Escherichia coli* OmpF channel. *Antimicrob. Agents Chemother.* **44**, 311–315

Curriculum Vitae

NAME Miss Jaruwan Siritapetawee

DATE OF BIRTH 3 October 1972

PLACE OF BIRTH Bangkok, Thailand

INSTITUTION ATTENDED

Khon Kaen University, Khon Kaen, Thailand,
1991-1995, Bachelor of Science (Medical
Technology)

Khon Kaen University, Khon Kaen, Thailand,
1996-1998, Master of Science (Biochemistry)

Suranaree University of Technology, Nakhon
Ratchasima, Thailand, 2000-2004,
Doctor of Philosophy (Biochemistry)

AWARDS AND SCHOLARSHIPS

Shell studentship, The shell centenary scholarship
Fund, 2003.